Droplet-based microfluidic systems to incorporate nucleic acids into cationic liposomes and to transfect mammalian cells in vitro

Micaela Vitor

NNT : 2017SACLX020

THESE DE DOCTORAT
DE
UNIVERSIDADE ESTADUAL DE CAMPINAS (UNICAMP)
ET DE
L'UNIVERSITE PARIS-SACLAY
PREPAREE A
L'ECOLE POLYTECHNIQUE

ECOLE DOCTORALE N° 573:
Interfaces: approches interdisciplinaires, fondements, applications et innovation

Spécialité de doctorat: Sciences et technologies industrielles

Par

Mme Micaela Tamara Vitor

Droplet-based microfluidic systems to incorporate nucleic acids into cationic liposomes and to transfect mammalian cells *in vitro*

Thèse présentée et soutenue au Brésil, le 26 avril 2017:

Composition du Jury :

M Hernandes Faustino de Carvalho	Professeur, Université de Campinas	Président
Mme Stephanie Descroix	Chargée de recherche, Institut Curie	Rapporteur
Mme Séverine Le Gac	Professeur agrégé, University of Twente	Rapporteur
Mme Rosiane Lopes da Cunha	Professeur, Université de Campinas	Examinateur
M Charles Baroud	Professeur associé, Ecole Polytechnique	Directeur de thèse
Mme Lucimara Gaziola de la Torre	Professeur, Université de Campinas	Co-directeur de thèse

Titre : Système microfluidique de gouttes pour incorporer des acides nucléiques dans des liposomes cationiques et pour la transfection de cellules mammifères *in vitro*

Mots clés : microfluidique des gouttes, liposomes cationiques, acides nucléiques, délivrance de gènes, cellules dendritiques, cellules CHO.

Résumé : Ce travail a consisté à utiliser deux systèmes microfluidiques de gouttes pour incorporer d'une part des acides nucléiques dans des liposomes cationiques et d'autre part étudier la dynamique de transfection dans des cellules mammifères. La première micropuce a permis d'insérer de l'ADN dans des liposomes cationiques afin d'obtenir de manière reproductible des lipoplexes appropriés à la transfection de cellules dendritiques (DC). Plusieurs paramètres expérimentaux ont été tout d'abord étudiés. Ensuite, les lipoplexes produits dans une micropuce avec un grand canal en serpentin et une région de division des gouttes, fonctionnant à un rapport de débit eau/huile 0,25 et aux rapports molaire de charge ($R_{+/-}$) 1,5; 3; 5; 7 et 10; ont été utilisés pour transfecter des DCs *in vitro*. Tous les lipoplexes ont transfecté les DCs, tout en offrant une activation des DCs. La seconde étape a consisté à utiliser une micropuce à l'échelle de la cellule unique afin de transfecter des cellules ovariennes de hamster Chinois (CHO-S) avec lipoplexes au différent chargement d'ADN ($R_{+/-}$ 1,5; 3; 5), dont la dynamique de transfection a été suivie par la production de protéines vertes fluorescentes (GFP) et par la viabilité cellulaire. Cette micropuce a permis d'évaluer l'hétérogénéité des cellules transfectées, révélant la présence d'une sous-population produisant des niveaux particulièrement élevés de GFP. Ces hautes productrices (HP) ont présenté une taille cellulaire plus importante que celle de la population moyenne. Le lipoplex chargé positif $R_{+/-}$ 5 a produit plus de HPs. Le $R_{+/-}$ 1,5, avec plus d'ADN, a augmenté la productivité spécifique de GFP des HPs. Cette thèse a été réalisée dans le cadre d'un programme de co-tutelle entre l'Université de Campinas, au Brésil, et l'École Polytechnique, en France. Ce travail a principalement présenté des contributions originales aux domaines de microfluidique et de délivrance de gènes.

Title: Droplet-based microfluidic systems to incorporate nucleic acids into cationic liposomes and to transfect mammalian cells *in vitro*

Keywords: droplet-based microfluidic system, cationic liposomes, nucleic acids, gene delivery, dendritic cells, CHO cells.

Abstract: This work aimed at using one droplet-based microfluidic systems to incorporate nucleic acids into cationic liposomes and another one to study the mammalian cell transfection process. In the first part of this study we used a droplet-based microfluidic system to complex cationic liposomes with pDNA in order to obtain reproducible and suitable lipoplexes to dendritic cells (DCs) transfection. For this purpose, some experimental parameters were investigated. Lipoplexes produced in a microchip with large serpentine channel and split region, operating at ratio aqueous/oil flow rate 0.25 and molar charge ratios ($R_{+/-}$) 1.5, 3, 5, 7 and 10 were used to transfect DCs *in vitro*. All lipoplexes transfected DCs and resulted in cell activation. In the second part of this study we used a single-cell microfluidic platform to transfect Chinese hamster ovary cells (CHO-S) with lipoplexes at different DNA loading ($R_{+/-}$ 1.5, 3, 5) and monitored by green fluorescent protein (GFP) production and cell viability. The single-cell platform enables to assess the heterogeneities of CHO-S population, revealing the presence of a subpopulation producing significantly high levels of GFP. These high producers (HP) showed increased cell size in comparison to the average population. Moreover, the positive charged lipoplex $R_{+/-}$ 5 produced more HPs. Additionally, the $R_{+/-}$ 1.5, loading more amount of pDNA, increased GFP specific productivity of HPs. This thesis was developed under the joint graduate program of the University of Campinas, Brazil and École Polytechnique, France. In general, this work presents original contributions in the areas of microfluidics and gene delivery.

I dedicate this work
to my family and friends,
for the understanding and affection.

ACKNOWLEDGEMENTS

The development of this work was possible thanks to the collaboration between École Polytechnique (France) and University of Campinas (Unicamp). At first I would like to thank my advisors, Professor Lucimara Gaziola de la Torre and Professor Charles Baroud, for the confidence in my competence, guidance and encouragement to develop this research. I also would like to thank Dr Sebastien Sart, Professor Marcelo Bispo de Jesus and Professor Ronei Luciano Mamoni for the scientific assistance in biological field. I would like to acknowledge Professor Rosiane Lopes da Cunha, Professor Maria Helena Andrade Santana, Condensed Matter Physics Laboratory (PMC) at École Polytechnique and Microfabrication Laboratory at Brazilian Center for Research in Energy and Materials (CNPEM) for the availability to use their laboratory structures to the experiments. The financial support of São Paulo Research Foundation (FAPESP), National Counsel of Technological and Scientific Development (CNPq) and European Research Council (ERC).

I specially would like to thanks the researchers and colleagues at Unicamp, Gilson Maia Jr., Andréa Shimojo, Bruna Melo, Amanda Marcelino, Fernanda Lopes, Patrícia Severino, André Lima, Lívia Furquim de Castro, Caroline Sipoli, Aline Oliveira, Ismail Eş, Amanda Pessoa and Franciele Flores for their support and encouragement. École Polytechnique and Hydrodynamics Laboratory (LadHyX) staff, Audrey Lemarechal, Coralie Talet, Caroline Frot, Avin Babataheri, Daniel Guy, Delphine L'huillier, Magali Tutou, Thérèse Lescuyer, Do Chi Toaï Vu for technical support and comprehension. Researchers, colleagues and friends at Hydrodynamics Laboratory (LadHyX), Professor Abdul Barakat, Professor Christophe Clanet, Professor Gabriel Amselem, Professor Julien Husson, Irma Liascukiene, Raphaël Tomasi, Cyprien Guermonprez, Antoine Barizien, Benoît Drogue, Nicolas Taccoen, Carlo Natale, Julie Lafaurie, Elizabeth Antoine, Brenna Hogan, François Cornat, Lionel Guillou, Johanne Mensah for great discussions and friendly reception. At last, I would like to thank my friends from my stay in France, Denize Monaris, Marcela Silva, Zouhaïr Adnani and Meyer family for the caring with me.

"Life is not easy for any of us.
But what of that?
We must have perseverance and
above all confidence in ourselves.
We must believe that we are gifted for
something and that this thing must be attained."
Marie Curie

FIGURE CAPTIONS

Chapter IV

TABLE CAPTIONS

Chapter II

Chapter III

Annex II

NOMENCLATURE

ANOVA:	analysis of variance;
Ca:	capillary number;
CHO-S:	Chinese hamster ovary cells;
CL:	cationic liposomes;
DCs:	dendritic cells;
DNA:	deoxyribonucleic acid;
DOPE:	1,2dioleoylsn-glycero-3 phosphoethanolamine;
DOTAP:	1,2-dioleoyl-3-trimethylammonium-propane;
EPC:	Egg phosphatidylcholine;
FITC:	fluorescein fluorochrome;
GFP:	green fluoresce protein;
GFP:	green fluorescent protein;
HP:	high producer CHO-S cells;
Lipoplexes:	cationic liposomes/pDNA complexes;
LP:	low producer CHO-S cells;
MFI:	median fluorescence intensity;
PdI:	Polydispersity Index;
pDNA:	DNA plasmidial;
$\mathbf{R_{+/-}}$:	cationic lipid:DNA molar charge ratios;
Re:	Reynolds number;
S.D.:	Standard Deviation;
SSC:	side scatter - cells granularity/complexity;
ST:	stable transfection;
TC:	thin serpentine channel;
TE:	transfection efficiency;
TGE:	transient gene expression technology;
THP-1:	human monocyte cells;
Volume fraction:	ratio aqueous/oil flow rate;
WC:	wide serpentine channel;

SUMMARY

Chapitre I - Introduction

1. Introduction

La thérapie génique se réfère à la transmission d'un acide nucléique codant un gène d'intérêt dans les cellules ou organes ciblés avec conséquente expression du transgène (1). Un facteur clé dans le succès de la thérapie génique est le développement de systèmes d'administration capables de transférer efficacement les gènes (2). Les nanovecteurs sont généralement classés comme viraux et non-viraux, et dans ces derniers, les liposomes cationiques sont particulièrement prometteurs (1,3). Les liposomes cationiques sont principalement composés de lipides cationiques pour assurer leur charge superficielle positive, ce qui les conduit à interagir électrostatiquement avec les acides nucléiques chargés négativement, pour former des complexes capables d'entrer dans les cellules (3). Les liposomes cationiques sont supérieurs aux vecteurs viraux en termes de reproductibilité, de sécurité d'utilisation, en plus d'être biocompatibles et biodégradables. Cependant, ils sont inférieurs aux vecteurs viraux en termes d'efficacité de transfection (4).

Les progrès récents de la microfluidique ont créés de nouvelles et passionnantes perspectives de thérapie génique. L'environnement à micro-échelle dans les systèmes microfluidiques permet un contrôle et une optimisation précis des processus et techniques multiples utilisés dans le transférer des gènes et dans la production des systèmes d'administration de gènes et de médicaments (5). En particulier, les microgouttes d'eau dans l'huile fournissent un autre format expérimental, car les microgouttes définissent des compartiments de réaction, entraînant une réduction de volume de réaction requis. Il a également été démontré que les microgouttes générées par des dispositifs microfluidiques sont extrêmement uniformes, ce qui est apparemment adéquat pour l'encapsulation de cellules individuelles et pour la synthèse des systèmes non-viraux (6,7).

Les systèmes microfluidiques de gouttes désignés avec certaines géométries peuvent fournir un mélange rapide de réactifs (8). Les microsystèmes fonctionnant

uniquement avec des flux parallèles ont le mélange de fluides favorisé principalement par la diffusion, alors que les microsystèmes de gouttes peuvent ajouter une contribution d'advection chaotique qui augmente le mélange dans le système (9). Les micromélangeurs ont des applications importantes telles que le contrôle de réactions chimiques (10), la contribution à la cristallisation des protéines (11), l'amélioration d'analyses biochimiques (12) et la complexation des nanoparticules avec les acides nucléiques (lipoplexes) (7).

Les méthodes classiques d'obtention de lipoplexes impliquent uniquement le mélange fourni par le « hand shaking » ou par le vortex pour atteindre la complexation des liposomes cationiques avec des acides nucléiques. Cependant, ces méthodes conventionnelles introduisent une grande variabilité dans la formation de lipoplexes et, par conséquent, fournissent des rendements de transfection incompatibles (7). Certaines cellules difficiles à transfecter, comme les cellules dendritiques (DC) (13), utilisent des voies de transfection extrêmement dépendantes de la taille et de la polydispersité des lipoplexes (14). Les cellules dendritiques chargées avec des antigènes tumoraux sont importantes pour des approches immunothérapeutiques (15). Ainsi, l'étude des méthodologies de formation des lipoplexes est très importante afin d'obtenir lipoplexes avec des propriétés spécifiques à différentes lignée cellulaire d'une manière reproductible et contrôlable (16). Hsieh *et al.* (7) ont développé un système microfluidique de gouttes afin de complexer liposomes commerciaux avec ADN. Ils ont montré la robustesse du microsystème pour produire des lipoplexes reproductibles et aussi pour transfecter des cellules, ainsi arrivant à une méthode alternative aux conventionnelles (7).

En outre, les systèmes microfluidiques de gouttes peuvent être utilisés pour analyser des cellules individualisées, car les gouttes permettent la détection rapide de molécules sécrétées par les cellules en raison du faible volume entourant chaque cellule encapsulée. Le risque de contamination croisée diminue et les cellules peuvent être étudiées individuellement par des techniques de fluorescence (17). Les micropuces liées à des équipements de fluorescence permettent l'analyse des cellules de mammifères adhérentes et non adhérentes, la

manipulation et l'étude du contenu de cellules individualisées (18). En plus, les cellules encapsulées dans les gouttes peuvent être surveillées pendant toute la période de culture cellulaire, au lieu de seulement quelques instants, ce qui met en évidence la réponse de chaque cellule même si le signal de la population cellulaire semble relativement homogène pendant l'expérience (19). Cependant, maintenir la viabilité cellulaire dans les gouttes est un défi, car il existe des risques de coalescence, d'appauvrissement des nutriments ou d'accumulation de métabolites toxiques. Ainsi, ces points doivent être considérés avant de faire une analyse robuste sur des longues périodes de culture cellulaire (17). Malgré ces inconvénients, un groupe de recherche a montré que la culture cellulaire dans des plateformes à l'échelle de la cellule unique est possible (20).

L'application d'une plateforme microfluidique pour suivre dynamiquement les réponses cellulaires individualisées ouvre la possibilité de mieux comprendre l'hétérogénéité cellulaire auprès de l'expression transitoire des gènes (21). L'industrie de la biotechnologie utilise largement les cellules ovariennes de hamster Chinois (CHO) pour produire des protéines recombinantes par transfection transitoire. Généralement, ce type de transfection est plus approprié pour la production de protéines en haute quantité et de manière rapide, qui est dont utilisé dans les premières étapes du développement de médicaments (22). Par conséquent, en vue d'optimiser les rendements de production, la transfection par un gène d'expression transitoire à l'échelle de la cellule unique est souhaitable afin de mieux comprendre le processus et de mieux contrôler les conditions de transfection.

Dans ce contexte, l'application de la technologie microfluidique de gouttes pour synthétiser lipoplexes et pour transfecter des cellules de mammifères *in vitro* de manière transitoire peuvent contribuer aux progrès de la technique de délivrance de gène. A cet effet, dans la première partie de ce travail, certains paramètres qui influencent la synthèse de lipoplexes ont été étudiés dans la plateforme de gouttes. Le but était de synthétiser lipoplexes dans des conditions microfluidiques, avec des propriétés physico-chimiques appropriées pour la transfection *in vitro* des cellules dendritiques. En outre, à l'échelle de la cellule

unique, cellules CHO-S ont été transfectées dans une plateforme microfluidique universelle pour des tests biologiques. La transfection transitoire a été réalisée par lipoplexes au différent chargement d'ADN, rapport molaire de charge entre lipides cationiques et des acides nucléiques ($R_{+/-}$) 1,5; 3; 5. Avec ce système, c'était possible de conclure sur l'influence des lipoplexes dans l'hétérogénéité de la population de cellules en exprimant une protéine recombinante. Cette thèse a été développée dans le cadre d'une programme de cotutelle entre l'Université de Campinas - Brésil et de l'Ecole Polytechnique – France, grâce à la collaboration entre la Professeur Lucimara de la Torre, spécialiste en systèmes non-viraux de transfert de gènes au Brésil, et le Professeur Charles Baroud, spécialiste en microfluidique pour les applications biologiques en France.

2. Objectifs

L'objectif général du projet était de contribuer aux domaines de la nanobiotechnologie, de la microfluidique et du transfert de gènes. En particulier, ce travail visait à appliquer des systèmes microfluidiques de gouttes afin de synthétiser des lipoplexes présentant des caractéristiques physico-chimiques pour transfecter les cellules dendritiques et d'étudier le processus de transfection de cellules CHO-S par l'analyse de cellules individualisées pendant la période de culture cellulaire. Ainsi, le premier objectif était de maintenir les propriétés des liposomes cationiques après le traitement dans le système microfluidique de gouttes et de former lipoplexes avec les caractéristiques requises pour transférer les DCs. Ensuite, le deuxième objectif était d'étudier plus profondément l'influence de lipoplexes au différent chargement d'ADN ($R_{+/-}$) sur la transfection de cellules de mammifères. Pour cela, une plateforme microfluidique universelle à l'échelle de la cellule unique a été utilisée pour transfecter les cellules CHO-S par lipoplexes. Avec l'analyse de cellules individualisées fournie par la plateforme, c'était possible d'associer l'influence de lipoplexes au différent chargement d'ADN sur hétérogénéité dans la production de GFP par la population de cellules CHO-S.

Pour atteindre ces objectifs, la recherche a suivi ces buts:

• Synthèse de lipoplexes dans un dispositif microfluidique de gouttes pour transfecter les cellules dendritiques:

Investiguer comment les paramètres microfluidiques expérimentaux influencent sur les propriétés physico-chimiques des lipoplexes afin d'obtenir des lipoplexes reproductibles et appropriés à la transfection des DC.

• Transfection des cellules CHO-S dans une plateforme microfluidique à l'échelle de la cellule unique:

Évaluez la manière dont les lipoplexes au différent chargement d'ADN influencent sur la transfection transitoire des cellules CHO-S par l'analyse de cellules individualisées.

3. Organization de la thèse

La thèse est organisée en six chapitres, comme décrit ci-dessous. Les résultats expérimentaux ont été présentés sous forme des articles scientifiques (Chapitre III et IV) qui seront soumis à des revues internationales, selon le contenu abordé. Par conséquent, les sections: introduction, matériel et méthodes, résultats et discussion et conclusion; de chaque partie de la thèse sont inclus dans les articles scientifiques de leur respectif chapitre.

- *Chapitre I* – Introduction

- *Chapitre II* – Revue de littérature

Ce chapitre présente une vision globale de la thérapie génique, des liposomes cationiques, de la microfluidique, des systèmes microfluidique de gouttes et leur application dans la synthèse des lipoplexes et dans la transfection des cellules de mammifères *in vitro* dans l'approche de cellules individualisées. Le texte a été adapté à partir d'un chapitre du livre ("Trends on microfluidic liposome production through hydrodynamic flow-focusing and microdroplet techniques for gene delivery applications") et d'un article de révision ("Droplet-based microfluidic systems for production and transfection *in vitro* of non-viral vectors for gene delivery ") publiés au cours de la thèse, avec Micaela Tamara Vitor comme co-auteur.

- *Chapitre III* – Droplet Microfluidic-Assisted Synthesis of Lipoplexes for DC Transfection

Ce chapitre montre l'application d'un système microfluidique de gouttes pour étudier la complexation des liposomes cationiques EPC/DOTAP/DOPE avec l'ADN pour obtenir des lipoplexes reproductibles et appropriés à la transfection des cellules dendritiques. À cette fin, certains paramètres expérimentaux ont été étudiés, tels que les débits d'entrée et les propriétés physico-chimiques des liposomes cationiques après le microsystème de gouttes. Avec le système fonctionnant avec un rapport débit aqueux/huile 0,25, les gouttes ont été formées avec une taille de 1,5 fois du canal de serpentin. Les liposomes cationiques maintiennent leurs propriétés après le traitement, même avec un résidu de tensioactif dans la phase aqueuse. Ensuite, les caractéristiques des lipoplexes ont été étudiées en fonction du rapport molaire de charge ($R_{+/-}$) et de la géométrie de la micropuce. Une condition optimale de synthèse des lipoplexes a été obtenue en utilisant le système microfluidique de goutes avec un canal serpentin large et une région de séparation, fonctionnant au rapport débit aqueux/huile 0,25 et dans les rapports molaire de charge $R_{+/-}$ 1,5 ; 3 ; 5 ; 7 et 10. Ensuite, ces lipoplexes ont été évalués dans leur capacité à transfecter les cellules dendritiques *in vitro*, lors de l'activation des cellules. La meilleure efficacité de transfection a été obtenue avec lipoplexes $R_{+/-}$ 10 qui ont également activé les DCs, un effet important pour les applications immunologiques.

- *Chapitre IV* – Tracking the Heterogeneities of CHO Cells Transiently Transfected on a Chip

Ce chapitre montre l'utilisation d'une plateforme universelle pour transfecter de cellules CHO-S en utilisant lipoplexes au différent chargement d'ADN ($R_{+/-}$ 1,5; 3; 5). En vue d'optimiser les rendements de production de protéines recombinantes dans la transfection transitoire, les hétérogénéités de la population CHO-S ont été explorées par l'analyse de cellules individualisées fournie par la plateforme. La cinétique de production de GFP a révélé la présence d'une sous-population produisant des niveaux significativement élevés de protéines recombinantes. Ces

cellules hautes productrices (HP) ont montré une augmentation de la taille par rapport à la population moyenne, ce qui suggère qu'elles étaient dans le cycle de division cellulaire. Lipoplexes avec une charge positive et moins d'ADN ($R_{+/-}$ 5) ont produit plus de HP. Lipoplexes avec une charge négative et plus d'ADN ($R_{+/-}$ 1,5) ont augmenté la productivité spécifique de GFP des HP.

- *Chapitre V* – Conclusions

- *Chapitre VI* – Perspectives

ANNEXE I – Vecteurs plasmidiques

ANNEXE II – Etudes préliminaires dans le système microfluidique de gouttes pour synthétiser les lipoplexes

L'étude des débits sur la formation de gouttes dans une émulsion eau / huile en utilisant des réactifs moins coûteux et l'étude de la formation de liposomes cationiques dans différents diluants afin d'obtenir des nanoparticules ayant des caractéristiques physico-chimiques requises pour la transfection des cellules dendritiques.

ANNEXE III – Etudes préliminaires dans le système microfluidique de gouttes pour transfecter les cellules CHO-S

Avant d'atteindre le système présenté au Chapitre III pour transfecter les cellules CHO-S, d'autres cellules et d'autres microdispositifs ont été explorés. Ils n'ont pas été utilisés pour écrire l'article scientifique en raison de la faible viabilité ou efficacité de transfection. Par contre, la micropuce a montré son potentielle dans la compréhension des paramètres clés qui influent sur le processus de transfection des cellules de mammifères *in vitro*, et à cause de cela, les expériences ont été présentées dans cette annexe.

4. Références

1. Guang Liu W, De Yao K. Chitosan and its derivatives—a promising non-viral vector for gene transfection. J Control Release. 2002;83(1):1–11.

2. Verma IM, Weitzman MD. Gene therapy: twenty-first century medicine. Annu Rev Biochem. 2005;74:711–38.

3. Miller AD. Cationic liposomes for gene therapy. Angew Chemie Int Ed. 1998;37(13–14):1768–85.

4. Serikawa T, Kikuchi A, Sugaya S, Suzuki N, Kikuchi H, Tanaka K. In vitro and in vivo evaluation of novel cationic liposomes utilized for cancer gene therapy. J Control Release. 2006;113(3):255–60.

5. Kim J, Hwang I, Britain D, Chung TD, Sun Y, Kim D-H. Microfluidic approaches for gene delivery and gene therapy. Lab Chip. The Royal Society of Chemistry; 2011;11(23):3941–8.

6. Kintses B, van Vliet LD, Devenish SRA, Hollfelder F. Microfluidic droplets: new integrated workflows for biological experiments. Curr Opin Chem Biol. 2010;14(5):548–55.

7. Hsieh AT-H, Hori N, Massoudi R, Pan PJ-H, Sasaki H, Lin YA, et al. Nonviral gene vector formation in monodispersed picolitre incubator for consistent gene delivery. Lab Chip. The Royal Society of Chemistry; 2009;9(18):2638–43.

8. Bringer MR, Gerdts CJ, Song H, Tice JD, Ismagilov RF. Microfluidic systems for chemical kinetics that rely on chaotic mixing in droplets. Philos Trans R Soc London A Math Phys Eng Sci. The Royal Society; 2004;362(1818):1087–104.

9. Lin B. Microfluidics: technologies and applications. Springer; 2011.

10. Song H, Tice JD, Ismagilov RF. A Microfluidic System for Controlling Reaction Networks in Time. Angew Chemie Int Ed. WILEY-VCH Verlag; 2003;42(7):768–72.

11. Zheng B, Tice JD, Ismagilov RF. Formation of droplets of alternating composition in microfluidic channels and applications to indexing of concentrations in droplet-based assays. Anal Chem. 2004;76(17):4977–82.

12. Brouzes E, Medkova M, Savenelli N, Marran D, Twardowski M, Hutchison JB, et al. Droplet microfluidic technology for single-cell high-throughput screening. Proc Natl Acad Sci. 2009 Aug 25;106(34):14195–200.

13. Bowles R, Patil S, Pincas H, Sealfon SC. Optimized protocol for efficient transfection of dendritic cells without cell maturation. JoVE (Journal Vis Exp. 2011;(53):e2766–e2766.

14. De Haes W, Van Mol G, Merlin C, De Smedt SC, Vanham G, Rejman J. Internalization of mRNA lipoplexes by dendritic cells. Mol Pharm.

2012;9(10):2942–9.

15. Barbuto JAM, Ensina LFC, Neves AR, Bergami-Santos PC, Leite KRM, Marques R, et al. Dendritic cell–tumor cell hybrid vaccination for metastatic cancer. Cancer Immunol Immunother. Springer Berlin / Heidelberg; 2004;53(12):1111–8.

16. Hsieh AT-H, Pan PJ-H, Lee AP. Rapid label-free DNA analysis in picoliter microfluidic droplets using FRET probes. Microfluid Nanofluidics. 2009;6(3):391–401.

17. Lindstrom S, Andersson-Svahn H. Overview of single-cell analyses: microdevices and applications. Lab Chip. The Royal Society of Chemistry; 2010;10(24):3363–72.

18. Sims CE, Allbritton NL. Analysis of single mammalian cells on-chip. Lab Chip. The Royal Society of Chemistry; 2007;7(4):423–40.

19. Schaerli Y, Hollfelder F. The potential of microfluidic water-in-oil droplets in experimental biology. Mol Biosyst. The Royal Society of Chemistry; 2009;5(12):1392–404.

20. Clausell-Tormos J, Lieber D, Baret J-C, El-Harrak A, Miller OJ, Frenz L, et al. Droplet-Based Microfluidic Platforms for the Encapsulation and Screening of Mammalian Cells and Multicellular Organisms. Chem Biol. Cell Press; 2008;15(5):427–37.

21. Subramanian S, Srienc F. Quantitative analysis of transient gene expression in mammalian cells using the green fluorescent protein. J Biotechnol. 1996;49(1):137–51.

22. Derouazi M, Girard P, Van Tilborgh F, Iglesias K, Muller N, Bertschinger M, et al. Serum-free large-scale transient transfection of CHO cells. Biotechnol Bioeng. 2004;87(4):537–45.

Chapter II – Literature review

The literature review text was adapted from the book chapter and the review article co-authored by Micaela Tamara Vitor

De La Torre LG, Balbino TA, Sipoli CC, Vitor MT, Oliveira AF. Trends on Microfluidic Liposome Production through Hydrodynamic Flow-focusing and Microdroplet Techniques for Gene Delivery Applications. In: Finney L, Eds. Advances in Liposomes Research. New York: Nova Science Publishers; 2014. ISBN: 978-1-63117-074-4.

Vitor, M. T., Sipoli, C.C., & De La Torre, L.G. (2015). Droplet-based Microfluidic Systems for Production and Transfection In Vitro of Non-Viral Vectors for Gene Delivery. Journal of Pharmacy and Pharmaceutical Sciences, 4(4), 1-17.

1. Introduction

Gene delivery is a promising technique that involves the insertion of nucleic acid inside target cells for curing a disease or at least improving the clinical status of a patient (1). One important step of gene therapy is the transfection process that introduces foreign nucleic acids into cells to produce genetically modified cells (2). In this context, the development of delivery systems capable of efficient and safe gene transfer (3), while protecting the genetic material from different barriers (extracellular matrix, cell membrane, cytosol, nuclear membrane) (4), is necessary. Among the delivery systems, cationic liposomes stand out due to their reproducibility, safety of use, biocompatibility and biodegradability (5). However, besides the promising results of cationic liposomes, the development of methods to insert nucleic acids into cationic liposomes in a control and reproducible way is still a challenge. Depending on cell lines, the production of lipoplexes with specific physico-chemical properties is required for transfection (6).

On the other hand, microfluidics, technology that manipulates small amounts of reactants inside microchannels, appears as a powerful strategy to overcome these drawbacks (7). The microenvironment of microfluidic systems allows precise control and optimization of multiple processes and techniques used in gene therapy (8). Moreover, droplet-based microfluidic systems define microreactors that reduce of many orders the volume manipulated, being attractive for molecular biology assays (9). Droplets moving in some microfluidic systems with specific geometry become micromixers that provide a rapid mixing of reagents (10). Droplet-based microfluidic systems can be also used to transfect cells *in vitro*. Since microfluidics generates extremely uniform droplets, they are appropriate for single-cell encapsulation and/or for *in vitro* expression of single genes (11). Molecules secreted by cells are fast detected due to the low volume surrounding each cell, allowing investigation of transfection parameters in culture real time (9,12).

In this literature review, first we present an overview about gene therapy and the role of non-viral vectors. Then, we show the state-of-the-art of current microengineering methods based in droplet microfluidic platforms for the

production of lipoplexes and mammalian cell transfection. The understanding of this technology and how fluid dynamics influences the microscale for the production of controllable and stable droplets give the insight to understand how to form complexes for gene delivery applications. At last, we show methods of transfection inside droplets comparing with the conventional transfection in wells.

2. Nanoparticles as non-viral vectors for gene delivery

Gene therapy refers to the transfer of genetic material encoding a therapeutic gene of interest into a cell, tissue, or whole organ with consequent expression of the transgene in order to treat a disease. However, for the success of gene therapy, the development of sophisticated and efficient delivery systems capable of transfering genes is a key factor (3,13). In brief, we can describe two classes of efficient nucleic acid carriers: viral and non-viral vectors. These delivery systems should protect nucleic acids from degradation, while providing a safe intracellular delivery (14). Over a decade ago, patients with immunodeficiency-X1 were treated with gene therapy assays based on the use of cDNA in a retrovirus (15,16). After that, gene therapy based on retrovirus vector was used to treat French patients with T cell leukemia, producing aberrant transcription and expression of LMO2 (17). These facts opened an optimistic vision about gene therapy research. Nowadays, gene therapy clinical trials are present in worldwide, mainly in United States of America (62.6%), United Kingdom (10.3%) and Germany (4.1%). These therapies are usually used in the treatment of cancer (63.8%), monogenic diseases (8.9%) and infectious diseases (8.2%) (18). The most commonly vectors used in gene therapy are still virus vectors, highlighting adenovirus (22.5%) and retrovirus (18.8%), but also lipofection (5.2%) and naked pDNA (17.5%) are raising their use (18). Notwithstanding the high efficient transfection provided by viral vectors, they can invoke immune responses or proto-oncogene activations. In this context, the non-viral vectors, particularly cationic liposomes, have a promise and potential future, taking into account their reproducibility and safety of use (5).

Cationic liposomes are non-viral vectors mainly composed of cationic lipids, which guarantee their positive superficial charge. Examples of synthetic cationic

lipids used in cationic liposome composition are DOTAP (1,2-dioleoyl-3-trimethylammonium propane), DOTMA (2,3-bis(oleyl)oxypropyl-trimethylammonium chloride), DDAB (dimethyl dioctadecyl ammonium bromide), DC-Chol (3 β [*N-(N',N'*-dimethylaminoethane)-carbamoyl]cholesterol), DMRIE (*N*-(2-hydroxyethyl)-*N,N*-dimethyl-2,3-bis(tetradecyloxy)-1-propanaminium bromide), DOGS (dioctadecyl amino glycyl spermine), DOSPA (2,3 dioleyloxy-*N*-[2(spermine carboxaminino)ethyl]-*N,N*-dimethyl-1-propanaminium trifluoroacetate). However, the use of cationic lipids can generate cell toxicity, and so the inclusion of others lipids, *e.g.* egg phosphatidylcholine (EPC), in cationic liposome composition is required to decrease the cytotoxicity (19,20). On the other hand, the positive charge of cationic liposomes provides an electrostatic interaction with negatively charged nucleic acids, forming complexes with net positive charge (21). Hence, these positive charged complexes can enter easily inside cells, whose surface membrane is negatively charged (22). Once into cells, the complexes should release the nucleic acids in cytosol, in case of RNA for rapid synthesis of a target protein (23), or in cell nucleus, in case of DNA to control gene expression for a more long-term. The inclusion of helper lipids, *e.g.* phosphatidylethanolamines (DOPE), in cationic liposomes composition facilitates the nucleic acid to escape inside the cytosol (24). Felgner *et al.* (22) were pioneers in the development of cationic liposomes for gene delivery. They produced liposomes composed of 1:1 ratio of DOTMA and DOPE, which were then commercialized as Lipofectin. For example, these cationic liposomes were used *in vitro* to carrier efficiently hepatitis C virus proteins into a human hepatocyte cell line (HUH7) (25) and *in vivo* to delivery linamarase gene for the treatment of brain tumors in animals or humans (26). Recently, other commercial cationic liposomes, such as Lipofectamine, DMRIE-C, Oligofectamine, Ambion, 293fectin, Optifecta, Invivofectamine, FuGENE, TransFast, TransFection and CLONfectin, are being used in gene therapy due to their well-established protocols and to provide high efficiency of transfection in some specific cells and with some specific nucleic acids. Our research group (27) also showed the feasibility of dehydrated-rehydrated liposomes composed of EPC, DOTAP and DOPE (50/25/25% molar, respectively)

carrying polynucleotides encoding HSP65, for prevention and treatment of tuberculosis. And more recently, we obtained the same cationic liposomes produced in a large scale by ethanol injection method to delivery nucleic acid into dendritic cells (DCs) as a potential tool for cancer immunotherapy (28).

Dendritic cells are professional antigen-presenting cells widely used in immunotherapeutic approaches, particularly in immunotherapies against cancer. Since loaded with tumor antigens, mature DCs can induce an immune response against cancer by recruiting patients' immune system (29). Different strategies are currently used to load DCs with antigens, *e.g.* peptide pulsing, pulsing with tumor cell lysates, infection with viral vectors, direct nucleic acid loading, or ingestion/fusion with tumor cells (30). Moreover, cationic liposomes stand out in this function as gene carriers, since besides to transfect DCs, they can also activated them (31). Particularly, our research group (32,33) showed that cationic liposomes EPC/DOTAP/DOPE were uptake by DCs, while providing cells stimulation/activation. However, dendritic cells require that these cationic liposomes have a very specific properties (size < 100 nm and polydispersity <0.2) to be internalized (32), due to the use of macropinocytosis and/or phagocytosis as transfection pathways (34). Thus, the study of methodologies that enable to form lipoplexes modulated to specific cells lines in a reproducible and controllable way is very important (35). Conventional methods of obtaining lipoplexes involve just the mixing provided by hand shaking or vortexing to reach cationic liposomes complexation with nucleic acids. However, these conventional methods introduce variability in lipoplexes formation and, as a result, provide inconsistent transfection efficiencies (6). To effectively transfect cells, the physico-chemical properties of lipoplexes should be suitable to the pathway used by the cell line to internalize nanoparticles (36).

3. Microfluidic droplet technologies

The general concept of microfluidics is in the manipulation of small amounts of reactants inside microchannels with the capability to control and manipulate molecules in space and time (37). In microfluidics it is possible to work with small

amounts of reactants, the period of reactions is short, it is possible to work with parallel operations (38), large surface to volume ratio allows fast diffusion of compounds and fast mass/heat transfer (39). These advantages can be related to the flow in microfluidic devices, which is laminar and corresponds to a low Reynolds number (37,40). Another important consequence of this regime is that the mixture between two parallel flowing streams occurs mainly by diffusion (38).

The origin in microfluidic is in the 90´s for MicroElectroMechanical Systems area (MEMS) (39). Nowadays microfluidics has been exploited in numerous areas as:

Biological analyses - detection of biomolecules (41,42), manipulation and amplification (43) and separation of DNA by capillary electrophoresis (44).

Microbial growth - Screening of variables and kinetic parameters (45,46).

Nanoparticles production – polymeric particles (47,48), liposomes and lipid vesicles (49–51), metallic nanoparticles (52).

Gene Delivery/Transfection – electroporation (53), hydrodynamic force and optical energy (8).

Different materials can be used for the construction of microchannels and, for biological application, glass and polymers are detached (54). Glass is considered to be biocompatible, impermeable to gases (54,55), has physic and chemical stability and it is hydrophilic (54). The techniques to prepare microdevices in glass are laser ablation and wet etching (54). Microdevices can also be made by polymers which are not expensive, there is the possibility to change the chemical formulation (55), are stable (37) and hydrophobic (54). The elastomer which has been used extensively for microdevices construction is poly(dimethyl syloxane) well-known as PDMS , moreover the technique employed is soft lithography (56).

In addition, it is important to consider the wettability related to the microchannel material and the droplet system. Since the continuous phase wets the walls faster than the disperse phase and forms a thin film between droplet and walls (57). The droplet breakup occurs when the continuous phase wets the device walls instead the disperse phase, thus the droplet morphology is a result of the interaction between the material which the devices is formed and the continuous

phase (57). Summarizing hydrophobic channels are required to prepare water in oil systems, inversely hydrophilic channels are necessary for forming oil in in water emulsions (58). Considering the advantages of using PDMS for devices construction, in the literature different strategies are reported to change the wettability of the material, through chemical modifications (58,59).

Microfluidic systems can be classified according to the interfaces created by the fluid flows in microchannel as: pinned interfaces, in which fluids flow in parallel creating vertical interfaces, and floating interfaces, in which immiscible fluids produce droplets of precise shape (60). The use of segmented flow which the reactants are separated in different picoliter/nanoliter droplets has been used in cases when miniaturized systems has to be achieved (61). The segmented flow is the principle of emulsions which are a metastable colloidal systems (62) with two immiscible liquids. In this case there is one continuous phase and one disperse phase in droplets formats (57,61). Some advantages of droplet processes can be described in comparison with parallel flows processes. In parallel flows, in which solute are all distributed over the solvent, the efficiency of chemical reactions and the detection of some molecules inside the channels can be decreased, this phenomenon is called Taylor-Aris dispersion (63,64). The use of droplets processes cut out the contact with solid wall, reducing the probability of reagents adsorption into the channels walls (64). Droplets with samples inside can be seen as micro-reactors which allows the manipulation of small volumes (14,65). In addition, in droplets microfluidics it is possible to carry out many reactions without increasing the number and the channels size (13). Furthermore, considering the relation between the surface area and volume, the reactions inside droplets are faster because the heat and mass transfer times and also diffusion distances are shorter (13,66).

In order to form stable droplets, the use of appropriated surfactants is important. Surfactants are known as amphiphilic molecules with different groups and having affinity for different phases which are immiscible. Due to different groups in the structure, surfactant molecules go to interface and as a result the surface tension between the phases decreases (67). An essential requirement to

use droplets as microreactors is to avoid the coalescence of them. Thus the surfactant addition provides stabilization in the metastable state (62,67). Furthermore choose biocompatible surfactants is the rule for the success of droplet system application in biological fields (67). Fluorinated oils are promising to be used in biotechnology area; however few surfactants are available to stabilize water in oil interfaces emulsions (67). Different molecules are being studied and developed to microfluidic applications. Nowadays, block copolymer of perfluoropolyether and polyethylenoxide are the most interesting molecules existent. It is known that these molecules reduce protein adsorption or the interactions with cell membranes (67). Another important molecule is a triblock copolymer surfactant composed of perfluoropolyether (PFPE) and polyethylene glycol (PEG) blocks (68). However the problem is the limitation of surfactant modification which can be just by varying the molecular weight or chain-end functionalization. In this way, Wagner *et al* (68) proposed to synthetize and characterize polyglycerol-based triblock surfactants, and exemplified in droplet-based microfluidics their application in cell encapsulation and *in vitro* gene expression studies.

The droplet compartments formed in microfluidic systems have many functions. The uniformity and the little volume of these droplets allow them to be used for quantitative assays requiring reduced volumes of reagents, and as a result, providing a low cost for this technique (69). Moreover, droplets compartment design can furnish combined information about molecules function (activity or inhibitory functions), molecules identity and molecules ability to carry out its function by measuring, for example, a fluorescence product. In addition, droplets give the possibility to make several unit operations in a device, like droplets can be divided, fused, incubated, analyzed, sorted and broken up (70). Moreover, the compartments formed by droplets can be used as micromixers, providing efficient and controlled mixing over the reactants inside microcontainers (66).

4. Droplet-based microfluidic platforms for lipoplexes formation

The control and rapid mixing of reagents within droplet-based microfluidic systems (micromixers) can be used, for example, to make an effective complexation between nucleic acids and liposomes in order to form lipoplexes (35). Microsystems using parallel flows, the mixing is promoted mainly by the diffusion of reactants (31). In contrast to this, microdroplets devices can add a chaotic advection contribution to the system, increasing the promoted mixing. For example, serpentine channels can generate two recirculation flows within droplets due to the shear created between the droplets and channel wall (31) (Figure 2.1). For this, droplets should have a precise size to touch the inner surface channels and generate a fluid movement relative to the stationary walls of serpentine channel (10). On the whole, micromixers can be classified as passive and active. The passive micromixers require the use of different microchannel geometries and/or liquid flow rates to generate mixing (54). On the other hand, active micromixers demand an external energy to enhance the mixing, such as pneumatic or mechanical vibration (71). Active mixers require more complex fabrication processes and they are more difficult to integrate with other microfluidic components. The passive mixers usually adopt longer mixing channels without external agitation (72).

Nevertheless, some parameters of the system have to be taken into account to provide an effective mixing within droplets. One of the most important parameter is capillary number (Ca), which should be low in order to form droplets in the system (73). The Ca is proportional to the average flow velocity (U) and inversely proportional to the interfacial velocity (γ/μ_C, where γ is the surface tension between two immiscible phases and μ_C is the dynamic viscosity of continuous phase). Hence, when the flow velocity is much lower, Ca is reduced and the surface tension controls the system. In high Ca, the shear force dominates (73). As consequence, the viscosity of fluids is another parameter that interferes in interfacial velocity and in droplets mixing (74). Tice *et al.* (74) concluded that combination of viscous and non-viscous fluids promotes a more efficiently mixing inside droplets than the use of only non-viscous fluids. Thus, the use of fluids with

approximated viscosities decreases the interfacial velocity of the system, inducing a decrease in droplets mixing (74). Moreover, the channel configuration is also fundamental in a good mixing within droplets. The channel width is often used to control the local flow velocity, when the channel depth and flow rate being kept constant (75). Furthermore, microsystems should be operate in a Peclet number between 1000 times and 100,000 times greater than Reynolds for a good mixing (76). According to the Peclet number, it is possible to determine if the convection mixing (UL, where L is a characteristic length scale) or the diffusion mixing (D, where D is a characteristic diffusion coefficient) dominates in the system (77).

Besides setting operational parameters in the droplet microfluidic system, to achieve a chaotic mixing in passive micromixers, especial geometries, such as serpentine channels outlined in Figure 2.1, can be adopted (77). Chaotic advection provides an accelerated mixing within droplet-based microfluidic devices, stretching and folding the fluid into droplets as long as they pass in these channels (40). Droplets moving downstream and upstream in serpentine channels offer an alternating motion time periodically influenced by the walls, creating fluid vortexes (40). In brief, the mechanism can be explained as follows: the part of droplet in contact with the outside arc of the channel prompts greater contact between the interface of the droplet and the channel wall, leading to a longer recirculation flow; on the other side, part of droplet in contact with the inner arc of the channel prompts smaller shear, leading to a smaller recirculation flow (13). This process repeats along the channel, in such a way that recirculating flows vary alternately on each side of the drop, generating a chaos within it (13). Passive micromixers with chaotic advection have a promising future in microfluidic field, since they allow an effective mixing on a millisecond scale without requiring moving parts in devices (76).

The chaotic mixing in droplet-based microfluidic devices have various applications such as: controlling chemical reactions (40), promoting protein crystallization (73) and improving biochemical analysis (78). Among the applications, we can emphasize the complex formation between nucleic acids and liposomes (Figure 2.1) as an essential step in gene delivery process.

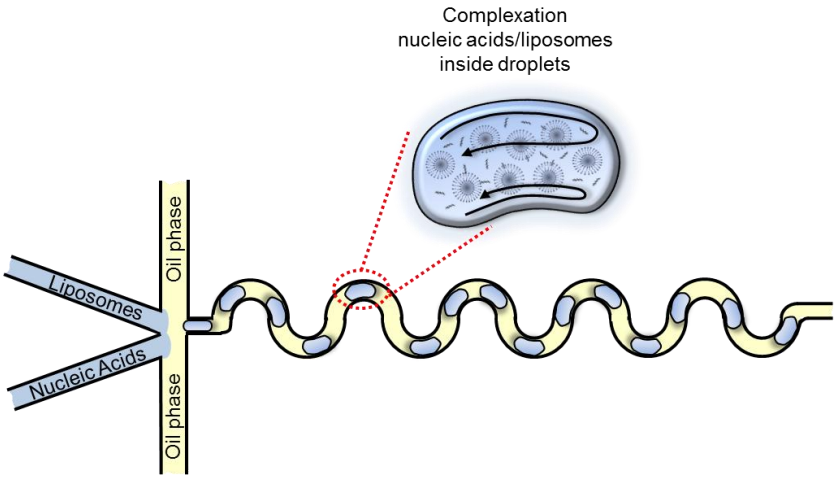

Figure 2.1 - Scheme of liposomes complexation with nucleic acids within droplets in a droplet-based microfluidic system. Arrows represent flow within droplet.

It is well known that cationic liposomes (positively charged) spontaneously make complexes with nucleic acids (negatively charged) by electrostatic complexation, which can be formed simply by agitation, e.g. hand-shaking or vortexing (22). However, the complex cationic liposomes/nucleic acids obtained in these processes are commonly not reproducible and exhibit high size and heterogeneous population, reflecting in lipoplex uptake by cells (35). Depending on the strategy used by cells to internalize lipoplexes, such as by endocytosis process (79), complexes showing small size (smaller than the endosome diameter that is about 200 nm) (80) and narrow size distribution (polydispersity values below 0.2) (81) are requested.

In this context, researchers have been exploring the use of droplet-based microfluidic systems to obtain complexes with low size and polydispersity for gene delivery applications. For example, Ho *et al.* (82) showed microfluidics-assisted confinement in picoliter droplets to control electrostatic self-assembly between pDNA encoding GFP and polymeric reagents. They obtained complexes with approximately 300 nm in size and 0.12 of polydispersity by microfluidics, in contrast with approximately 400 nm in size and 0.16 of polydispersity of complexes obtained by the bulk method (82). *In vitro* assays with HEK293 cells showed that nanocomplexes produced in droplet-based microfluidic devices presented narrower size distribution, lower cytotoxicity, and higher transfection efficiency compared to those produced by the bulk method (82). Particularly in lipoplexes field, Hsieh *et al.*

(35) developed a picoliter incubator based on the microfluidic system, which was used to constantly and uniformly mix the cationic liposomes (Lipofectin composed of DOTMA and DOPE) with pEGFP-C1 DNA vector in a serpentine mixing region. The major part of the complex population generated in the microfluidic system presented size of approximately 200 nm and polydispersity index between 0.4 and 0.45. On the other hand, hand-shaking generated a polydisperse complex exhibiting nearly three populations, one with approximately 300 nm in size, another with 700 nm and a third with 900 nm (35). Comparing the transfection efficiencies of the two complexes through GFP expression by U2OS cells, they concluded that complexes prepared in the microfluidic system provided more consistent gene transfection (coefficient of variation of 0.05) than complexes prepared by hand-shaking (coefficient of variation of 0.30) (35). Therefore, the employment of a passive chaotic mixing in droplet-based microfluidic devices aiming at the nucleic acid incorporation in liposomes has a promising future.

5. Droplet-based microfluidic platforms for *in vitro* transfection

Besides the use for lipoplexes formation, droplet-based microfluidic platforms can be used to transfect cells *in vitro*. Transfection, the procedure to introduce nucleic acids into cells, can be used to study gene and protein function and regulation (2). Thus, cells are commonly transfected in culture systems on well plates for then be inserted *in vivo* (83,84) or only be analyzed *in vitro* (85). Briefly, there are three transfection methods: physical, biological and chemical, which are chosen according to cell type and purpose (2). Physical-mediated methods are comprised of microinjection (86), biolistic particles delivery (87), electroporation (88), optical gene transfection (89), sonoporation (90) and magnetic nanoparticles (91). Biological methods include those with virus as vector (92), chemical methods consist of lipid and polymeric vectors (93,94) and calcium phosphate (95). Transfection method is chosen in order to have high transfection efficiency, with safety, reproducibility, low cytotoxicity and should be easy to use (2).

Although, when studying cellular uptake of nanoparticles for *in vitro* transfection, usually the physiologically relevant stimulus of fluid flow is overlooked

and internalization assays are carried out under static conditions. But, both in theory (96) and practice (97), it has been shown that the mechanical stimulus of fluid flow is an important factor to achieve an optimal transfection efficiency (98). In conventional transfection methods performed in wells, there is only diffusive transport of nanoparticles to the cellular targets surface. In microfluidic systems, a convective contribution can be added to the process, increasing the collision rate between nanoparticles and cell surface, and consequently, showing more controllable and easier transfection (99).

Thus, droplet-based microfluidic devices can be used for *in vitro* transfection, in which one droplet defines a picoliter compartment that allows single cell encapsulation and *in vitro* expression of genes, using fewer reagent than conventional methods (11). Microfluidic environment also offers unique possibility to mimic dynamic conditions, opening new possibilities to investigate. So, processes and techniques used in gene delivery, such as used in physical methods, can be better controlled and optimized in the micro-scaled environment (8). To summarize, we made a comparative table showing differences between both, conventional transfection in wells and in microfluidic systems (Table 2.1).

Table 2.1 - Comparative table summarizing differences between *in vitro* transfection by conventional transfection in wells and by droplet-based microfluidic systems.

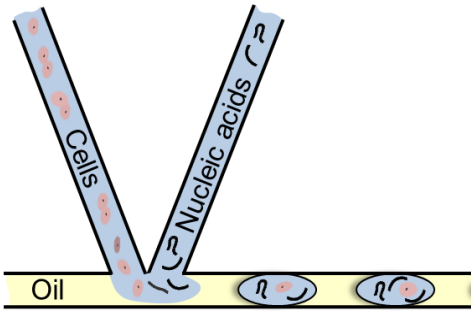

	Conventional transfection in wells	**Droplet-based microfluidic systems**
Operation	Fast and easy	Slow (employ low flows) and require microfluidic knowledge
Reagents	Large quantity	Little quantity
Accuracy	Detect only large quantities of biomarkers	Able to detect little quantities of biomarkers
Transfection efficiency	Measured at the end	Real-time measurement
Nucleic acids transport to cells	Diffusion	Diffusion and chaotic advection
Analysis	Cell population	Single cell

Microfluidics, and more specifically, cell transfection inside microchannels for parameters analysis, is a current topic. As a result, in the last decade, many patents involving these issues were filed. For example, cells can be merged in microfluidic devices developed for handle cell with electroporation and electrofusion (100,101) or they can be analyzed and sorted individually by measuring the signal of an optical-detectable molecule (102,103). Thus, the integration of these steps can create a biological environment similar to those presented on macroscopic scale, but with advantageous engineering features of the microscopic format. Like explained previously, droplet microfluidics provides some advantages that are particularly important for *in vitro* cell transfection such as: the laminar flow behavior that improve heat and mass transfer phenomena (9),

the higher sensibility for biomarker that amplify the detection of extremely low levels of biomarker molecules (12,104), the rapid mixing of reagents in case of droplets applied as micromixers in which a chaotic advection contribution can be added to the system (40,104), the compartmentalization that reduces the interaction of reagents from different droplets and let an easy parallelization of independent experiments (14).

From the point of view of the *in vitro* transfection, droplets in microfluidic systems can be applied as single cells compartment. Some patents have been published about cells encapsulation one by one in droplets, independent of cells densities (105). Or also encapsulate cells in nested labeled matrices, which can be compared to cell tissues, enabling to track or identify different cell populations (106). Thus, in a similar way to molecule assays, single cells analysis in this type of system allows a rapid detection of cell-secreted molecules, due to the low volume surrounding each encapsulated cell. Moreover, as the risk of cross-contamination decreases, cells can be analyzed by various techniques mainly by fluorescence detection (12). Furthermore, fluorescence detection can be applied for both adherent and non-adherent single cells, enabling the manipulation of isolated single cells and also the investigation of contents from disrupted single cells (107). For example, Huebner *et al.* (108) described the preparation of microdroplets containing few or individual cells to detect fluorescent protein expression by cells while measure droplet size, fluorescence and cell occupancy. Equally important is the possibility to carry out spot-checks of single cells in the time courses, since the response of cell population at the end, not always describes the behavior of a single cell in certain times (9). This technology lets us to obtain more data about transfection characteristics, like the real point when transfection started, the ideal cell lines to be used in a transfection with a specific nucleic acid and delivery system. To verify the potential utility of this technique, Schmitz *et al.* (109) used drop spots devices to monitor the levels of β-galactosidase in a population of single yeasts using the reporter enzyme fluorescence technology and also to monitor yeast growth rates. Boedicker *et al.* (110) showed another important application for this technique: rapid detection and drug susceptibility screening of bacteria in

samples without pre-incubation, that can likely generate rapid and effective patient-specific treatment of bacterial infections. They determined the antibiogram of methicillin-resistant *Staphylococcus aureus* (MRSA), an antibiotic sensitivity strain, against many antibiotics. They measured the minimal inhibitory concentration (MIC) of the drug cefoxitin against MRSA and also signalized sensitive and resistant strain of *S. aureus* in complex samples, like human blood plasma (110).

On the other hand, hydrogel droplets can be used to mimic *in vitro* multicellular organisms providing a 3D microenvironment for adherent and non-adherent mammalian cells. In contrast to vast majority of *in vitro* cell biology studies, which are performed using cell monolayers cultured on flat substrates, 3D microenvironment recapitulates the architecture of living tissues and involves a dynamic interplay between biochemical and mechanical signals provided by the extracellular matrix (ECM), cell–cell interactions and soluble factors (111,112). These hydrogel droplets, composed by natural or synthetic polymers, should provide cells attachment and proliferation (113). Adherent cells need relatively resistant substrates, like collagen, to anchor and pull on their surroundings, since they are dependent on myosin-based contractility and cellular adhesion (114). Moreover, hydrogels can be engineered to promote efficient gene transfer with non-viral vectors (115) and can be also used to investigate cellular pathways to internalize nanoparticles (116). Dhaliwal *et al.* (115) identified extracellular matrix (ECM) proteins and their combinations as a microenvironment that significantly enhance mouse mesenchymal stem cells (mMSCs) transgene expression. They showed that proteins that enhanced cell proliferation and spreading, increased cell gene expression as well (115). Additionally, studying transgene expression pathway, Dhaliwal *et al.* (117) showed that RhoGTPases, which mediate the crosstalk between cell and fibronectin (structural component of ECM), regulate internalization and effective intracellular processing of nanovectors, resulting in efficient gene transfer.

However, there are some drawbacks that have to be taken into account before encapsulate cells, particularly when using robust analysis over longer periods of time, like how to maintain viability of cells within the droplets, risks of

coalescence, nutrient depletion or the accumulation of toxic metabolites (12). Thus, to minimize these obstacles by preventing droplet coalescence, biocompatible surfactant-oil formulations that allow oxygen diffusion and prevent molecules leaking out into the oil phase have been developed (118–123). Clausell-Tormos *et al.* (118) demonstrated the feasibility of using this strategy for long periods by culturing adherent and non-adherent mammalian cells into aqueous microdroplets of water-in-oil emulsion systems for up to two weeks. They applied the technique of spot-checks to analyze cells viability in the device and they also broke the emulsions to recover cells after a couple of days.

In the case of microfluidic droplets, that involves immiscible phases, other important topics to be considered are the dominant physical mechanisms related with microfluidic scales, such as surface tension and diffusion. Our research group (124) explored these parameters, coupled with quantitative measurements within droplets, for the purpose of advance biological science and technology. Hence, in order to keep a droplet stationary for long term observation and to provide combinatorial measurements on a single image, Fradet *et al.* (125) combined rails and anchors in microfluidic system with laser forcing, enabling the creation of highly controllable 2D droplet arrays. Additionally, in microfluidic droplet systems a more rapid mass transfer can be expected than in single-phase microfluidic systems, since the interfacial area ratio between different fluids per unit volume is larger (126). Then, Abbyad *et al.* (127) applied this rails and anchors design to control the transport oxygen for cell cultures or to induce a temporal or spatial variation of gas content in droplets, thus verifying the polymerization of intracellular hemoglobin by deoxygenating droplets that encapsulate red blood cells from patients suffering from sickle cell disease.

Furthermore, with microfluidic systems we can investigate how the shear stress induced by flow can affect the transfection efficiency. Shin *et al.* (128) described a microfluidic device to investigate shear stress effect upon transfection efficiency of liposomes/DNA complexes in primary cultured neurons, achieving 45% of transfection. Particularly in droplet-based systems, the phenomenon of mixing that accelerate mass transport inside droplets is highly studied by

computational (129–131) or experimental instruments (73,74,132). Kinoshita *et al.* (133) used a high-speed confocal micro-particle image velocimetry (PIV) to measure the droplet internal flow, concluding that a three-dimensional and complex circulating flow is formed inside the droplet. Therefore, to correlate the hydrodynamic effect of mixing inside droplets to the transfection efficiency is still a challenge, because of the complexity of circulating flow inside the droplets.

Nevertheless, droplet-based tools for single-cell analysis draw attention of many researchers for *in vitro* cell transfection, mainly due to the potential of high-throughput screening and the benefits of enclosed individual microchambers (12). Moreover, Chinese hamster ovary (CHO) cells are widely used as cell line model for this application. CHO cells are the most popular host to express stably or transiently recombinant therapeutic proteins (134). There are many advantages for using CHO cells as protein expression system (135,136). One is that regulatory agencies like the FDA tends to easier approve recombinant proteins produced from CHO cells, since this cell line showed to be safe hosts for the past two decades. Another advantage is that CHO cells are a powerful gene amplification system, which grows to high cell densities in suspension and can be easily transfected. This cell line has also the capacity to adapt to the growth in serum free media, suitable characteristic for transfection by nanovectors. At last, there are some CHO cell strains that produce recombinant proteins with glycoforms that are compatible with bioactive in humans (135,136). Additionally, to previously inquire cell lines in their ability to express recombinant proteins, the green fluorescent protein (GFP) is often used as a model assay. GFP with its small size, formidable stability and relative ease of use, can report great exploratory results before cell line use for a target protein production (137). In this context, we summarize in Table 2.2 different methods to transfect single cells using droplet-based microfluidic platforms. In these microsystems, cells are placed in contact with nucleic acids inside droplets and physic or chemical transfection methods can be used to provide nucleic acids insertion inside cells.

Table 2.2 - Description of different methods (electroporation, microinjection and nanoparticles) to provide single-cell transfection in droplet-based microfluidics platforms.

Transfection methods	Description	References
Electroporation	Delivery genes into cells by applying an external electric field, with lower voltages compared to conventional electroporation. ✓Advantage: Higher transfection efficiency ✓Disadvantage: Lower cell viability	(138), (139)
Microinjection	Microneedles are used to inject nucleic acids and others bioactive compounds into the same target single-cell. ✓Advantage: Quantitative introduction of multiple components into the same cell ✓Disadvantage: Technical skills are required to prevent cell damage	(140)
Nanoparticles	Nanoparticles as non-viral vectors for safely and reproducible gene delivery into cells. ✓Advantage: Higher cell viability ✓Disadvantage: Lower transfection efficiency	(141), (142), (143)

The most commonly transfection in droplet-based microfluidic devices is the electrotransfection, which is a method for delivering genes into cells by applying an external electric field. Due to the compartmentalization, droplet systems require much lower voltages compared to conventional electroporation, thus enabling a higher cell viability (8). Zhan *et al.* (138) demonstrated a simple microfluidic device that encapsulated cells into aqueous droplets in oil flow and then electroporated the encapsulated cells. The results showed an enhancement in delivering green fluorescent protein (EGFP) plasmid into CHO-K1, reaching approximately 11% of transfected cells. Thus, to demonstrate the potentiality of this transfection method in other cells, Luo *et al.* (139) showed that fluorescein could be introduced into yeast cells by applying a low alternating current voltage to a couple of Au microelectrodes.

Additionally, microinjection can be used to transfect cells in air-liquid droplet systems, enabling the introduction of multiple bioactive compounds, including nucleic acids, into the same target single-cells, which are difficult to handle in conventional methods (144). Thus, Lee *et al.* (140) showed the feasibility of a

microinjector by engaging a microvalve in a microfluidic device to form a droplet at the microneedle tip allowing, for example, gene delivery in single-cells.

In a similar way, nanoparticles, generally composed by biopolymers or lipids, can be used as non-viral vectors for safely and reproducible gene delivery into cells. Chen and co-workers (141) transfected CHO-K1 cells with a plasmid encoding EGFP, by a chemical stimulus, PolyFect (activated-dendrimers) complexed with pDNA, reaching 25% of transfection efficiency. We highlighted two relevant points shown in the referred work, the first important point is the necessity to use fluorocarbon oils as continuous phase due to their biocompatibility with cells and smaller loss of nanoparticles from aqueous to oil phase. The second point is that smaller droplets provide an increase in efficiency transfection probably because of a better interaction between cell and complexes (141). Likewise, Hufnagel *et al.* (142) transfected CHO-K1 cells with the same reporter gene, pEGFP, but using polyplexes as nanovectors, achieving 20% of transfection efficiency. Even though, this work approaches a modular microfluidic system that allows several operations with cells inside it, such as seeding, cultivation, manipulation, detachment, collection, encapsulation and transfection (142). Therefore, microdroplets systems for cells transfection is a promising future, since many parameters can be investigate by them in order to approximate to *in vivo* transfection conditions and also to better understand the transfection process by single-cell analysis.

6. References

1. Perrie Y, Frederik PM, Gregoriadis G. Liposome-mediated DNA vaccination: the effect of vesicle composition. Vaccine. 2001;19(23–24):3301–10.

2. Kim TK, Eberwine JH. Mammalian cell transfection: The present and the future. Anal Bioanal Chem. 2010;397(8):3173–8.

3. Verma IM, Weitzman MD. Gene therapy: twenty-first century medicine. Annu Rev Biochem. 2005;74:711–38.

4. Tavernier G, Andries O, Demeester J, Sanders NN, De Smedt SC, Rejman J. mRNA as gene therapeutic: How to control protein expression. J Control Release. 2011;150(3):238–47.

5. Serikawa T, Kikuchi A, Sugaya S, Suzuki N, Kikuchi H, Tanaka K. In vitro and in vivo evaluation of novel cationic liposomes utilized for cancer gene therapy. J Control Release. 2006;113(3):255–60.

6. Hsieh AT-H, Hori N, Massoudi R, Pan PJ-H, Sasaki H, Lin YA, et al. Nonviral gene vector formation in monodispersed picolitre incubator for consistent gene delivery. Lab Chip. The Royal Society of Chemistry; 2009;9(18):2638–43.

7. Nie Z, Xu S, Seo M, Lewis PC, Kumacheva E. Polymer particles with various shapes and morphologies produced in continuous microfluidic reactors. J Am Chem Soc. 2005;127(22):8058–63.

8. Kim J, Hwang I, Britain D, Chung TD, Sun Y, Kim D-H. Microfluidic approaches for gene delivery and gene therapy. Lab Chip. The Royal Society of Chemistry; 2011;11(23):3941–8.

9. Schaerli Y, Hollfelder F. The potential of microfluidic water-in-oil droplets in experimental biology. Mol Biosyst. The Royal Society of Chemistry; 2009;5(12):1392–404.

10. Bringer MR, Gerdts CJ, Song H, Tice JD, Ismagilov RF. Microfluidic systems for chemical kinetics that rely on chaotic mixing in droplets. Philos Trans R Soc London A Math Phys Eng Sci. The Royal Society; 2004;362(1818):1087–104.

11. Kintses B, van Vliet LD, Devenish SRA, Hollfelder F. Microfluidic droplets: new integrated workflows for biological experiments. Curr Opin Chem Biol. 2010;14(5):548–55.

12. Lindstrom S, Andersson-Svahn H. Overview of single-cell analyses: microdevices and applications. Lab Chip. The Royal Society of Chemistry; 2010;10(24):3363–72.

13. Teh S-Y, Lin R, Hung L-H, Lee AP. Droplet microfluidics. Lab Chip. 2008;8(2):198–220.

14. Song H, Chen DL, Ismagilov RF. Reactions in Droplets in Microfluidic Channels. Angew Chemie Int Ed. WILEY-VCH Verlag; 2006;45(44):7336–56.

15. Cavazzana-Calvo M, Hacein-Bey S, Basile G de Saint, Gross F, Yvon E, Nusbaum P, et al. Gene Therapy of Human Severe Combined Immunodeficiency (SCID)-X1 Disease. Science. 2000;288(5466):669–72.

16. Hacein-Bey-Abina S, Le Deist F, Carlier F, Bouneaud C, Hue C, De Villartay J-P, et al. Sustained Correction of X-Linked Severe Combined Immunodeficiency by ex Vivo Gene Therapy. N Engl J Med. 2002;346(16):1185–93.

17. Hacein-Bey-Abina S, von Kalle C, Schmidt M, Le Deist F, Wulffraat N,

McIntyre E, et al. A serious adverse event after successful gene therapy for X-linked severe combined immunodeficiency. N Engl J Med. 2003;348(3):255–6.

18. The, Journal, of, Gene, Medicine. Gene Therapy Clinical Trials Worldwide. John Wiley and Sons; 2015.

19. Rosada RS, De La Torre LG, Frantz FG, Trombone AP, Zarate-Blades CR, Fonseca DM, et al. Protection against tuberculosis by a single intranasal administration of DNA-hsp65 vaccine complexed with cationic liposomes. BMC Immunol. 2008;9:38.

20. Balbino TA, Gasperini AAM, Oliveira CLP, Azzoni AR, Cavalcanti LP, De La Torre LG. Correlation of the Physicochemical and Structural Properties of pDNA/Cationic Liposome Complexes with Their in Vitro Transfection. Langmuir. American Chemical Society; 2012;28(31):11535–45.

21. Miller AD. Cationic liposomes for gene therapy. Angew Chemie Int Ed. 1998;37(13–14):1768–85.

22. Felgner PL, Gadek TR, Holm M, Roman R, Chan HW, Wenz M, et al. Lipofection: a highly efficient, lipid-mediated DNA-transfection procedure. Proc Natl Acad Sci USA. 1987;84(21):7413–7.

23. Vitor MT, Bergami-Santos PC, Barbuto JA, De La Torre LG. Cationic Liposomes as Non-viral Vector for RNA Delivery in Cancer Immunotherapy. Recent Pat Drug Deliv Formul. 2013;7(2):99–110.

24. Zhou X, Huang L. DNA transfection mediated by cationic liposomes containing lipopolylysine: characterization and mechanism of action. Biochim Biophys Acta - Biomembr. 1994;1189(2):195–203.

25. Hang JH, Spaete RR, Yoo BJ, Suh BS, Selby MJ, Houghton M. Methods and compositions for controlling translation of HCV proteins. Google Patents; 1996.

26. Cortés MLD, Izquierdo MP. Suicide gene therapy system for the treatment of brain tumours. Google Patents; 1999.

27. De La Torre LG, Rosada RS, Trombone APF, Frantz FG, Coelho-Castelo AAM, Silva CL, et al. The synergy between structural stability and DNA-binding controls the antibody production in EPC/DOTAP/DOPE liposomes and DOTAP/DOPE lipoplexes. Colloids Surfaces B Biointerfaces. 2009;73(2):175–84.

28. De La Torre LG, Vitor MT, Bergami-Santos PC, Barbuto JAM. Production procedure of liposomes, the product so obtained and their uses. Brazil; 2013.

29. Barbuto JAM, Ensina LFC, Neves AR, Bergami-Santos PC, Leite KRM, Marques R, et al. Dendritic cell–tumor cell hybrid vaccination for metastatic

cancer. Cancer Immunol Immunother. Springer Berlin / Heidelberg; 2004;53(12):1111–8.

30. Onaitis M, Kalady MF, Pruitt S, Tyler DS. Dendritic cell gene therapy. Surg Oncol Clin N Am. Elsevier; 2002;11(3):645–60.

31. Ma Y, Zhuang Y, Xie X, Wang C, Wang F, Zhou D, et al. The role of surface charge density in cationic liposome-promoted dendritic cell maturation and vaccine-induced immune responses. Nanoscale. The Royal Society of Chemistry; 2011;3(5):2307–14.

32. Vitor MT, Bergami-Santos PC, Piedade Cruz KS, Pinho MP, Marzagão Barbuto JA, La Torre LG De. Dendritic Cells Stimulated by Cationic Liposomes. J Nanosci Nanotechnol. 2016;16(1):270–9.

33. Vitor MT, Bergami-Santos PC, Zômpero RHF, Cruz KSP, Pinho MP, Barbuto JAM, et al. Cationic liposomes produced via ethanol injection method for dendritic cell therapy. J Liposome Res. 2016;7:1-15.

34. De Haes W, Van Mol G, Merlin C, De Smedt SC, Vanham G, Rejman J. Internalization of mRNA lipoplexes by dendritic cells. Mol Pharm. 2012;9(10):2942–9.

35. Hsieh AT-H, Pan PJ-H, Lee AP. Rapid label-free DNA analysis in picoliter microfluidic droplets using FRET probes. Microfluid Nanofluidics. 2009;6(3):391–401.

36. Chou LY, Ming K, Chan WC. Strategies for the intracellular delivery of nanoparticles. Chem Soc Rev. 2011;40(1):233–45.

37. Whitesides GM. The origins and the future of microfluidics. Nature. 2006;442(7101):368–73.

38. Beebe DJ, Mensing G a, Walker GM. Physics and applications of microfluidics in biology. Annu Rev Biomed Eng. 2002;4:261–86.

39. van den Berg A, Craighead HG, Yang P. From microfluidic applications to nanofluidic phenomena. Chem Soc Rev. 2010;39(3):899–900.

40. Song H, Tice JD, Ismagilov RF. A Microfluidic System for Controlling Reaction Networks in Time. Angew Chemie Int Ed. WILEY-VCH Verlag; 2003;42(7):768–72.

41. Jiang X, Ng JMK, Stroock AD, Dertinger SKW, Whitesides GM. A miniaturized, parallel, serially diluted immunoassay for analyzing multiple antigens. J Am Chem Soc. 2003;125(18):5294–5.

42. Sia SK, Whitesides GM. Microfluidic devices fabricated in poly(dimethylsiloxane) for biological studies. Electrophoresis. 2003;24(21):3563–76.

43. Zhang C, Xu J, Ma W, Zheng W. PCR microfluidic devices for DNA amplification. Biotechnol Adv. 2006;24(3):243–84.

44. Lagally ET, Simpson PC, Mathies R a. Monolithic integrated microfluidic DNA amplification and capillary electrophoresis analysis system. Sensors Actuators, B Chem. 2000;63(3):138–46.

45. Atencia J, Cooksey G a, Locascio LE. A robust diffusion-based gradient generator for dynamic cell assays. Lab Chip. 2012;12(2):309–16.

46. Oliveira AF, Pelegati VB, Carvalho HF, Cesar CL, Bastos RG, de la Torre LG. Cultivation of yeast in diffusion-based microfluidic device. Biochem Eng J. 2016;105:288–95.

47. Majedi FS, Hasani-Sadrabadi MM, Hojjati Emami S, Shokrgozar MA, VanDersarl JJ, Dashtimoghadam E, et al. Microfluidic assisted self-assembly of chitosan based nanoparticles as drug delivery agents. Lab Chip. The Royal Society of Chemistry; 2013;13(2):204–7.

48. Yang C-HC, Huang K-SS, Chang J-YY. Manufacturing monodisperse chitosan microparticles containing ampicillin using a microchannel chip. Biomed Microdevices. 2007;9(2):253–9.

49. Balbino TA, Aoki NT, Gasperini AAM, Oliveira CLP, Azzoni AR, Cavalcanti LP, et al. Continuous flow production of cationic liposomes at high lipid concentration in microfluidic devices for gene delivery applications. Chem Eng J. 2013;226(0):423–33.

50. Jahn A, Vreeland WN, DeVoe DL, Locascio LE, Gaitan M. Microfluidic Directed Formation of Liposomes of Controlled Size. Langmuir. American Chemical Society; 2007;23(11):6289–93.

51. Teh S-Y, Khnouf R, Fan H, Lee AP. Stable, biocompatible lipid vesicle generation by solvent extraction-based droplet microfluidics. Biomicrofluidics. 2011;5(4):44113.

52. Lazarus LL, Yang AS-J, Chu S, Brutchey RL, Malmstadt N. Flow-focused synthesis of monodisperse gold nanoparticles using ionic liquids on a microfluidic platform. Lab Chip. 2010;10(24):3377–9.

53. Kim JA, Cho K, Shin YS, Jung N, Chung C, Chang JK. A multi-channel electroporation microchip for gene transfection in mammalian cells. Biosens Bioelectron. 2007;22:3273–7.

54. de la Torre LG, Balbino TA, C. SC, Vitor MT, Oliveira AF. Trends on Microfluidic Liposome Production through Hydrodynamic Flow- Focusing and Microdroplet Techniques for Gene Delivery Applications. In: Advances in Liposomes Research. 2014. p. 195.

55. Nge PN, Rogers CI, Woolley AT. Advances in microfluidic materials,

functions, integration, and applications. Chem Rev. 2013;113(4):2550–83.

56. McDonald JC, Whitesides GM. Poly (dimethylsiloxane) as a Material for Fabricating Microfluidic Devices. Acc Chem Res. 2002;35(7):491–9.

57. Christopher GF, Anna SL. Microfluidic methods for generating continuous droplet streams. J Phys D Appl Phys. 2007;40(19):R319.

58. Seemann R, Brinkmann M, Pfohl T, Herminghaus S. Droplet based microfluidics. Reports Prog Phys. 2012;75(1):16601.

59. Abate AR, Lee D, Do T, Holtze C, Weitz D a. Glass coating for PDMS microfluidic channels by sol-gel methods. Lab Chip. 2008;8(4):516–8.

60. Atencia J, Beebe DJ. Controlled microfluidic interfaces. Nature. 2005 Sep 29;437(7059):648–55.

61. Casadevall i Solvas X, deMello A. Droplet microfluidics: recent developments and future applications. Chem Commun. The Royal Society of Chemistry; 2011;47(7):1936–42.

62. Bibette J, Calderon FL, Poulin P. Emulsions: basic principles. Reports Prog Phys. 1999;62(6):969.

63. Taylor G. Dispersion of Soluble Matter in Solvent Flowing Slowly through a Tube. Proc R Soc London Ser A Math Phys Sci. 1953;219(1137):186–203.

64. Gu H, Duits MHG, Mugele F. Droplets formation and merging in two-phase flow microfluidics. Int J Mol Sci. 2011;12(4):2572–97.

65. Baroud CN, Gallaire F, Dangla RR. Dynamics of microfluidic droplets. Lab Chip. The Royal Society of Chemistry; 2010;10(16):2032–45.

66. Zhao C-X, He L, Qiao SZ, Middelberg APJ. Nanoparticle synthesis in microreactors. Chem Eng Sci. 2011;66(7):1463–79.

67. Baret J-C. Surfactants in droplet-based microfluidics. Lab Chip. 2012;12(3):422.

68. Wagner O, Thiele J, Weinhart M, Mazutis L, David A. Weitz C, Huckb WTS, et al. Biocompatible fluorinated polyglycerols for droplet microfluidics as an alternative to PEGbased copolymer surfactants. Lab Chip. 2015;1–5.

69. Li D. Encyclopedia of microfluidics and nanofluidics. Springer Science & Business Media; 2008.

70. Umbanhowar PB, Prasad V, Weitz DA. Monodisperse emulsion generation via drop break off in a coflowing stream. Langmuir. 2000;16(2):347–51.

71. Hessel V, Löwe H, Schönfeld F. Micromixers—a review on passive and active mixing principles. Chem Eng Sci. 2005;60(8):2479–501.

72. Kim DS, Lee SH, Kwon TH, Ahn CH. A serpentine laminating micromixer combining splitting/recombination and advection. Lab Chip. 2005;5(7):739–47.

73. Zheng B, Tice JD, Ismagilov RF. Formation of droplets of alternating composition in microfluidic channels and applications to indexing of concentrations in droplet-based assays. Anal Chem. 2004;76(17):4977–82.

74. Tice JD, Lyon AD, Ismagilov RF. Effects of viscosity on droplet formation and mixing in microfluidic channels. Anal Chim Acta. 2004;507(1):73–7.

75. de Lozar A, Hazel AL, Juel A. Scaling properties of coating flows in rectangular channels. Phys Rev Lett. 2007;99(23):234501.

76. Nguyen N-T. Micromixers: fundamentals, design and fabrication. William Andrew; 2011.

77. Ho C-M. Micro/nano technology systems for biomedical applications: microfluidics, optics, and surface chemistry. Oxford University Press; 2010.

78. Brouzes E, Medkova M, Savenelli N, Marran D, Twardowski M, Hutchison JB, et al. Droplet microfluidic technology for single-cell high-throughput screening. Proc Natl Acad Sci. 2009 Aug 25;106(34):14195–200.

79. Colosimo A, Serafino A, Sangiuolo F, Di Sario S, Bruscia E, Amicucci P, et al. Gene transfection efficiency of tracheal epithelial cells by DC-Chol–DOPE/DNA complexes. Biochim Biophys Acta (BBA)-Biomembranes. 1999;1419(2):186–94.

80. Rejman J, Oberle V, Zuhorn IS, Hoekstra D. Size-dependent internalization of particles via the pathways of clathrin- and caveolae-mediated endocytosis. Biochem J. 2004;377(Pt 1):159–69.

81. Muthu MS, Kulkarni SA, Raju A, Feng SS. Theranostic liposomes of TPGS coating for targeted co-delivery of docetaxel and quantum dots. Biomaterials. 2012;33(12):3494–501.

82. Ho Y-P, Grigsby CL, Zhao F, Leong KW. Tuning Physical Properties of Nanocomplexes through Microfluidics-Assisted Confinement. Nano Lett. American Chemical Society; 2011;11(5):2178–82.

83. Itaka K, Uchida S, Matsui A, Yanagihara K, Ikegami M, Endo T, et al. Gene transfection toward spheroid cells on micropatterned culture plates for genetically-modified cell transplantation. JoVE (Journal Vis Exp. 2015;(101):e52384–e52384.

84. Wurm FM. Production of recombinant protein therapeutics in cultivated mammalian cells. Nat Biotechnol. 2004;22(11):1393–8.

85. Nikić I, Kang JH, Girona GE, Aramburu IV, Lemke EA. Labeling proteins on

live mammalian cells using click chemistry. Nat Protoc. 2015;10(5):780–91.

86. Cottle RN, Lee CM, Archer D, Bao G. Controlled delivery of β-globin-targeting TALENs and CRISPR/Cas9 into mammalian cells for genome editing using microinjection. Sci Rep. 2015;5.

87. Drummond MC, Barzik M, Bird JE, Zhang D-S, Lechene CP, Corey DP, et al. Live-cell imaging of actin dynamics reveals mechanisms of stereocilia length regulation in the inner ear. Nat Commun. 2015;6.

88. Takahashi M, Kikkawa T, Osumi N. Gene transfer into cultured mammalian embryos by electroporation. Electroporation Methods Neurosci. 2015;141–57.

89. Uchugonova A, Breunig HG, Batista A, König K. Optical reprogramming with ultrashort femtosecond laser pulses. In: SPIE BiOS. International Society for Optics and Photonics; 2015. p. 93290U–93290U–6.

90. Wang Y, Chen Y, Zhang W, Yang Y, Bai W, Shen E, et al. Upregulation of ULK1 expression in PC‐3 cells following tumor protein P53 transfection by sonoporation. Oncol Lett. 2016;11(1):699–704.

91. Shi W, Liu X, Wei C, Xu ZJ, Sim SSW, Liu L, et al. Micro-optical coherence tomography tracking of magnetic gene transfection via Au–Fe 3 O 4 dumbbell nanoparticles. Nanoscale. 2015;7(41):17249–53.

92. Tokunaga Y, Liu D, Nakano J, Zhang X, Nii K, Go T, et al. Potent effect of adenoviral vector expressing short hairpin RNA targeting ribonucleotide reductase large subunit M1 on cell viability and chemotherapeutic sensitivity to gemcitabine in non-small cell lung cancer cells. Eur J Cancer. 2015;51(16):2480–9.

93. Bartman CM, Egelston J, Ren X, Das R, Phiel CJ. A simple and efficient method for transfecting mouse embryonic stem cells using polyethylenimine. Exp Cell Res. 2015;330(1):178–85.

94. Zhang L. Polymeric nanoparticle-based delivery of microRNA-199a-3p inhibits proliferation and growth of osteosarcoma cells. Int J Nanomedicine. 2015;10:2913.

95. Mostaghaci B, Susewind J, Kickelbick G, Lehr C-M, Loretz B. Transfection System of Amino-Functionalized Calcium Phosphate Nanoparticles: In Vitro Efficacy, Biodegradability, and Immunogenicity Study. ACS Appl Mater Interfaces. 2015;7(9):5124–33.

96. Decuzzi P, Ferrari M. Design maps for nanoparticles targeting the diseased microvasculature. Biomaterials. 2008;29(3):377–84.

97. Farokhzad OC, Khademhosseini A, Jon S, Hermmann A, Cheng J, Chin C, et al. Microfluidic system for studying the interaction of nanoparticles and

microparticles with cells. Anal Chem. American Chemical Society; 2005;77(17): 5453-59.

98. Meer van der AD, Kamphuis MMJ, Poot AA, Feijen J, Vermes I. A microfluidic device for monitoring siRNA delivery under fluid flow. J Control Release. 2008;132(3):e42–4.

99. Harris SS, Giorgio TD. Convective flow increases lipoplex delivery rate to in vitro cellular monolayers. Gene Ther. 2005;12(6):512–20.

100. Fuhr G, Gradl G, Mueller T, Schnelle T, Shirley SG. Microsystem for cell permeation and cell fusion. Google Patents; 2000.

101. Lee LP, Seo J, Ionescu-Zanetti C, Khine M, Lau A. Cell handling, electroporation and electrofusion in microfluidic systems. Google Patents; 2012.

102. Quake S, Volksmuth W. Method and apparatus for analysis and sorting of polynucleotides based on size. Google Patents; 2006.

103. Ata E, Esener S, Wang M. Optical switching and sorting of biological samples and microparticles transported in a micro-fluidic device, including integrated bio-chip devices. Google Patents; 2002.

104. Song H, Ismagilov RF. Millisecond Kinetics on a Microfluidic Chip Using Nanoliters of Reagents. J Am Chem Soc. American Chemical Society; 2003;125(47):14613–9.

105. Lee A, Fisher J. Microfluidic device for the encapsulation of cells with low and high cell densities. Google Patents; 2006.

106. Choo Y, Johnson CJ, Odenwälder PK, Jayasinghe SN. Nested cell encapsulation. Google Patents; 2012.

107. Sims CE, Allbritton NL. Analysis of single mammalian cells on-chip. Lab Chip. The Royal Society of Chemistry; 2007;7(4):423–40.

108. Huebner A, Srisa-Art M, Holt D, Abell C, Hollfelder F, deMello AJ, et al. Quantitative detection of protein expression in single cells using droplet microfluidics. Chem Commun. The Royal Society of Chemistry; 2007;(12):1218–20.

109. Schmitz CHJ, Rowat AC, Köster S, Weitz DA. Dropspots: a picoliter array in a microfluidic device. Lab Chip. 2009;9(1):44–9.

110. Boedicker JQ, Li L, Kline TR, Ismagilov RF. Detecting bacteria and determining their susceptibility to antibiotics by stochastic confinement in nanoliter droplets using plug-based microfluidics. Lab Chip. 2008;8(8):1265–72.

111. Alessandri K, Sarangi BR, Gurchenkov VV, Sinha B, Kießling TR, Fetler L, et al. Cellular capsules as a tool for multicellular spheroid production and for investigating the mechanics of tumor progression in vitro. Proc Natl Acad Sci. 2013;110(37):14843–8.

112. Ranga A, Gobaa S, Okawa Y, Mosiewicz K, Negro A, Lutolf MP. 3D niche microarrays for systems-level analyses of cell fate. Nat Commun. 2014;5.

113. Fedorovich NE, Alblas J, de Wijn JR, Hennink WE, Verbout AJ, Dhert WJA. Hydrogels as extracellular matrices for skeletal tissue engineering: state-of-the-art and novel application in organ printing. Tissue Eng. 2007;13(8):1905–25.

114. Discher DE, Janmey P, Wang Y. Tissue cells feel and respond to the stiffness of their substrate. Science. 2005;310(5751):1139–43.

115. Dhaliwal A, Lam J, Maldonado M, Lin C, Segura T. Extracellular matrix modulates non-viral gene transfer to mouse mesenchymal stem cells. Soft Matter. 2012;8(5):1451–9.

116. Mih JD, Marinkovic A, Liu F, Sharif AS, Tschumperlin DJ. Matrix stiffness reverses the effect of actomyosin tension on cell proliferation. J Cell Sci. 2012;125(Pt 24):5974–83.

117. Dhaliwal A, Maldonado M, Lin C, Segura T. Cellular cytoskeleton dynamics modulates non-viral gene delivery through RhoGTPases. PLoS One. 2012;7(4):e35046.

118. Clausell-Tormos J, Lieber D, Baret J-C, El-Harrak A, Miller OJ, Frenz L, et al. Droplet-Based Microfluidic Platforms for the Encapsulation and Screening of Mammalian Cells and Multicellular Organisms. Chem Biol. Cell Press; 2008;15(5):427–37.

119. Courtois F, Olguin LF, Whyte G, Theberge AB, Huck WTS, Hollfelder F, et al. Controlling the Retention of Small Molecules in Emulsion Microdroplets for Use in Cell-Based Assays. Anal Chem. American Chemical Society; 2009;81(8):3008–16.

120. Courtois F, Olguin LF, Whyte G, Bratton D, Huck WTS, Abell C, et al. An Integrated Device for Monitoring Time-Dependent in vitro Expression From Single Genes in Picolitre Droplets. ChemBioChem. WILEY-VCH Verlag; 2008;9(3):439–46.

121. Ghadessy FJ, Holliger P. A novel emulsion mixture for in vitro compartmentalization of transcription and translation in the rabbit reticulocyte system. Protein Eng Des Sel. 2004;17(3):201–4.

122. Holtze C, Rowat AC, Agresti JJ, Hutchison JB, Angile FE, Schmitz CHJ, et al. Biocompatible surfactants for water-in-fluorocarbon emulsions. Lab Chip. The Royal Society of Chemistry; 2008;8(10):1632–9.

123. Roach LS, Song H, Ismagilov RF. Controlling Nonspecific Protein Adsorption in a Plug-Based Microfluidic System by Controlling Interfacial Chemistry Using Fluorous-Phase Surfactants. Anal Chem. American Chemical Society; 2004;77(3):785–96.

124. Abbyad P, Tharaux P-L, Martin J-L, Baroud CN, Alexandrou A. Sickling of red blood cells through rapid oxygen exchange in microfluidic drops. Lab Chip. 2010;10(19):2505–12.

125. Fradet E, McDougall C, Abbyad P, Dangla R, McGloin D, Baroud CN. Combining rails and anchors with laser forcing for selective manipulation within 2D droplet arrays. Lab Chip. The Royal Society of Chemistry; 2011;11(24):4228–34.

126. Kim DH. Microdroplets for the Study of Mass Transfer. In: Nakajima DH, editor. Mass Transfer - Advanced Aspects. InTech; 2011. p. 805–24.

127. Abbyad P, Dangla R, Alexandrou A, Baroud CN. Rails and anchors: guiding and trapping droplet microreactors in two dimensions. Lab Chip. The Royal Society of Chemistry; 2011;11(5):813–21.

128. Shin HS, Kim HJ, Sim SJ, Jeon NL. Shear Stress Effect on Transfection of Neurons Cultured in Microfluidic Devices. J Nanosci Nanotechnol. 2009;9(12):7330–5.

129. Alam A, Afzal A, Kim K-Y. Mixing performance of a planar micromixer with circular obstructions in a curved microchannel. Chem Eng Res Des. 2014;92(3):423–34.

130. Liau A, Karnik R, Majumdar A, Cate JHD. Mixing crowded biological solutions in milliseconds. Anal Chem. 2005;77(23):7618–25.

131. Muradoglu M, Stone HA. Mixing in a drop moving through a serpentine channel: a computational study. Phys Fluids. 2005;17(7):73305.

132. Tice JD, Song H, Lyon AD, Ismagilov RF. Formation of droplets and mixing in multiphase microfluidics at low values of the Reynolds and the capillary numbers. Langmuir. 2003;19(22):9127–33.

133. Kinoshita H, Kaneda S, Fujii T, Oshima M. Three-dimensional measurement and visualization of internal flow of a moving droplet using confocal micro-PIV. Lab Chip. Royal Society of Chemistry; 2007;7(3):338–46.

134. Jayapal KP, Wlaschin KF, Hu W, Yap MGS. Recombinant protein therapeutics from CHO cells-20 years and counting. Chem Eng Prog. AICHE AMERICAN INSTITUTE OF CHEMICAL; 2007;103(10):40.

135. Hacker DL, Balasubramanian S. Recombinant protein production from stable mammalian cell lines and pools. Current Opinion in Structural Biology. 2016. p. 129–36.

136. Kim JY, Kim Y-G, Lee GM. CHO cells in biotechnology for production of recombinant proteins: current state and further potential. Appl Microbiol Biotechnol. Springer; 2012;93(3):917–30.

137. March JC, Rao G, Bentley WE. Biotechnological applications of green fluorescent protein. Appl Microbiol Biotechnol. Springer; 2003;62(4):303–15.

138. Zhan Y, Wang J, Bao N, Lu C. Electroporation of Cells in Microfluidic Droplets. Anal Chem. American Chemical Society; 2009;81(5):2027–31.

139. Luo C, Yang X, Fu Q, Sun M, Ouyang Q, Chen Y, et al. Picoliter-volume aqueous droplets in oil: Electrochemical detection and yeast cell electroporation. Electrophoresis. 2006;27(10):1977–83.

140. Lee S, Jeong W, Beebe DJ. Microfluidic valve with cored glass microneedle for microinjection. Lab Chip. 2003;3(3):164–7.

141. Chen F, Zhan Y, Geng T, Lian H, Xu P, Lu C. Chemical transfection of cells in picoliter aqueous droplets in fluorocarbon oil. Anal Chem. 2011;83(22):8816–20.

142. Hufnagel H, Huebner A, Gulch C, Guse K, Abell C, Hollfelder F. An integrated cell culture lab on a chip: modular microdevices for cultivation of mammalian cells and delivery into microfluidic microdroplets. Lab Chip. The Royal Society of Chemistry; 2009;9(11):1576–82.

143. Lee APICA, Hsieh AT-HICA. Microfluidic device for forming monodisperse lipoplexes. Google Patents; 2010.

144. Matsuoka H, Komazaki T, Mukai Y, Shibusawa M, Akane H, Chaki A, et al. High throughput easy microinjection with a single-cell manipulation supporting robot. J Biotechnol. 2005;116(2):185–94.

Chapter III – Droplet Microfluidic-Assisted Synthesis of Lipoplexes for DC Transfection

Micaela Tamara Vitor[1,2], André Luiz Paes de Lima[1], Lívia Furquim de Castro[3], Ronei Luciano Mamoni[3], Charles N. Baroud[2], Lucimara Gaziola De La Torre[1*]

[1] School of Chemical Engineering, Department of Bioprocesses and Materials Engineering, University of Campinas (Unicamp), Av. Albert Einstein, 500, Campinas, SP, 13083-852, Brazil

[2] LadHyX and Department of Mechanics, Ecole Polytechnique, CNRS-UMR, 91128 Palaiseau, France

[3] Department of Clinical Pathology, Faculty of Medical Sciences, University of Campinas (Unicamp), Rua Tessália Vieira de Camargo, 126, Campinas, SP, 13083-887, Brazil

*Corresponding author: latorre@feq.unicamp.br

To be submitted to *Chemical Engineering Journal*

Abstract

Dendritic cells (DCs), professional antigen-presenting cells, are widely used in immunotherapeutic approaches. When loaded with tumor antigens, mature DCs can induce an immune response against cancer. Particularly, cationic liposomes show as a promising gene carrier for DCs, since besides to be internalized, they can also activate them. However, DCs transfection dependence of lipoplexes size and polydispersity makes the process a challenge. In this context, droplet-based microfluidic system can be applied in order to obtain reproducible and suitable lipoplexes to DCs transfection. For this purpose, we investigated a droplet-based microfluidic system with serpentine and split regions to synthesize lipoplexes. We first investigated operational parameters that influence in droplets formation, like inlet flow rates. Thus, we chose to operate the system at ratio aqueous/oil flow rate 0.25. Then, we ensured that cationic liposomes maintain their properties after droplet processing. We investigated the influence of molar charge ratio in lipoplexes formation and we also evaluated different microchip designs, exploring the effect of residence time and droplet size in lipoplexes physico-chemical properties. The droplet-based system allowed the incorporation of more amount of pDNA to CL while maintaining lipoplexes monodisperse and with positive charge. Mixing provided by small droplets flowing in the serpentine channel was more important than residence time to decrease lipoplexes polydispersity. Lipoplexes were able to transfect DCs, besides activating cells. However, lipoplexes loading lower amount of DNA were more efficient in transfect DCs. Thus, droplet-based microfluidic system showed to be a potential tool in lipoplexes properties modulation according to specific cell lines.

Keywords: lipoplex, transfection, microfluidics, water fraction, capillary number, molar charge ratio

1. Introduction

Gene therapy is the insertion of genetic materials into cells or organs in order to treat genetic defects. For this, gene therapy requires safety and efficient gene

delivery systems, classified as viral and non-viral vectors. Viral vectors delivery efficiently the target gene into the host cell, but as consequence, immune and oncogenic responses can be activated. To overcome these drawbacks, non-viral vectors were developed reproducing viral gene delivery function, in a more secure and reproducible way, even though without reaching the high transfection level verified by virus vectors (1). Within the current range of non-viral vectors, cationic liposomes are particularly promising (2). The electrostatic interaction between the positive charge of cationic lipids from liposomes and negative charges from phosphate groups from nucleic acids form complexes capable of entering cells, named lipoplexes (3).

In the field of gene delivery, one specific challenge is the transfection of dendritic cells (DCs). DCs are professional antigen-presenting cells widely used in immunotherapeutic approaches, particularly in immunotherapies against cancer. Since loaded with tumor antigens, mature DCs can induce an immune response against cancer by recruiting patients' immune system (4). Different strategies are currently used to load mature DCs *in vitro* with tumor antigens (5). Cationic liposomes stand out in this function as gene carriers, since besides to transfect DCs, they can also activated them (6). The cationic liposomes composed of Egg phosphatidylcholine (EPC), 1,2-dioleoyl-sn-glycero-3-phosphoethanolamine (DOPE) and 1,2-dioleoyl-3-trimethylammonium-propane (DOTAP) (50/25/25% molar) showed as a potential tool for DC-based immunotherapeutic approaches, since they were uptaken by DCs providing cell stimulation/activation (7,8). DCs uses preferentially macropinocytosis and/or phagocytosis as transfection pathway, and so, extremely dependent of lipoplexes size and polydispersity for transfection (9). Thus, the study of methodologies that enable to form lipoplexes modulated to specific cells lines in a reproducible and controllable way is very important (10).

Conventional methods of obtaining lipoplexes involve just the mixing provided by hand shaking or vortexing to reach cationic liposomes complexation with nucleic acids. However, these conventional methods introduce variability in lipoplexes formation and, as a result, provide inconsistent transfection efficiencies (11). To

effectively transfect cells, the physico-chemical properties of lipoplexes should be suitable to the pathway used by the cell line to internalize nanoparticles (12).

On the other hand, to circumvent the above difficulties, the micro-scaled environment of microfluidic systems allows precise control and optimization of multiple processes and techniques used in gene therapy (1). Droplet-based microfluidic systems define microcontainers that reduce of many orders the volumes manipulated, making these systems attractive for performing experiments in molecular biology. Moreover, droplets moving in microfluidic systems become micromixers that provide a rapid mixing of reagents (13). Microsystems working only with parallel streams have the fluid mixing mainly promoted by diffusion, whereas droplet-based microsystems can have the addition of chaotic advection that increases the mixing in the system (14). The chaotic advection in serpentine channel is generated by two recirculation flows inside droplets due to the shear created between droplet and channel walls (15). Micromixers have important applications such as control chemical reactions (16), promote protein crystallization (17), improve biochemical analysis (18) and complex nanoparticles and nucleic acids (11). Hsieh e*t al.* (11) developed a picolitre incubator based microfluidic system to complex commercial liposomes lipofectin with pDNA encoding GFP. They showed the robusteness of the microsystem to produce reproducible lipoplexes and also to transfect human osteosarcoma U2OS cells (11). Thus, droplet-based microfluidic platforms emerge as an alternative to conventional methods, which provide more controllable environment for direct synthesis of lipoplexes adequate for gene therapy applications (19). To produce lipoplexes according to the cell line requirements, some parameters, such as flow rates, viscosity of fluids and microchip design, which influence on mixing in droplet-based platforms, should take into account (20,21).

Therefore, this work aimed to investigate the complexation of EPC/DOTAP/DOPE liposomes with plasmidial DNA (pDNA) by droplet-based microfluidic system, based on microchip already designed by Hsieh e*t al.* (11) in order to obtain reproducible and suitable lipoplexes to DCs transfection. For this purpose, some experimental parameters were investigated, such as flow rates to

ensure droplets formation in the system, liposomes physico-chemical properties after droplet processing, lipoplex characteristics as function of molar charge ratio ($R_{+/-}$) and microchip design. Then, lipoplexes produced in the microfluidic system operating in the chose parameters were evaluated in their capacity to transfect DCs *in vitro* while stimulating cells.

2. Materials and Methods

2.1. Microfabrication

Cationic liposomes (CLs) and lipoplexes (CL/pDNA complexes) were synthesized in PDMS/glass microfluidic devices fabricated according to Moreira *et al.* (22). The designs of the devices were projected using the software AutoCAD 2002. All microchannels had a rectangular cross section constructed using soft lithography methods in PDMS and irreversibly sealed to glass through O_2 plasma surface activation (22).

The cationic liposomes production was carried out in a cross-junction device, like used by Balbino *et al.* (23) and illustrated in Figure 3.1A. Channels had a rectangular cross section with a depth of 100 µm and a width of 140 µm. Otherwise, the devices designed for lipoplexes formation (Figure 3.1B) was based on Hsieh e*t al.* (11), with slight modifications. The device had rectangular cross section with 50 µm of depth in all channel. The serpentine channel was classified as: (i) thin channel (TC) with 200 µm of width (D) and 9600 µm of linear length (L), and (ii) wide channel (WC) with 400 µm of width (D) and 19200 µm of linear length (L) (Figure 3.1B). Number of curves in serpentine channel was fixed in 13 for both WC and TC. Mix between pDNA and CL occurred in the serpentine channel due to a chaotic advection (11), and so this part of the chip was used to calculate the average flow velocity of the system. Furthermore, droplet microfluidic device can have or not a split region (Figure 3.1B) in the end of the design with 50 µm of width to accelerate the mixing efficiency of reagents inside microdroplets (10).

PDMS microchips bonded with glass slide by plasma oxygen rendered surface hydrophilic. Thus, for the use of fluorinated oil as continuous phase of the emulsion system (Figure 3.1B), a treatment with Novec 1700 Electronic Grade 3M

Coating solution (MN, USA) was done, deposing a layer of fluoropolymer in the inner surfaces. For this, microdevices were filled with the electronic coating solution and heated at 150 °C for 30 minutes; this procedure was repeated three times. Then, microchips were cooled in room temperature and microchannels were filled with pure FC-40 oil, which remained in the system until the use.

A

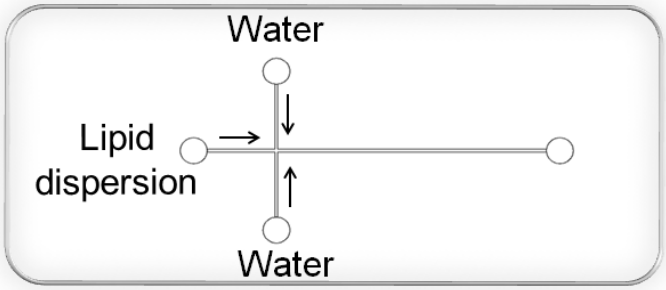

B

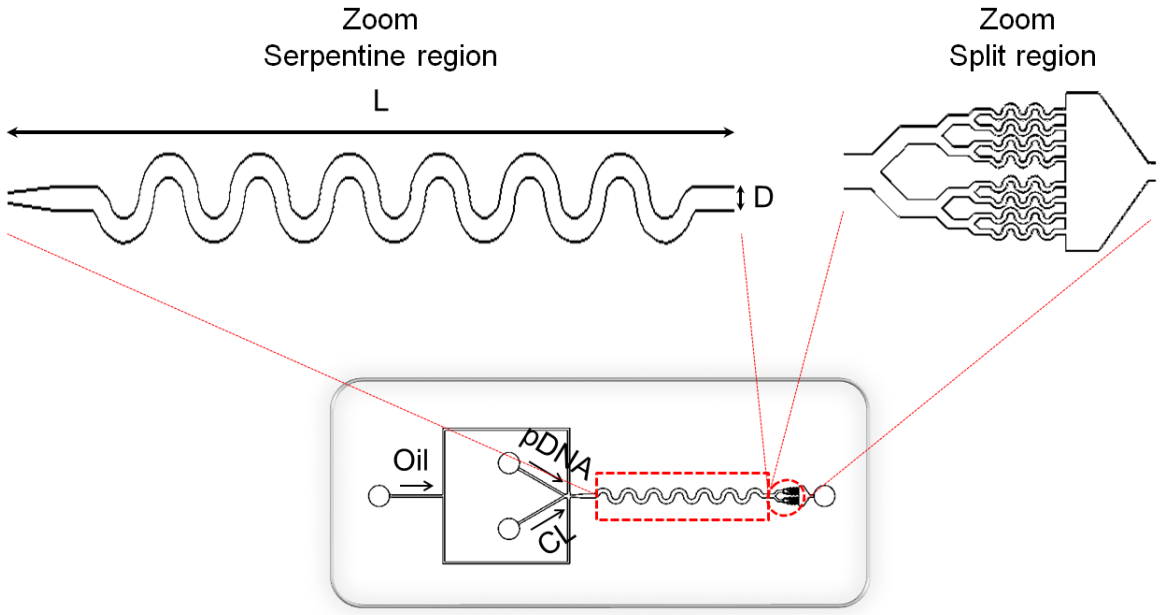

Figure 3.1 - Microfluidic devices. Cross-junction device for liposome production by a single hydrodynamic flow focusing (A) and droplet-based device for CL complexation with pDNA with serpentine channel and split regions (B). The droplet-based devices designed varying the serpentine width (thin-TC and wide-WC channels). TC: 200 µm of width (D) and 9600 µm of linear length (L); WC: 400 µm of width (D) and 19200 µm of linear length (L). The channel in the split region have 50 µm of width (devices without split region were also investigated).

2.2. Cationic Liposome Production

Cationic liposomes composed of egg phosphatidylcholine (EPC) (96% of purity), 1,2-dioleoyl-sn-glycero-3-phosphoethanolamine (DOPE) (99.8% of purity) and 1,2-dioleoyl-3-trimethylammonium-propane (DOTAP) (98% of purity) (Lipoid GmbH, Ludwigshafen, Germany) (50/25/25 % molar, respectively) were produced by single hydrodynamic flow focusing in a cross-junction device like Balbino *et al.* (23) (Figure 3.1A). Basically, the three lipids were dispersed in anhydrous ethanol to achieve 25 mM of total lipid concentration. To form cationic liposomes for gene delivery with this lipid composition is very important the order in which lipids are dispersed in the alcoholic solution, the grade purity of lipids, the method used to form liposomes and their concentration (24). The lipid dispersion was injected as center flow at 10.92 μL min^{-1} with a glass syringe (Hamilton, NV, USA) by syringe pump (KDScientific, model KDS-200, USA). Simultaneously, water (Samtec, SP, Brazil) were inserted at 54.6 μL min^{-1} by two sides of cross-junction chip. Liposome samples were collected and leaved for at least 2 hours at 4 °C. Then, samples were collected to physico-chemical characterization. Before choosing water as aqueous phase, others biocompatible solutions, like PBS buffer and OptiMEM culture medium were also tested. However, cationic liposomes in water had the best characteristics for the specific application of DCs transfection (see Annex II).

2.3. Lipoplexes Synthesis and Recovery from A/O Emulsion

Aqueous flows, cationic liposomes and pDNA, and the oil flow were injected in their respective inlets (Figure 3.1B) by syringe pumps Harvard (model HA3000W, MA, USA). The oil flow (FC40/Pico-Surf 1) was composed of perfluorocarbon oil Fluorinert Electronic Liquid FC-40 from 3M (Zwijndrecht, Belgium) with 5% v/v of Pico-Surf 1 from Sphere Fluidics (Cambridge, UK). The pDNA used was a plasmid pEGFP-N1 from Clontech (CA, USA) encoding green fluorescent protein (see Annex I) that was previously amplified using competent *E. Coli* bacteria and purified (kit Maxiprep PureLink from Invitrogen, CA, USA) (25). During complexation, the microchip was placed over a Peltier system (Watronix, CA, USA) to maintain temperature at 4 °C (23). After complexation process, the

obtained emulsion was centrifuged at 10,000 rpm for 4 minutes to separate phases. In the supernatant of emulsion lipoplexes were recovered, for then being characterized in terms of physico-chemical properties and/or applied for biological evaluation.

It is important to highlight that this recovered procedure by centrifugation was used as the last step for all process that occurred in the droplet-based microfluidic device in order to obtain the aqueous phase from emulsion.

2.4. Capillary (Ca) and Reynolds (Re) Numbers

The capillary number (Ca) is a dimensionless number that relates viscous forces and surface tension between two immiscible phases, as demonstrated in Equation 3.1.

$$Ca = \frac{\mu_C U}{\gamma} \qquad \text{(Equation 3.1)}$$

where μ_C is the dynamic viscosity of continuous phase, U is the average flow velocity and γ is the surface tension between two immiscible phases. The dynamic viscosity of the continuous phase (μ_{oil} = 7.43 mPa s) was obtained by analyzing the material in Anton Paar rheometer (model Physica MCR301, Graz, Austria). The surface tension (γ = 15.82 mN m^{-1}) was obtained by pendant drop method performed in Teclis tensiometer (model Tracker-S, Longessaigne, France). The average oil flow velocity (U) was determined in the serpentine region from measured area section.

In microfluidic systems only laminar regime occurs (26). Thus, we used the Reynolds number obtained by Equation 3.2 to investigate mixing inside droplets provided by the serpentine geometry.

$$\mathrm{Re} = \frac{\rho_C U d_h}{\mu_C} \qquad \text{(Equation 3.2)}$$

where ρ_C is the density of continuous phase (ρ_{oil} = 1.85 kg m^{-3}), U is the average flow velocity, d_h is the hydraulic diameter (80 µm for TC or 89 µm for WC) and μ_C is the dynamic viscosity of continuous phase.

2.5. Physico-Chemical Characterization of Cationic Liposomes and Lipoplexes

To characterize nanoparticles properties, the cationic liposomes and lipoplexes were diluted in water at 25 °C until 0.25 mM. The average hydrodynamic diameter, the size distribution, polydispersity index and zeta potential were measured by dynamic light scattering (Malvern Zetasizer Nano Series, model ZEN3600 - UK) using a Ne–He laser. The mean diameter and the distribution of particle sizes were calculated using CONTIN algorithm. Nanoparticles' size was presented in number mean, number-weighted hydrodynamic mean diameter.

Each experiment was conducted at least three times and statistical analysis performed with MS Excell 2007. The data was analyzed by ANOVA to compare the results in each group followed by Tukey's test at a p-value < 0.10.

2.6. Biological Evaluation of Lipoplexes

2.6.1. Generation of DCs from THP-1 Cell Line and Transfection With Lipoplexes

THP-1 cells, derived from human monocytic leukemia cell line, were differentiated into dendritic cells as described by Berges *et al.* (27). THP-1 cells were cultivated in culture medium RPMI 1640 from Gibco-Invitrogen (NY, USA) supplemented with 0.1 M (2%) L-glutamine, fetal bovine serum (10%) and gentamycin (0.05%), at a concentration of 5 x 10^5 cells mL^{-1}. To induce DC differentiation, the cytokines from Peprotech (NJ, USA) rhIL-4 (50 ng mL^{-1}) and rhGM-CSF (50 ng mL^{-1}) were added. Cells were cultured for 5 days to acquire the properties of immature dendritic cells (iDCs). Medium exchange was performed on the second day with fresh cytokine-supplemented medium. On the fifth day, iDCs were collected and seeded on 24-well plate in OptiMEM medium (reduced-serum medium from Gibco-Invitrogen, USA) for transfection. Cells were stimulated with cytokine rhTNF-α (50 ng mL^{-1}) to induce mature dendritic cells (mDCs) as positive control, or with lipoplexes $R_{+/-}$ 1.5, 3, 5, 7 and 10 (2 µg pDNA / well) or cationic liposomes (1 mM) diluted in OptiMEM, or as negative control, no stimulant was added (iDC). Then, they were incubated for 3-4 hours at 37 °C and 5% CO_2. Subsequently, liposome and lipoplexes were washed out and medium exchanged

by RPMI supplemented again. After this step, the DCs were incubated for more 2 days to evaluate the transfection efficiency (TE).

2.6.2. Flow Cytometry

After 2 days post-transfection, dendritic cells were harvested and incubated for 20 min at 4°C with antibodies CD80, CD11c, CD86 and HLA-DR (Biolegend, CA, USA) conjugated to APC, PE-Cy5, PE and APC-Cy7, respectively. After incubation, cells were washed, fixed (2% paraformaldehyde) and the samples were acquired in a Flow Cytometer (FACScanto, BD Biosciences, CA, USA). At least 10,000 events were acquired per sample. The data was analyzed using the FlowJo 7.6 software (Tree Star, Inc., CA, USA). Cells were marked with anti-CD11c and anti-HLA-DR to identify dendritic cells in the population (see strategy of DCs analysis in Supplementary data, Figure S.2). The other antibodies, anti-CD80 and anti-CD86, were used in order to determinate DCs activation. Then, transfection efficiency was indirectly measured by quantification of GFP production through FITC fluorescence filter (see strategy of GFP analysis in Supplementary data, Figure S.3), procedure widely used for exploratory results of transfection (28).

3. Results and Discussion

3.1. Establishment of the best condition for droplet generation

The first step was the establishment of processing conditions ensuring droplet formation with suitable performance and shape in the microfluidic device with serpentine (TC) and split regions. For this, we determined the capacity of droplet generation as function of aqueous flow rate ($Q_{aqueous}$), containing only CLs, to reach the best inlet flow rates in which droplets were formed. The oil phase was composed by FC40/Pico-Surf 1 solution, with flow rate fixed at (Q_{oil}) fixed at 2 µL min^{-1}. In this situation, the assays were performed at 25 °C with Ca fixed at $3x10^{-3}$. Previous study determined $Q_{aqueous}$ range used in this work (see Annex II).

Thus, Figure 3.2 illustrates some different flow regimes as function of $Q_{aqueous}$. Considering the nondimensional drop size (λ), ratio of the droplet size to the serpentine channel width (20), in $Q_{aqueous}$ range between 0.22 and 0.47 µL min^{-1}

was formed small droplets (Figure 3.2A) with λ = 0.82. Droplets formed in $Q_{aqueous}$ = 0.50 µL min^{-1} matched λ = 1.31, *i.e.* almost 1.5 times the width of the channel (Figure 3.2B). On the other hand, in $Q_{aqueous}$ between 0.53 and 1.33 µL min^{-1} (Figure 3.2C) were formed plugs (26) of λ = 2.10. At last, in $Q_{aqueous}$ above 2.00 µL min^{-1} (Figure 3.2D) streams flowed in parallel. Thus, investigating the droplets size and shorter operating time, we chose the follow flow rates $Q_{aqueous}$ = 0.50 µL min^{-1} and Q_{oil}= 2 µL min^{-1} (Figure 3.2B) to form droplets in microchip with serpentine TC and split region. For further steps we fixed the volume fraction, ratio between $Q_{aqueous}$ and Q_{oil}, at 0.25.

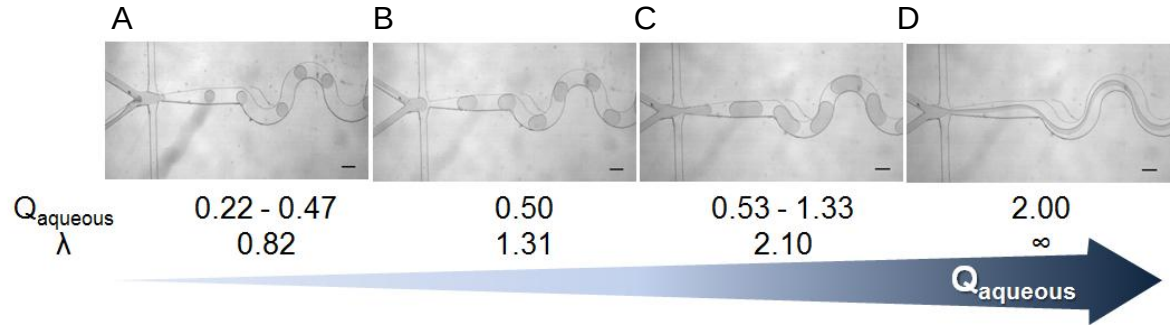

Figure 3.2 - Images of droplet formation in microfluidic system as function of aqueous flow rate ($Q_{aqueous}$): (A) 0.22 - 0.47 µL min^{-1} with small droplets, (B) 0.50 µL min^{-1} forms ideal droplets, (C) 0.53 - 1.33 µL min^{-1} forms plugs and (C) above 2.00 µL min^{-1} produces parallel flow streams. The drop size (λ), ratio of the droplet size to the serpentine channel width, varies from λ = 0.82 (A), 1.31 (B) until 2.10 (C). The assays were developed with fixed Ca = $3x10^{-3}$, Q_{oil} = 2 µL min^{-1} and lipids from cationic liposomes at 2mM.

3.2. Physico-Chemical properties of Cationic Liposome after droplet-based microfluidic processing

The CL are formed by the self-assembly of two zwitterionic phospholipids, EPC and DOPE, and only one monocationic lipid, DOTAP. Since these lipids are amphiphilic molecules, one possibility is the interaction between the surfactant from the oil phase with liposomes, disrupting membranes or modifying the physico-chemical properties, compromising lipoplex and transfection applications. To monitor possible changes in CL properties due to interaction between CL and Pico-Surf 1surfactant, we measured the physico-chemical properties of CL before and

after being processed in the droplet system, as shown in Figure 3.3. In order to access CL properties after droplet-microfluidic processing, CL were injected at 0.67 µL min^{-1} into the droplet-based microfluidic system (Figure 3.1B, serpentine-TC with split region), while the FC-40/Pico-Surf 1 was injected at 2 µL min^{-1} (device and flow rates similar to those used by Lee and Hsieh (29)). At the end, aqueous phase was recovered from w/o emulsion and characterized in terms of size, polydispersity and zeta potential. The size of cationic liposome before (95.54 ± 15.38 nm) and after (86.85 ± 13.52 nm) droplet processing, the polydispersity index before (0.144 ± 0.016) and after (0.164 ± 0.022) and the zeta potential (60.50 ± 3.36 mV before and 57.60 ± 2.57 mV after) were similar (Supplementary data, Table S.1). Additionally, Figure 3.3 shows more clearly that there was no variation in liposome size distribution before and after processing in the droplet-based microfluidic device.

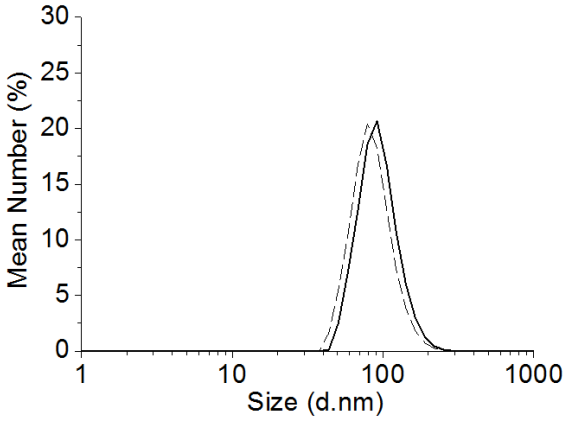

Figure 3.3 - Number-weighted size distribution (diameter) of cationic liposomes before (solid line) and after (dashed line) being inserted in droplet-based microfluidic system. Each solid and dashed line represent mean of triplicate from independent experiments.

Furthermore, following similar procedure, we replaced cationic liposomes by water as aqueous solution in order to verify a possible formation of surfactant micelles in the system. We verified the presence of colloidal structures close to 30 nm in the water (data not shown) *via* dynamic light scattering. Thus, indicating that part of surfactant remained in the aqueous phase as micelles and it may be inserted in liposomes. However, observing results obtained with cationic liposomes (Figure 3.3), we confirmed that this residual surfactant was not appreciable to

change physico-chemical characteristics of the liposomes. In addition, oil FC-40 and perfluoro-derived surfactants, like Pico-Surf 1, are biocompatible (30), so it is expected that the residual surfactant will not affect biological application of lipoplexes.

3.3. Lipoplexes Synthesis: Influence of Molar Charge Ratio ($R_{+/-}$) and Microchip Design

The mainly factors that govern lipoplexes formation are cationic lipid/DNA charge ratio that affects the complexation kinetics (31) and the time and speed of mixing that influence the complex size distributions (32). Thus, we investigated the effect of molar charge ratio (ratio between cationic lipids from liposomes and nucleic acids) and microdevice design on the final physico-chemical properties of lipoplexes (Figure 3.4 and Supplementary data, Table S.2). First of all, we studied the operational parameter capillary number. For this, we used the microchip with serpentine-TC and split region (Figure 3.1B), fixed the $R_{+/-}$ at 3, the volume fraction at 0.25 and the capillary number ranged from $8x10^{-4}$ to $5x10^{-3}$ by varying the average flow velocity of the system (Supplementary data, Figure S.1). There was no tendency in lipoplexes properties according to Ca. Thus, we fixed the operational parameters volume fraction at 0.25 and capillary number at $3x10^{-3}$ (average flow velocity $6x10^{-3}$ m s^{-1}) for further steps investigation.

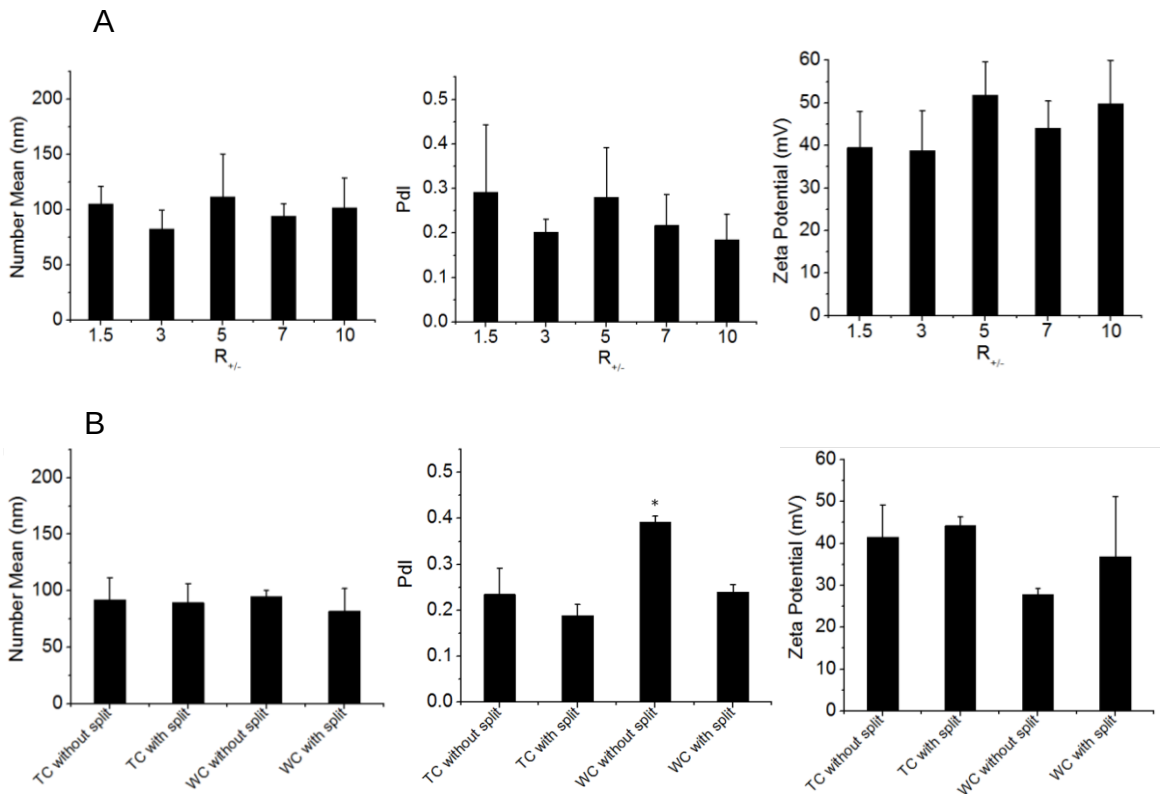

Figure 3.4 – Impact of experimental parameters $R_{+/-}$ (A) and microchip design (B) on lipoplexes characteristics in terms of average diameter (number mean), polydispersity (PdI) and zeta potential. Volume fraction was set at 0.25 and capillary number at $3x10^{-3}$. The droplet-based microfluidic system with serpentine-TC and split region (Figure 3.1B) was used to investigate $R_{+/-}$ varying of 1.5, 3, 5, 7 and 10. For microchip design evaluation, $R_{+/-}$ was fixed at 3.0 and tested droplet-based platforms with serpentine region (thin-TC and wide-WC channels) and in the presence or absence of split region (Figure 3.1B). The error bars represent standard deviation of means (n = 3). Means statistically significant different by Tukey's test ($P<0.10$) were flagged with an asterisk (*).

The influence of droplet system method in lipoplex formation was studied by varying $R_{+/-}$ of 1.5, 3, 5, 7 and 10 in microchip serpentine-TC with split region (Figure 3.4A). Surprisingly, all lipoplexes produced showed monodisperse population around 100 nm and PdI 0.2 and zeta potential around 40 mV. Conventional lipoplex preparation by hand shaking or vortexing usually provides the large size distribution of lipoplexes with increasing amount of DNA added (31,33). Balbino *et al.* (34) investigated microfluidic synthesis of EPC/DOTAP/DOPE lipoplexes in only aqueous phase. The authors showed similar profiles of lipoplexes at the same $R_{+/-}$ range studied, with exception of $R_{+/-}$ 1.5 (with

more quantity of pDNA). In this R+/- they found lipoplexes, with negative charge, polydispersity 0.5 and size about 500 nm. As a result, the droplet microfluidic system presented in this work can load more amount of pDNA in CL while maintaining lipoplexes monodisperse and with positive charge, characteristics specially required for some therapeutic vaccines (35). Moreover, *in vitro* studies demonstrated that nanoparticles of size between 100 and 200 nm and polydispersity less than 0.2 (homogeneous size distribution) are more easily internalized by mammalian cells, assuming that they would expend less energy in their capture (36,37). Cells usually have a negative surface charge, thus lipoplexes with positive charge were easier internalized (3), besides indicating storage stability of complexes over time. Therefore, it was expected that all lipoplexes investigated would be able to transfect dendritic cells. Moreover, the differences obtained from Balbino *et al.* (34) and this current work strongly suggest the superiority of droplet microfluidic systems in generate lipoplexes with high DNA loading, keeping the physico-chemical properties close to proper characteristics for transfection.

Then, we investigated the influence of residence time and droplet mixing in complex properties by using different microdevice designs in lipoplexes formation (Figure 3.1B). For a given average flow velocity (U), the residence time of the liquid is increased by increasing the length of the channel so as to ensure complete mixing (39). In this work, we changed the residence time by modifying serpentine channel length and also the mixing by modifying serpentine channel width. The serpentine channel width interfere in the chaotic mixing inside droplets due to the fluid movement relative to the stationary walls (13). In some designs the mixing channel is branched into multiple narrower channels (split region) to ensure mixing in a shorter residence time (38). Thus, we used four different droplet-based microfluidic systems (Figure 3.1B), two types of serpentine widths (TC-200 µm and WC-400 µm) and in the presence or absence of split mixing region, to obtain lipoplexes with $R_{+/-}$ 3. Thus, the microchip with wide serpentine channel had the linear length 2 times the thin channel, leading to a residence time in WC (3.2 s) 2 times greater than in TC (1.6 s), for a constant flow velocity ($U = 6x10^{-3}$ m s^{-1}).

Droplet-based microfluidic systems with thin and wide serpentine channels presented Re values of $1.3x10^{-4}$ and $1.2x10^{-4}$, respectively. The mixing contribution in this Re range is not dramatic (20).

We can observe in Figure 3.4B that lipoplexes produced in all microchips presented average diameter next to 200 nm and PdI 0.2, exception of microfluidic system with wide serpentine channel without split region that showed higher PdI (0.392 ± 0.013). In this case, the use of serpentine-WC/without split presented negative influence on PdI index, suggesting poor mixture. The residence time in serpentine-WC/without split greater than in serpentine-TC/without split was not sufficient to decrease the lipoplexes PdI. However, the higher PdI value obtained in the serpentine-WC/without split is overcome with the addition of split region, favoring mixture. The serpentine-TC/without split showed that the mixing provided by the split region (10) it is not mandatory to control lipoplex PdI, since only generation of small droplets due to the constriction of serpentine channel width already lead to this result. Handique and Burns (39) modeled the mixing of solutes present in a drop moving in a slit-type microchannel. They showed that shorter plugs will mix in a shorter distance and therefore in a shorter time, considering a constant average flow velocity. Thus, to complex CL with pDNA the most important parameter in this droplet-microfluidic system is the mixing generated in the thin serpentine channel. Rakhmanov *et al.* (32) compared different methods of lipoplexes production, a slow preparation by magnetically stirred and a quick preparation by pipette shaking. As a result, for the low concentrated solutions, the most monodisperse lipoplex population was formed by magnetically stirred method, showing the relevance of a controlled mixing. Moreover, zeta potential of lipoplexes remained around 40 mV, independent of microdevice design used (Figure 3.4B). The choice between microchip with thin or wide serpentine channel should not be only related to the mixing provided by them, but also the ease of system handling. Wide serpentine channel is easier and faster to operate than thin channel, because of the higher flow used and less chance of clogging. Additionally, the connection of a split region to this serpentine-WC channel improves mixing inside droplets. Thus, we decided to use the droplet-based microfluidic systems

with wide serpentine channel and split region to produce lipoplexes for DCs transfection.

3.4. Biological Evaluation of Lipoplexes to Transfect DCs

Lipoplexes produced in the chosen microfluidic system parameters, droplet-based microfluidic system with serpentine-WC with split region operating at fixed volume fraction 0.25, capillary number at $3x10^{-3}$ and $R_{+/-}$ varying in 1.5, 3, 5, 7 and 10, were evaluated in their capacity to transfect DCs. For this, at first, lipoplexes were characterized in terms of average diameter, PdI and zeta potential as shown in Figure 3.5.

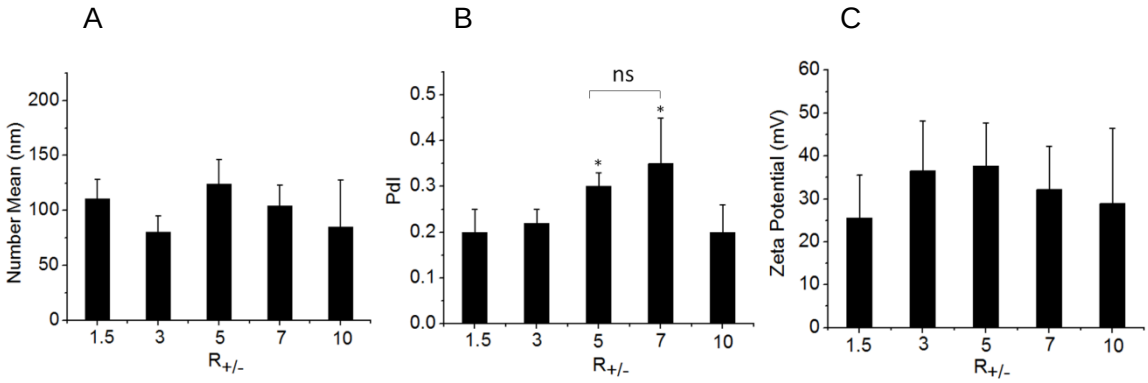

Figure 3.5 – Physico-chemical properties of lipoplexes produced in microfluidic system in terms of average diameter (number mean) (A), polydispersity (PdI) (B) and zeta potential (C). The droplet-based microfluidic system with wide serpentine channel (WC) and split region was operated with volume fraction 0.25, Ca = $3x10^{-3}$, Q_{oil} = 6.5 µL min^{-1} and $R_{+/-}$ varying in 1.5, 3, 5, 7 and 10. The error bars represent standard deviation of means (n = 4). Means statistically significant different by Tukey's test (P<0.10) were flagged with an asterisk (*) and non-different means with "ns".

Similarly as lipoplexes synthesized in microchip with serpentine-TC with split region (Figure 3.1B), lipoplexes obtained in the chosen conditions (Figure 3.5) showed size around 100 nm and PdI 0.20. However, lipoplexes $R_{+/-}$ 5 and 7 obtained in chosen conditions (Figure 3.5B) showed higher PdI (0.30 ± 0.03 and 0.35 ± 0.10, respectively). This is probably due to irregular motion of the syringe pumps that induced fluctuations in relative flow rates (26); reflecting in the mixing for lipoplex formation kinetics. Charge of lipoplexes decreased from 40 mV

in thin serpentine channel (Figure 3.4B) to 30 mV when synthesized in wide channel (Figure 3.5C). The better mixing provided by thin channel lead a lower reduction in liposome charge with pDNA addition, than in wide channel. After characterized, these lipoplexes synthesized in microchip serpentine-WC with split were evaluated in terms of efficacy to transfect (TE) dendritic cells *in vitro* by analyzing cell GFP production (Figure 3.6).

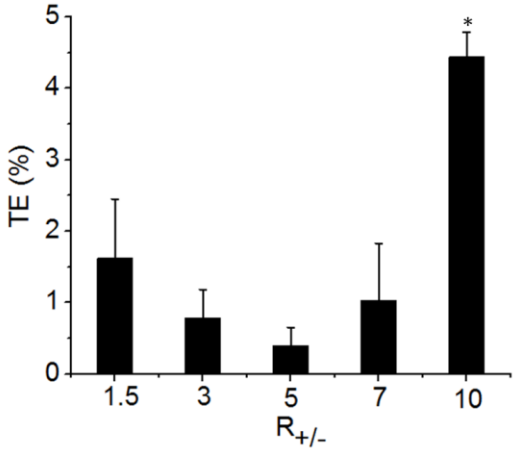

Figure 3.6 - *In vitro* transfection efficacy (TE) of dendritic cells using lipoplexes at different molar charge ratios ($R_{+/-}$ 1.5, 3, 5, 7 and 10) synthesized by microfluidics method. The droplet-based microfluidic system with wide serpentine channel (WC) and split region was operated with volume fraction 0.25, Ca = $3x10^{-3}$, Q_{oil} = 6.5 µL min^{-1} and $R_{+/-}$ varying in 1.5, 3, 5, 7 and 10. The error bars represent standard deviation of means (n = 4). Means statistically significant different by Tukey's test ($P<0.10$) were flagged with an asterisk (*).

DCs showed higher transfection efficiency when using lipoplexes $R_{+/-}$ 10 produced by microfluidic method (4.44 ± 0.35%) (Figure 3.6). The low transfection efficiency of DCs *via* lipofection is already known. VAN TENDELOO *et al.* (5) transfected monocyte-derived DCs with mRNA encoding GFP by lipofection achieving 4% of TE. DCs use phagocytosis and/or macropyocytosis as effective pathway for transfection (9), which requires more precise lipoplex size and PdI to transfect (42). Besides the statically analysis, lipoplexes $R_{+/-}$ 10 showed tendency to lower size (85.27 nm) and PdI (0.20) than the others. Moreover, transfected DC with lipoplexes containing less nucleic acid ($R_{+/-}$ 10) can be advantageous, since DCs exposed to high concentration of nucleic acids can significantly express less cytokines and activation markers (43).

Besides transfecting, lipoplexes should activate DCs in order to allow antigen presenting cells to play their role as immunological response starter. For this, the increase of costimulatory molecules expression by dendritic cells was evaluated for lipoplexes synthetized by microfluidic method. Figure 3.7 showed DC expression of CD80 and CD86 when treated with lipoplexes $R_{+/-}$ 1.5, 3, 5, 7 and 10.

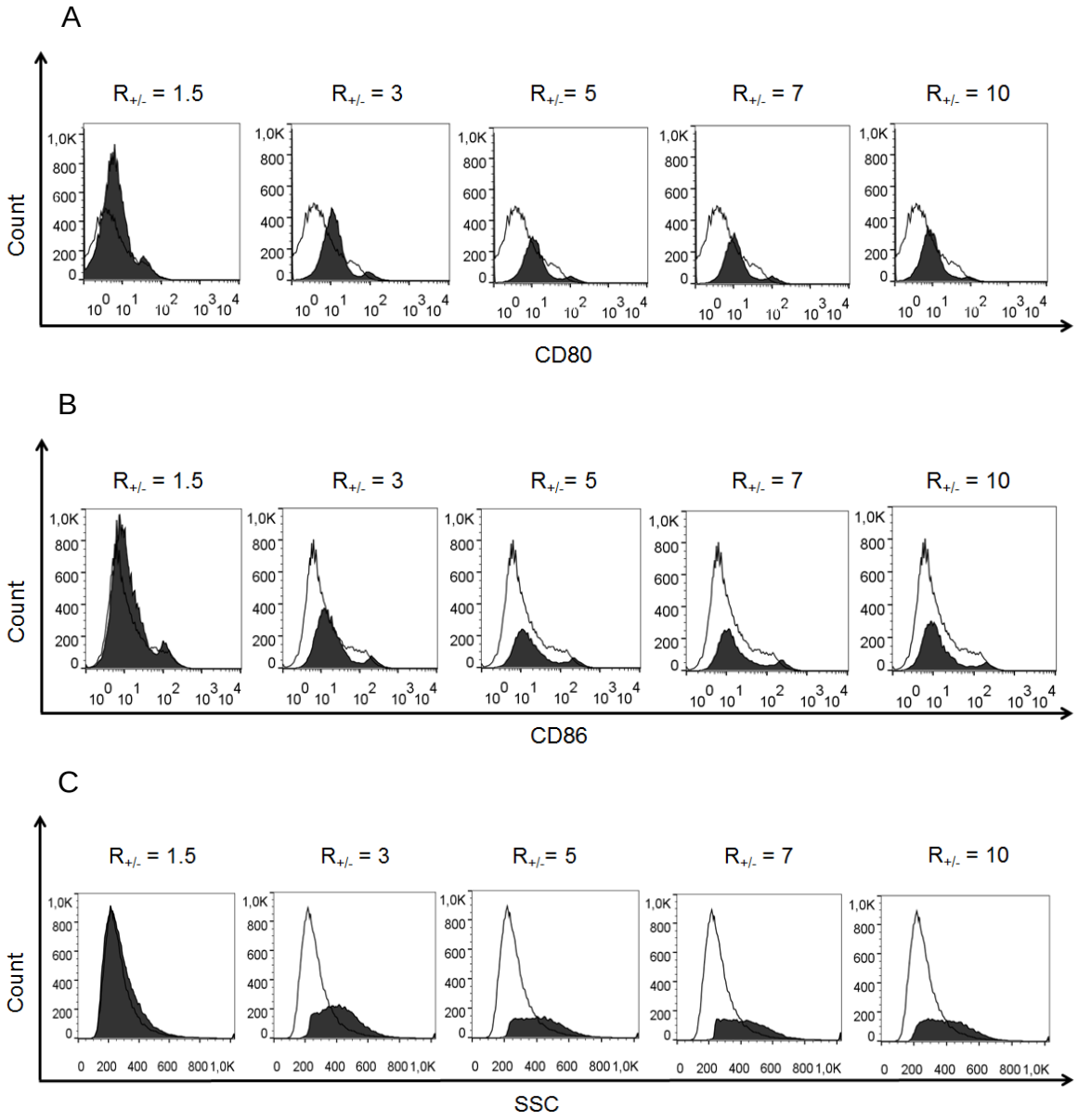

Figure 3.7 - DCs activation after transfection with lipoplexes produced by microfluidics method. The droplet-based microfluidic system with wide serpentine channel (WC) and split region was operated with volume fraction 0.25, Ca = $3x10^{-3}$, Q_{oil} = 6.5 µL min^{-1} and $R_{+/-}$ varying in 1.5, 3, 5, 7 and 10. Histograms of CD80 (A) and CD86 (B) (costimulatory molecules B7-1 and B7-2, respectively) expressed by

DCs is shown. Histograms of DC granulocyte (SSC – side scatter) (C) indicate lipoplex internalization by cells. Histograms are composed of iDC (immature dendritic cells) represented by solid dark lines overlaid by histogram of DCs treated with corresponding type of lipoplex represented by solid-filled background.

The median fluorescence intensity (MFI) of CD80 expressed by DCs transfected with lipoplexes $R_{+/-}$ 1.5 (MFI = 5.73), 3 (11.00), 5 (11.10), 7 (10.60) and 10 (8.74) increased in relation to iDC (3.92), as shown by Figure 3.7A shifting the corresponding curve to right. In a similar way, the MFI of CD86 expression increased for all lipoplexes $R_{+/-}$ 1.5 (10.30), 3 (15.40), 5 (15.10), 7 (13.70) and 10 (11.00) regarding to iDC (8.74) (Figure 3.7B). The positive control (mDC – mature dendritc cells) also increased the MFI of CD80 (4.49) and CD86 (9.56) expression. Beyond that, we verified, such as in previously studies (7,8), that empty cationic liposomes EPC/DOTAP/DOPE activated DCs (MFI of CD80 increased to 7.23 and for CD86 to 12.20). The lipofection action upon DCs activation was also showed by Denis-Mize *et al.* (42) by co-culturing transfected DCs *via* cationic microparticles with antigen-specific T cells. They verified an increase in IL-2 production by the culture in function of microparticle tested.

Another parameter evaluate was the variation in DC granularity (SSC) according to lipoplexes used (Figure 3.7C). DCs showed to increase granularity (internal structure and complexity) when incorporating this cationic liposomes (7). Thus, median of SSC of DCs increased when transfected with all lipoplexes tested $R_{+/-}$ 1.5 (median of SSC = 258), 3 (410), 5 (415), 7 (422) and 10 (399) comparing to iDC (248) and mDC (217). Even though easier uptake by DCs, lipoplex $R_{+/-}$ 7 did not present the best TE since there is a specific pathway that lipoplexes should be internalized to effectively produce the recombinant protein (9).

4. Conclusion

The droplet-based microfluidic system was used to produce lipoplexes in reproducible and suitable strategy to transfect DCs. Droplet system operating at volume fraction, ratio between $Q_{aqueous}$ and Q_{oil}, 0.25 ensure the droplet formation with size 1.5 times the serpentine channel. Cationic liposomes maintain their properties after processing, even if surfactant residual in the aqueous phase. Thus,

allowing the use of these cationic liposomes in other droplet devices. This droplet microfluidic system allow the incorporation of more amount of pDNA to CL (R+/-=1.5) than conventional method, while maintaining lipoplexes monodisperse and with positive charge. Mixing provided by droplets formed in thin serpentine channel (200 µm of width) lead to decrease lipoplexes polydispersity. Lipoplexes R+/- 10, exhibiting lower size and PdI tendency, provided the higher transfection efficiency in DCs, besides activating them. Therefore the droplet-based microfluidic system showed as a potential tool to modulate lipoplexes properties on demand.

5. Acknowledgements

The study was financially supported by the São Paulo Research Foundation (FAPESP process number 2014/24797-2). The microfluidic devices were fabricated at Microfabrication Laboratory (LMF) in Brazilian Synchrotron Light Laboratory (LNLS). We would like to thank Professor Marcelo Bispo de Jesus to pDNA providing and technical support in biological field, Professor Rosiane Lopes da Cunha to provide the use of Malvern Zetasizer equipment acquired with project EMU (FAPESP process number 2009/54137-1), Anton Paar rheometer and Teclis tensiometer and also Professor Maria Helena Andrade Santana for the use of Malvern Zetasizer equipment.

6. References

1. Kim J, Hwang I, Britain D, Chung TD, Sun Y, Kim D-H. Microfluidic approaches for gene delivery and gene therapy. Lab Chip. 2011;11(23):3941–8.

2. Serikawa T, Kikuchi A, Sugaya S, Suzuki N, Kikuchi H, Tanaka K. In vitro and in vivo evaluation of novel cationic liposomes utilized for cancer gene therapy. J Control Release. 2006;113(3):255–60.

3. Felgner PL, Gadek TR, Holm M, Roman R, Chan HW, Wenz M, et al. Lipofection: a highly efficient, lipid-mediated DNA-transfection procedure. Proc Natl Acad Sci USA. 1987;84(21):7413–7.

4. Barbuto JAM, Ensina LFC, Neves AR, Bergami-Santos PC, Leite KRM, Marques R, et al. Dendritic cell–tumor cell hybrid vaccination for metastatic cancer. Cancer Immunol Immunother. 2004;53(12):1111–8.

5. Van Tendeloo VFI, Ponsaerts P, Lardon F, Nijs G, Lenjou M, Van Broeckhoven C, et al. Highly efficient gene delivery by mRNA electroporation in human hematopoietic cells: superiority to lipofection and passive pulsing of mRNA and to electroporation of plasmid cDNA for tumor antigen loading of dendritic cells. Blood. 2001;98(1):49–56.

6. Ma Y, Zhuang Y, Xie X, Wang C, Wang F, Zhou D, et al. The role of surface charge density in cationic liposome-promoted dendritic cell maturation and vaccine-induced immune responses. Nanoscale. 2011;3(5):2307–14.

7. Vitor MT, Bergami-Santos PC, Piedade Cruz KS, Pinho MP, Marzagão Barbuto JA, La Torre LG De. Dendritic Cells Stimulated by Cationic Liposomes. J Nanosci Nanotechnol. 2016;16(1):270–9.

8. Vitor MT, Bergami-Santos PC, Z?mpero RHF, Cruz KSP, Pinho MP, Barbuto JAM, et al. Cationic liposomes produced via ethanol injection method for dendritic cell therapy. J Liposome Res. 2016;

9. De Haes W, Van Mol G, Merlin C, De Smedt SC, Vanham G, Rejman J. Internalization of mRNA lipoplexes by dendritic cells. Mol Pharm. 2012;9(10):2942–9.

10. Hsieh AT-H, Pan PJ-H, Lee AP. Rapid label-free DNA analysis in picoliter microfluidic droplets using FRET probes. Microfluid Nanofluidics. 2009;6(3):391–401.

11. Hsieh AT-H, Hori N, Massoudi R, Pan PJ-H, Sasaki H, Lin YA, et al. Nonviral gene vector formation in monodispersed picolitre incubator for consistent gene delivery. Lab Chip. 2009;9(18):2638–43.

12. Chou LY, Ming K, Chan WC. Strategies for the intracellular delivery of nanoparticles. Chem Soc Rev. 2011;40(1):233–45.

13. Bringer MR, Gerdts CJ, Song H, Tice JD, Ismagilov RF. Microfluidic systems for chemical kinetics that rely on chaotic mixing in droplets. Philos Trans R Soc London A Math Phys Eng Sci. 2004;362(1818):1087–104.

14. Lin B. Microfluidics: technologies and applications. Vol. 304. Springer; 2011.

15. Teh S-Y, Lin R, Hung L-H, Lee AP. Droplet microfluidics. Lab Chip. 2008;8(2):198–220.

16. Song H, Tice JD, Ismagilov RF. A Microfluidic System for Controlling Reaction Networks in Time. Angew Chemie Int Ed. 2003;42(7):768–72.

17. Zheng B, Tice JD, Ismagilov RF. Formation of droplets of alternating composition in microfluidic channels and applications to indexing of concentrations in droplet-based assays. Anal Chem. 2004;76(17):4977–82.

18. Brouzes E, Medkova M, Savenelli N, Marran D, Twardowski M, Hutchison JB, et al. Droplet microfluidic technology for single-cell high-throughput screening. Proc Natl Acad Sci. 2009;106(34):14195–200.

19. Chan HF, Ma S, Leong KW. Can microfluidics address biomanufacturing challenges in drug/gene/cell therapies? Regen Biomater. 2016;rbw009.

20. Muradoglu M, Stone HA. Mixing in a drop moving through a serpentine channel: a computational study. Phys Fluids. 2005;17(7):73305.

21. Tice JD, Lyon AD, Ismagilov RF. Effects of viscosity on droplet formation and mixing in microfluidic channels. Anal Chim Acta. 2004;507(1):73–7.

22. Moreira NH, de Jesus de Almeida AL, de Oliveira Piazzeta MH, de Jesus DP, Deblire A, Gobbi AL, et al. Fabrication of a multichannel PDMS/glass analytical microsystem with integrated electrodes for amperometric detection. Lab Chip. 2009;9(1):115–21.

23. Balbino TA, Aoki NT, Gasperini AAM, Oliveira CLP, Azzoni AR, Cavalcanti LP, et al. Continuous flow production of cationic liposomes at high lipid concentration in microfluidic devices for gene delivery applications. Chem Eng J. 2013;226(0):423–33.

24. Rigoletto TP, Silva CL, Santana MH, Rosada RS, De La Torre LG. Effects of extrusion, lipid concentration and purity on physico-chemical and biological properties of cationic liposomes for gene vaccine applications. J Microencapsul. 2012;29(8):759–69.

25. Radaic A, Paula E De, Jesus MB De. Factorial design and development of solid lipid nanoparticles (SLN) for gene delivery. J Nanosci Nanotechnol. 2015;15(2):1793–800.

26. Tice JD, Song H, Lyon AD, Ismagilov RF. Formation of droplets and mixing in multiphase microfluidics at low values of the Reynolds and the capillary numbers. Langmuir. 2003;19(22):9127–33.

27. Berges C, Naujokat C, Tinapp S, Wieczorek H, Höh A, Sadeghi M, et al. A cell line model for the differentiation of human dendritic cells. Biochem Biophys Res Commun. 2005;333(3):896–907.

28. March JC, Rao G, Bentley WE. Biotechnological applications of green fluorescent protein. Appl Microbiol Biotechnol. 2003;62(4):303–15.

29. Lee APICA, Hsieh AT-HICA. Microfluidic device for forming monodisperse lipoplexes. Vol. 11746024. US: US 2004/0068019 A1 (Apr, 2004) Higuchi et al. 516/9; WO 2004/071638 (Aug, 2004) ; WO /96/32116 (Oct, 1996); 2010.

30. Clausell-Tormos J, Lieber D, Baret J-C, El-Harrak A, Miller OJ, Frenz L, et al.

Droplet-Based Microfluidic Platforms for the Encapsulation and Screening of Mammalian Cells and Multicellular Organisms. Chem Biol. 2008;15(5):427–37.

31. Lai E, van Zanten JH. Real time monitoring of lipoplex molar mass, size and density. J Control release. 2002;82(1):149–58.

32. Rakhmanova VA, Pozharski E V, MacDonald RC. Mechanisms of Lipoplex Formation: Dependence of the Biological Properties ofTransfection Complexes on Formulation Procedures. J Membr Biol. 2004;200(1):35–45.

33. Bordi F, Cametti C, Diociaiuti M, Gaudino D, Gili T, Sennato S. Complexation of anionic polyelectrolytes with cationic liposomes: evidence of reentrant condensation and lipoplex formation. Langmuir. 2004;20(13):5214–22.

34. Balbino TA, Gasperini AAM, Oliveira CLP, Azzoni AR, Cavalcanti LP, De La Torre LG. Correlation of the Physicochemical and Structural Properties of pDNA/Cationic Liposome Complexes with Their in Vitro Transfection. Langmuir. 2012;28(31):11535–45.

35. Rosada RS, Silva CL, Santana MH, Nakaie CR, De La Torre LG. Effectiveness, against tuberculosis, of pseudo-ternary complexes: peptide-DNA-cationic liposome. J Colloid Interface Sci. 2012;373(1):102–9.

36. Muthu MS, Kulkarni SA, Raju A, Feng SS. Theranostic liposomes of TPGS coating for targeted co-delivery of docetaxel and quantum dots. Biomaterials. 2012;33(12):3494–501.

37. Rejman J, Oberle V, Zuhorn IS, Hoekstra D. Size-dependent internalization of particles via the pathways of clathrin- and caveolae-mediated endocytosis. Biochem J. 2004;377(Pt 1):159–69.

38. Jacobson SC, McKnight TE, Ramsey JM. Microfluidic devices for electrokinetically driven parallel and serial mixing. Anal Chem. 1999;71(20):4455–9.

39. Handique K, Burns MA. Mathematical modeling of drop mixing in a slit-type microchannel. J Micromechanics Microengineering. 2001;11(5):548.

40. Kumacheva E, Garstecki P. Formation of Droplets in Microfluidic Systems. In: Microfluidic Reactors for Polymer Particles. John Wiley & Sons, Ltd; 2011. p. 41–94.

41. Baroud CN, Gallaire F, Dangla RR. Dynamics of microfluidic droplets. Lab Chip. 2010;10(16):2032–45.

42. Denis-Mize KS, Dupuis M, MacKichan ML, Singh M, Doe B, O'Hagan D, et al. Plasmid DNA adsorbed onto cationic microparticles mediates target gene

expression and antigen presentation by dendritic cells. Gene Ther. 2000;7(24):2105.

43. Karikó K, Buckstein M, Ni H, Weissman D. Suppression of RNA recognition by Toll-like receptors: the impact of nucleoside modification and the evolutionary origin of RNA. Immunity. 2005;23(2):165–75.

7. Supplementary data

7.1. Physico-Chemical properties of Cationic Liposome Stability after droplet-based microfluidic processing

Investigation of cationic liposomes stability in w/o emulsion by measuring physico-chemical properties of cationic liposomes before and after processing in droplet-based microfluidic device (Table S.1).

Table S.1 - Physico-chemical properties of cationic liposomes before and after droplet-based microfluidic processing.

Cationic liposomes	Mean diameter (± S.D.) nm and distribution (± S.D.) %[(i)]	PdI[(ii)]	Zeta potential (± S.D.) mV
Before droplet processing	95.54 ± 15.38 (100 ± 0)	0.144 ± 0.016	60.50 ± 3.36
After droplet processing	86.85 ± 13.52 (100 ± 0)	0.164 ± 0.022	57.60 ± 2.57

Results represent means ± S.D., n = 3.
[(i)] Number-weighted average diameter and distribution (N-distribution).
[(ii)]PdI: Polydispersity index of samples vary in ascending order from 0 to 1.

7.2. Investigation of experimental parameters: Capillary Number (Ca), Molar Charge Ratio ($R_{+/-}$) and Microchip Design

The effect of capillary number in lipoplexes physico-chemical properties was showed in Figure S.1. Comparing physico-chemical characteristics of lipoplexes formed in Ca ranging from $8x10^{-4}$ to $5x10^{-3}$ (Figure S.1), there was no difference in lipoplexes size around 100 nm, even the high standard deviation (144.03 ± 52.16 nm) presented by lipoplexes produced at Ca $1x10^{-3}$. In general, lipoplexes polydispersity remained about 0.2, exception of lipoplexes obtained at Ca $1x10^{-3}$ that presented higher polydispersity (0.467 ± 0.005). Moreover, considering zeta potential analysis, lipoplexes had a positive charge around 45 mV, even with pDNA

addiction in cationic liposomes. However, when produced at Ca $1x10^{-4}$ and $1x10^{-3}$, their charge decreased achieving 25.03 ± 6.64 mV and 30.87 ± 4.10 mV, respectively.

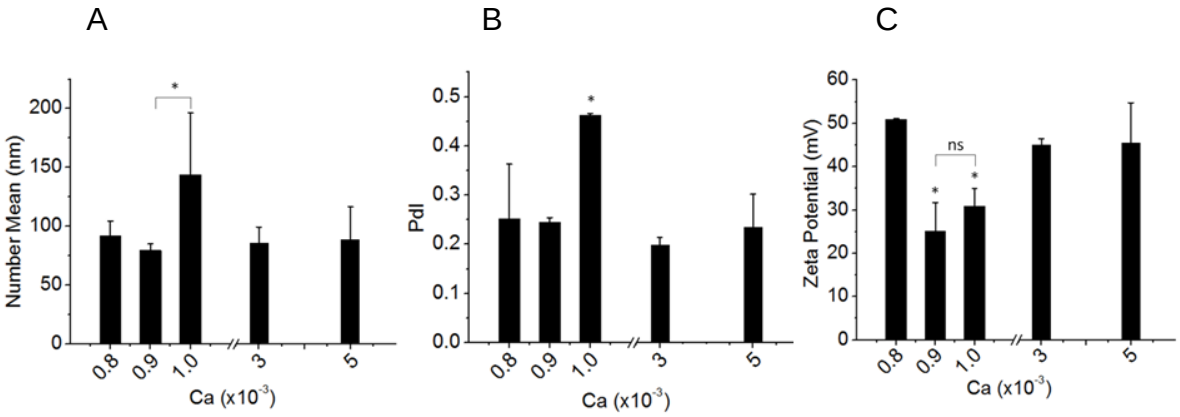

Figure S.1 – Impact of capillary number (Ca) on lipoplexes characteristics in terms of size (A), polydispersity (PdI) (B) and zeta potential (C). The droplet-based microfluidic system with serpentine-TC and split region (Figure 3.1B) was set at volume fraction 0.25, $R_{+/-}$ = 3 and varying Ca from $8x10^{-4}$ to $5x10^{-3}$. The error bars represent standard deviation of means (n = 3). Means statistically significant different by Tukey's test (P<0.10) were flagged with an asterisk (*) and non-different means with "ns".

Then, the effect of molar charge ratio and different microdevice designs on the final physico-chemical properties of lipoplexes synthesized in droplet-based microfluidic devices (Table S.2).

Table S.2 - The effect of molar charge ratio ($R_{+/-}$) and microchip design on physico-chemical properties of lipoplexes.

	Variable parameter	Mean diameter (± S.D.) nm and distribution (± S.D.) %[iii]	PdI[iv]	Zeta potential (± S.D.) mV
$R_{+/-}$[i]	1.5	176.95 ± 35.71 (100.0 ± 0)	0.292 ± 0.152	39.50 ± 8.51
	3.0	161.10 ± 15.98 (100.0 ± 0)	0.202 ± 0.029	38.83 ± 9.42
	5.0	158.45 ± 14.50 (100.0 ± 0)	0.281 ± 0.111	51.73 ± 7.91
	7.0	138.05 ± 2.48 (100.0 ± 0)	0.217 ± 0.069	44.10 ± 6.32
	10.0	151.75 ± 2.05 (100.0 ± 0)	0.185 ± 0.057	49.73 ± 10.30
Design[ii]	TC without split	249.35 ± 3.23 (56.2 ± 7.92) 107.34 ± 17.62 (43.8 ± 7.92)	0.235 ± 0.057	41.50 ± 7.64
	TC with split	159.80 ± 17.82 (100.0 ± 0)	0.189 ± 0.024	44.20 ± 2.12
	WC without split	249.4 ± 7.57 (58.3 ± 7.5) 99.58 ± 12.76 (41.7 ± 7.5)	0.392 ± 0.013	27.90 ± 1.41
	WC with split	159.07 ± 13.06 (100.0 ± 0)	0.240 ± 0.016	36.80 ± 14.40

At first, the droplet-based microfluidic system with serpentine-TC with split regions (Figure 3.1B) operated with volume fraction set at 0.25 and Ca at $3x10^{-3}$, $R_{+/-}$ varied of 1.5, 3, 5, 7 and 10. Then, to evaluate microchip design, volume fraction was set at 0.25, Ca at $3x10^{-3}$ and $R_{+/-}$ at 3.0. Droplet-based platform with thin (TC) and wide serpentine channel (WC) and with or without a split region (Figure 3.1B) were tested. Results represent means ± S.D., n = 3.
(i)$R_{+/-}$: molar charge ratio between nucleic acids and cationic lipids from liposomes.
*(ii)*Device design: Droplet-based microfluidic system with two types of serpentine widths (TC-200 µm and WC-400 µm) and in the presence or absence of split region (Figure 3.1B).
*(iii)*Intensity-weighted average diameter and distribution (I-distribution).
*(iv)*PdI: Polydispersity index of samples vary in ascending order from 0 to 1.

7.3. Strategy of dendritic cells and GFP analysis

For phenotypic characterization and evaluation of the liposomes incorporation, we delimited gate with cell size and granularity compatible with the DCs, by analysis of the "side scatter" (SSC) - granularity (internal structure and complexity) and the "forward scatter" (FSC) - relative size of the cells (Figure S.2A). Considering the analyzed region bounded by the gate, cells were analyzed through the expression of the myeloid marker CD11c and the antigen presenting cell marker, HLA-DR. Furthermore, when we analyzed the expression of co-stimulatory molecules, CD80 and CD86, within the population HLA-DR^+CD11c^+, called Gate R1 (Figure S.2B) in order to investigate DC activation.

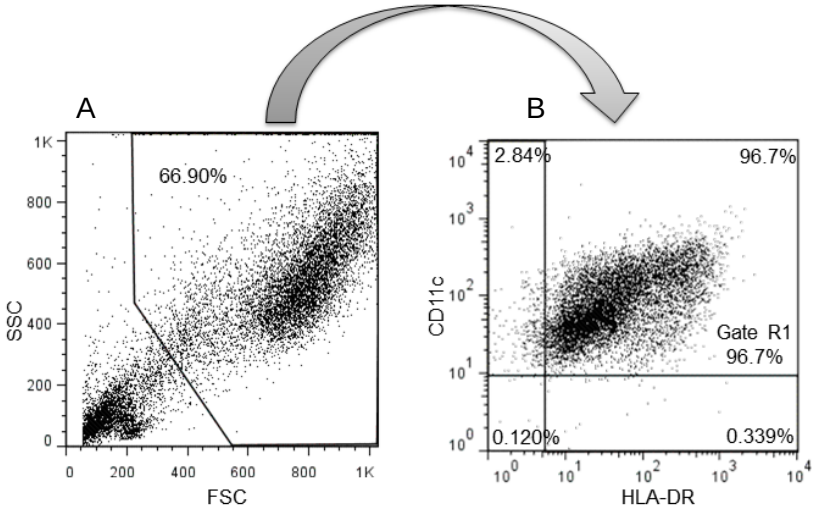

Figure S.2 – Strategy of dendritic cells analysis. (A) Dot Plot graph of SSC (side scatter) by FSC (forward scatter) to delimit DCs gate. (B) Graph of CD11c *versus* HLA-DR to delimit Gate R1, corresponding to cells double-positive.

Then, to determinate the transfection efficiency, we used FITC histograms of DCs treated with liposomes and lipoplexes, like showed in Figure S.3, in order to detect the GFP production and, consequently, the ratio between GFP producer cells and total of DCs in Gate R1. For this, we plotted FITC histogram of DCs in Gate R1 treated with liposomes (filled graph with solid line in Figure S.3) to define the gate of negative FITC that is around 99% of this population. Then, we overlaid the graph with the FITC histogram of DCs in Gate R1 treated with lipoplexes (empty graph with dot line in Figure S.3) to define the TE provided by the lipoplexes analyzed.

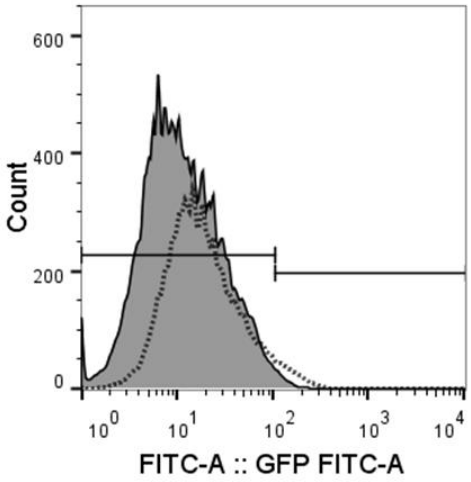

Figure S.3 – Strategy of transfection efficiency analysis. At first, we determined the negative gate of FITC that is around 99% of this population in the FITC histogram of DCs from Gate R1 treated with liposomes (filled graph with solid line). Then, we overlaid the graph with the FITC histogram of DCs from Gate R1 treated with lipoplexes (empty graph with dot line) in order to define the TE provided by the lipoplexes analyzed.

The procedure to define Gate R1 was performed for all samples, such as mature dendritic cells stimulated by TNF-α (positive control - mDC), immature dendritic cells (iDC), DCs treated with liposomes and lipoplexes. In case of transfection efficiency, the strategy showed below was applied for all DCs in Gate R1 treated with liposome and lipoplexes.

Chapter IV –Tracking the Heterogeneities of CHO Cells Transiently Transfected on a Chip

Micaela Tamara Vitor[1,2], Sébastien Sart[1], Antoine Barizien[1],

Lucimara Gaziola De La Torre[2] & Charles N. Baroud[1*]

[1]LadHyX and Department of Mechanics, Ecole Polytechnique, CNRS-UMR, 91128 Palaiseau, France

[2]School of Chemical Engineering, Department of Bioprocesses and Materials Engineering, University of Campinas (Unicamp), Av. Albert Einstein, 500, Campinas, SP, 13083-852, Brazil

*Corresponding author: baroud@ladhyx.polytechnique.fr

To be submitted to *Biotechnology and Bioengineering*

Abstract

Transient gene expression technology (TGE) enables the rapid production of large amount of recombinant proteins, without the need of fastidious screening of the producing cells required in conventional protocols using stable transfection (ST). However, several barriers require to be overcome before reaching the production yield achievable by ST. In view of optimizing the production yields in TGE, a better understanding and control over the transfection conditions at single cell level using are critically required. In this study, a universal droplet microfluidic platform was used to assess the heterogeneities of CHO-S population transiently transfected with different types of lipoplexes. A single cell analysis of GFP production kinetics revealed the presence of a subpopulation producing significantly high levels of recombinant proteins. The charge and the DNA content of the different lipoplexes regulated differentially HPs average size, their relative abundance and their specific productivity. These high producers showed increased cell size in comparison to the average population. Lipoplexes with positive charge produced more HPs. Lipoplexes loading more amount of pDNA showed the higher GFP specific productivity of HPs.

Keywords: droplet microfluidics, transient gene expression, cationic liposomes, single-cell analysis.

1. Introduction

In the past decades, Chinese Ovary cells (CHO) have emerged as one of the most powerful tool for the production of recombinant therapeutic proteins. CHO cells can secrete very high recombinant product yields, which glycosilation profile promotes their efficient bioactivity. Moreover, CHO cells have been successfully adapted for expansion in serum free media and for large-scale culture in stirred tank bioreactors (1,2). Consequently, current bioprocess making use of CHO cells can effectively meet the clinical demand (3).

The first step to achieve the production of recombinant proteins by CHO cells requires their genetic engineering. While CHO cells can be easily transfected,

current protocols require transgene integration in the host genome, which usually followed by lengthy procedure of clonal selection and adaption to large-scale and animal protein free culture conditions (3). Contrasting with these labor-intensive procedures of stable transfection (ST), transient gene expression technology (TGE) enables the rapid production of large amount of recombinant, without the need of fastidious screening of the producing cells. Moreover, no adaption to new culture condition is required (4). However, several barriers require to be overcome before reaching the production yield achievable by ST. Among them, because of the episomal location of transgene, exogenous DNA is lost after several rounds of cell division. As a consequence, the production occurs for significantly shorter time period than ST. In addition, the limited control over DNA delivery induces a large heterogeneity in the production rate of individual cells (5). Consequently, in view of optimizing the production yields, a better understanding and control over the transfection conditions at single cell level using TGE are critically required.

Several carrier systems, such as viral and nonviral vectors, are currently used for the delivery of recombinant nucleic acids into producing cells (6). While nonviral systems complexed with nucleic acids (e.g. lipoplexes and polyplexes) show significantly lower transfection efficiency, they demonstrate biological inertness, improved safety and they can be easily produced at large-scale, in contrast to viral systems. Consequently, current research efforts are directed to increase the efficiency of nonviral vectors for DNA delivery, by better understanding the mechanism of lipoplex uptake and internalization (7).

On other hand, the recent advances in microfluidics have created exciting prospects for gene delivery and therapy. The controlled hydrodynamics within microfluidic systems enables precise control of parameters involved in gene transfection, together with a significant reduction of the volumes of reagents (8). More recently, droplets microfluidics has enabled the development of new tools for cell manipulation, such as the encapsulation of individual cells, the biological compartmentalization etc (9,10). More importantly, the rapid accumulation of secreted protein in droplets enables their detection within shorter time period than conventional culture systems (e.g. culture flask, bioreactors etc.). In addition,

single-cells in droplets can be monitored for long time periods, which enables to dynamically track individualized response to biological stimuli by optical imaging (11). However, while investigations demonstrated the capability of such devices to support non-viral transfection (12), the full capability droplets to support the long term tracking and, consequently, to better understand the cell production heterogeneity after TGE has not been exploited so far.

Thus, this work aims at deeply investigating the response of a CHO-S (recombinant CHO cells suspension culture) population under different transient transfection conditions. For this purpose, the applications a droplets microfluidic platform will be extended to investigate, at the single cell level, the influence of different types of lipoplexes on production of recombinant GFP.

2. Materials and methods

2.1. Microfabrication

Standard dry soft lithography was used for the fabrication of the single-cell microchip and the liposome production device, as previously described (13). Briefly, dry film photoresists (Eternal Laminar, Taiwan) were sequentially laminated with an office laminator (PEAK PS320, UK) at 100°C on a glass slide, then exposed to UV light (LightningCure LC8, Hamamatsu, Japan) with the photo-masks. The molds were revealed using a 1% w/w K_2CO_3 (Sigma-Aldrich, USA). Polydimethylsiloxane (PDMS, Dow-Corning Sylgard 184, USA, 1/10 ratio of curing agent to bulk material) was poured on mold and cured 2 h at 70 °C. The replicate was covalently bonded to a glass slide using a plasma cleaner (Harrick, Ithaca, USA). In order to provide the manipulation of aqueous droplets in oil, the chips were filled 3 times with Novec Surface Modifer (3M, Paris, France), for 30 minutes at 110°C on a hot plate. In case of chip for liposome production, this surface treatment was not necessary.

The microchip design consists in a 2D chamber with two inlets and one outlet (Figure 4.1A). Single-cell droplets were trapped in 1495 square anchors of d = 120 µm of side, spaced by δ = 240 µm (Figure 4.1A). The chamber has h_1 = 35 µm of height and the anchors h = 135 µm (Figure 4.1B). Cationic liposomes (CL)

were produced in a single hydrodynamic focusing microfluidic device like Balbino *et al.* (14). The cross-junction design has a rectangular cross-section of depth 100 µm and height 135 µm.

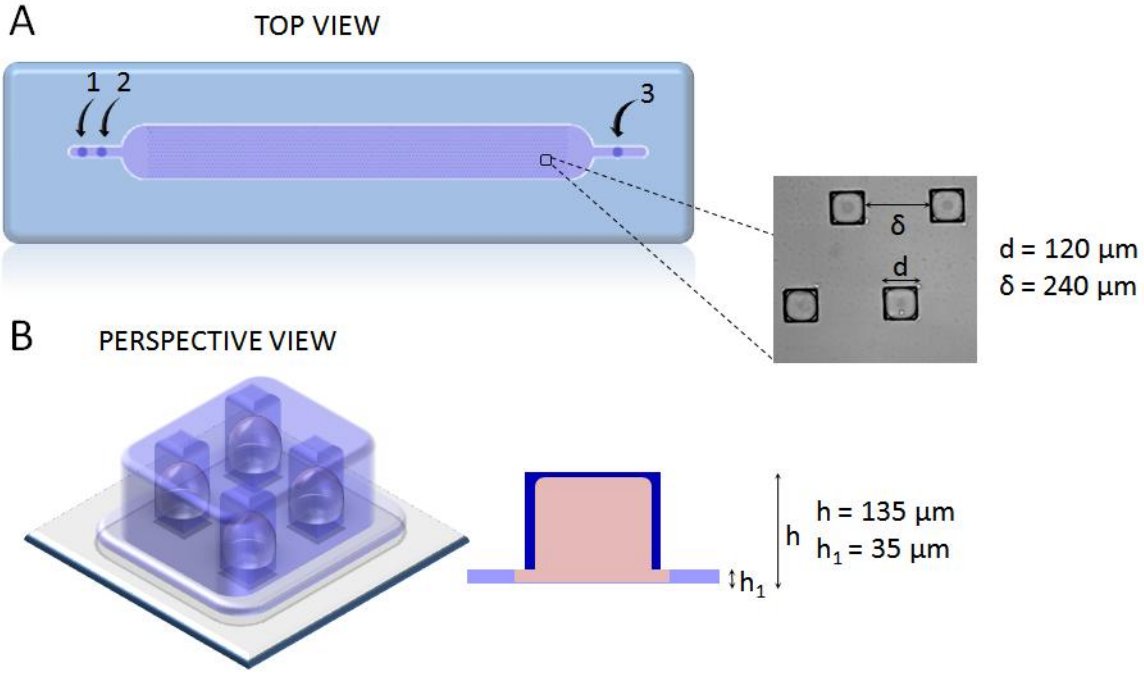

Figure 4.1 - Design of microchip where CHO-S cells were cultivated. The microchip dimension is 0.5 × 4.8 cm with 1495 square anchors (115 × 13). The microchip have two inlets: 1 for oil phase (FC-40/RAN) and 2 for aqueous phase (cells + lipoplexes + agarose), and one exit (3). Microchip top view (A) shows that each square anchor has d = 120 µm of side, spaced by δ = 240 µm. Lateral section (B) shows that the chamber height is h_1 = 35 µm and the anchor height h = 135 µm.

2.2. Production and Characterization of CL and their Complexes

Cationic liposomes were formed along the main channel of cross-junction microfluidic device. At first, EGG (egg phosphatidylcholine), DOTAP (1,2-dioleoyl-3-trimethylammonium-propane) and DOPE (1,2-dioleoyl-sn-glycero-3-phosphoethanolamine) (50/25/25 % molar) all from Lipoid (Germany) were dispersed in anhydrous ethanol to achieve 25 mM of total lipid concentration, following the protocol established by Rigoletto *et al.* (15). The lipid dispersion was injected into the center flow at 10.92 µL min^{-1}. Simultaneously, DEPC-treated water (Life Technologies, USA) were injected at 54.6 µL min^{-1} into two lateral sides.

Liposome samples were collected from the exit and leaved for at least 4 hours at 4 °C.

For lipoplexes formation, the CL and pDNA (pMAX GFP, Lonza – see Annex I) were mixed by vortexing for 30 seconds. Several liposomes/pMAX GFP molar ratios were used to produce different types of lipoplexes, characterized by $R_{+/-}$, the ratio between the positive charge from cationic liposomes and negative charge from pDNA. Cells were transfected setting pDNA at 0.07 µg and liposomes varying from 1.77 µL ($R_{+/-}$ = 5), 1.05 µL ($R_{+/-}$ = 3) and 0.53 µL ($R_{+/-}$ = 1.5).

To characterize the nanoparticles properties, CL and their lipoplexes were diluted in DEPC water. The average hydrodynamic diameter, the size distribution, polydispersity index and zeta potential were measured by dynamic light scattering (the scattering angle was 173°, backscattering) (Malvern Zetasizer Nano Series, model ZEN3600 - UK) using a Ne–He laser. The mean diameter and the distribution of particle sizes were calculated using CONTIN algorithm.

2.3. Cell Culture and Labeling

FreeStyle CHO-S (Life Technologies, CA, USA) cells were cultivated at 37°C into 25 cm^2 Ultra-Low Attachment flasks (Corning, USA) in a humidified incubation set up at 8% CO_2. The culture medium was composed of FreeStyle CHO Expression Medium supplemented with 8 mM GlutaMAX (Gibco, USA). The cells were passaged every 48–72 hours, by reseeding at a concentration of 1 x 10^5 cells.mL^{-1}.

To monitor the CHO-S behavior in culture, the cells were labeled with CellTracker Red CMTPX Dye (Thermo Scientific), following the manufacturer instructions. To measure the viability, the CHO-S were stained for ReadyProbes Cell Viability Imaging Kit Blue/Red (Thermo Scientific), according to the provided directions.

2.4. Gels

Type IX ultra-low-gelling Agarose (Sigma) was used to provide a mechanical support for the non-adherence cells to keep them stationary. The EEO

(electroendosmosis) of this specific type of agarose is low (i.e. <0.12), ensuring limited electrostatic interactions (either attractive or repulsive) between charged lipoplexes and the hydrogel. The average pore size of the agarose gels is of about 500 nm, thus significantly larger than the lipoplexes size. For the experiments, a 70 μL solution containing 5 x 10^3 cells in culture medium was mixed with a 0.3% liquid agarose solution. The concentration of resulting agarose gels was of about 1%. At this concentration, the mechanical properties of the agarose gel enable the cells to be firmly retained in the anchors (16). However, it was expected to observe a limited cell growth of the agarose encapsulated CHO-S, due to the low metastatic potential and the low degree of transformation of CHO-S at low passage number (17).

2.5. Chip Loading and *In-Situ* Transfection

The chip loading with cells was performed using a three-step protocol, as previously described (16). (1) The microchip is entirely filled with FC-40 (Fluorinert Electronic Liquid FC-40 from 3M, USA), a fluorinated oil, supplemented with 0.5% (w/v) a PEGylated surfactant (008-FluoroSurfactant, RAN Biotechnologies, USA); (2) the FC-40/surfactant flow is stopped and a solution containing 5 x 10^3 cells (70 µL), 3 % w/v ultra-low gelling agarose (Sigma) (30 µL) and 4 µL of lipoplexes at different molar charge ratio ($R_{+/-}$ = 1.5, 3 and 5) in culture medium is flowed at 10 µL min^{-1}, we used 10^{-5} µg pDNA/cell and aprox. 10^5 lipoplexes (number of particles)/cell for all conditions (see supplementary data); (3) once the chamber is filled the flow of cells/lipoplexes solution is stopped and FC-40/RAN inserted at a flow rate increasing from 5 to 50 µL min^{-1} to push the cells/lipoplexes solution towards the exit. This creates droplets containing the cells and the lipoplexes sample immobilized on each anchor (18). To promote the interaction between the cells and lipoplexes, the chip was placed for 1 hour in the CO_2 incubator. After incubation, the chip was flushed with pure FC-40 at 20 µL min^{-1} to wash surfactant and the agarose was gelled by placing the chip at 4 °C for 15 minutes. The solidification of the gel droplets allowed us to replace the oil with culture medium, which was flushed into the chip at 20 µL min^{-1} for 10 minutes in order to wash away

the remaining not internalized lipoplexes. Finally, the microchip was filled again with FC-40/surfactant, which surrounded the agarose spheres, thus isolating the droplets from each other. The GFP production was tracked by time lapse microscopy for 62 hours using a fluorescents microscope (Nikon Eclipse Ti-U, Japan), equipped with a EM-CCD (Andor Technology, Northern Ireland).

2.6. Image and Data Analysis

To track recombinant protein production, images were taken every two hours in bright field and in fluorescence to detect CellTracker Red (red filter) and GFP (green filter). Recombinant GFP production was measured by quantifying the green filter intensity evolution of each detected cell. A custom-made MATLAB R2015b program was used to process the images. First, the images with CellTracker Red signal in anchors were thresholded and converted into masks. The objects with a diameter comprised between 10 and 25 µm were considered as cells. The green signal intensity (I_{cell}) was then quantified for each mask derived from the red labeled objects. The green signal measured in rest of the anchors was considered as the background (I_{back}). The green signal per cell (I) was defined as the value of the green signal in the mask minus the green signal in the background: $I=I_{cell}-I_{back}$. In further calculations, it was useful to measure the variation in I between each time and the initial value (I_0). For this we define $\Delta I = I-I_0$.

To measure cell viability, single cells were identified as above from the DAPI signal (*i.e.* NucBlue™ - stained cells). The cells in the DAPI masks labeled for Propidum Iodide were considered as dead cells.

2.7. Statistical Analysis

Each experiment was conducted at least two times. To assess the statistical significance between three independent samples, we used the Kruskal-Wallis test and, to compare two related samples, we used Wilcoxon rank sum test. A p-value < 0.05 was considered statistically significant for both tests.

3. Results and Discussion

TGE enables the production of high recombinant protein yields, whithout the need of lenghty procedures of clonal selection. However, there have been few investigations on the contribution of individual cells on the rate of recombinant protein production of the global population. This work investigates the heterogeneities of GFP expression in a CHO-S population transfected with differents types of lipoplexes. The cationic liposomes EPC/DOTAP/DOPE were produced on a chip and then complex with recombinant DNA in various molar charge ratios ($R_{+/-}$). Lipoplexes were characterized based on their diameter, PdI and ζ. Then, CHO-S were individualized and *in situ* transfected using a universal droplet microfluidic chip (16).

3.1. Characterization of the Physico-Chemical Properties of Liposomes and Lipoplexes

Cationic liposomes (EPC/DOTAP/DOPE) and lipoplexes ($R_{+/-}$ = 1.5, 3, 5) had their properties (size; polydispersity, PdI; and zeta potential, ζ) analyzed and compared by dynamic light scattering (Figure 4.2).

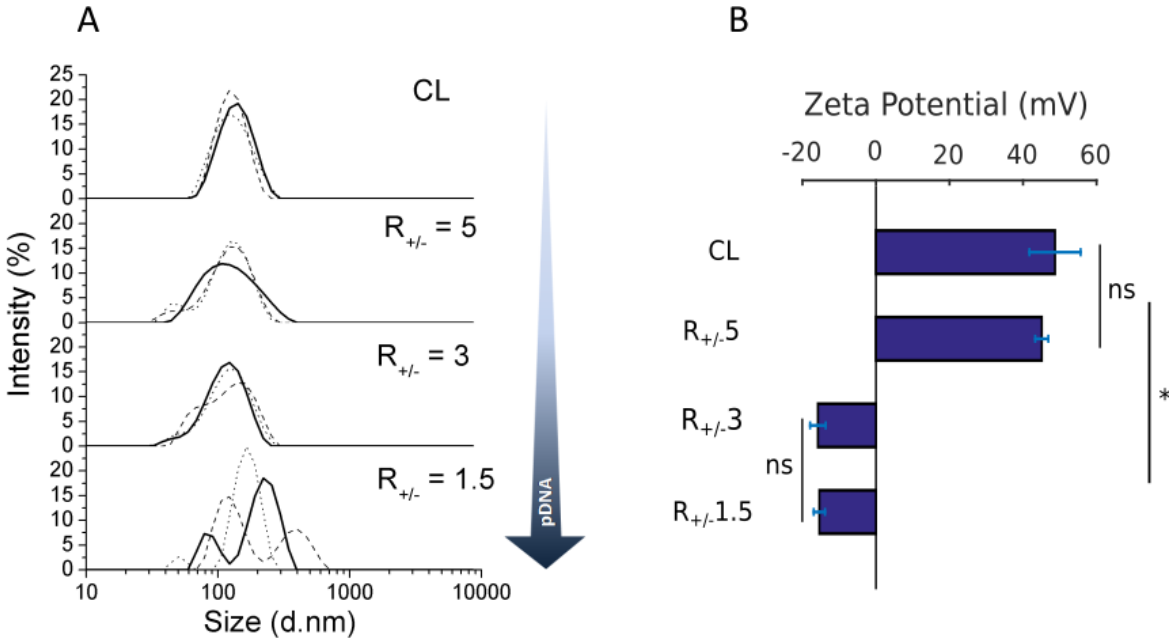

Figure 4.2 - Physico-chemical properties of CL (cationic liposomes EPC/DOTAP/DOPE) and their lipoplexes $R_{+/-}$ = 5, 3 and 1.5. (A) Size represented by intensity-weighted distribution disposed in a way to show the increase in ratio pDNA / liposomes when getting down, like represented by arrow in the right. The dotted, dashed and solid lines in each graph represent one independent size distribution. (B) Zeta potential was no significantly different (ns) between cationic liposome and lipoplexes $R_{+/}$ 5, and between lipoplexes $R_{+/-}$ 3 and 1.5, but different among groups by Wilcoxon rank sum test at 5% significance level. Measures were done in the same conditions as nanoparticles were mixed with cells, *i.e.*, CL and its lipoplexes was diluted in DEPC water. Results represent means ± S.D., n = 3.

The CL average diameter was of 113.56 ± 1.49 nm. The diameter of the liposome population presented a monomodal distribution, as shown by a single peak around 110 nm (Figure 2A). The PdI of the CL was of 0.193 ± 0.013. We can observe that increasing the pDNA content into the liposomes (*i.e.* decreasing $R_{+/-}$ values from 5 to 1.5), the intensity-weighted size distribution tend to increase its heterogeneity. This tendency has already been discussed by Balbino *et al.* (19), demonstrating that the number of double bilayers increases as pDNA content increases and specially for $R_{+/-}$ close to 1.8 it can be detected the presence of a fraction of aggregates with multiple bilayers.The lipoplex average size was 108.03 ± 1.20, 106.57 ± 1.36 and 157.67 ± 9.69 nm, for $R_{+/-}$ 5, 3 and 1.5, respectively. Besides the differences in heterogeneity, lipoplexes presented PdIs ranging from 0.15 to 0.21.

The electric charge of liposomes and the different lipoplexes was analyzed by measuring their zeta potential (ζ). The cationic liposomes EPC/DOTAP/DOPE presented cationic characteristic and showed similar ζ (i.e. 48.7 ± 13.92 mV) (Figure 2B). The net charge of $R_{+/-}$ 5 lipoplex was similar to the empty liposomes (ζ = 45.10 ± 3.57 mV). Surprisingly, the complexation with more pDNA significantly increased the electronegativity of $R_{+/-}$ 3 and 1.5 lipoplexes (*i.e.* - 15.80 ± 4.24 mV and - 15.40 ± 3.06 mV, respectively) (Figure 2B), since previous studies demonstrated that these lipoplexes presented positive zeta potential (19,20). The differences can be related to the conditions for liposome synthesis and pDNA complexation; this present work used DEPC-treated water as diluent while other studies with this liposome system used PBS (19) or sterile water for injection (20).

3.2. Single CHO-S Cell Trapping and Transfection on Chip

The chip consisted in a high aspect ratio chamber equipped with 1495 anchors. The protocol began with the entire chip filling with oil phase FC-40/RAN, which was then replaced by an aqueous phase containing CHO-S cells, liquid agarose and culture medium. The capillary anchors provided high confinement areas for the aqueous phase, contrasting with its lower confinement in the culture chamber. The oil flow in the chamber containing the aqueous phase induced a Rayleigh-Plateau instability around the anchors, a local minima of the surface energy of the aqueous–oil interfaces (21). Consequently, the procedure yielded to the formation of 1495 monodispersed aqueous droplets of a 2 nL volume, trapped in the anchors (Figure 4.3A). After trapping, the distribution of CHO-S cells inside the anchors follows a Poisson law (*i.e.* 33% of the anchors contained only one cell) (Figure 4.3B). In the following part of this study, only the anchors containing single CHO-S cell will be considered for the analysis. As the CHO-S cells were encapsulated in agarose, its gelation enabled to mechanically retain the cells in the anchors and to perform several rounds of phase change (*i.e.* oil-to-medium and medium-to-oil). This phase change was necessary to avoid cell nutrition depletion and toxic metabolites. Thus, the protocol resulted in the isolation of single CHO-S cells and it enabled long-term culture (at least up to 62h) with an individual cell

tracking. By the end to the culture period, the isolated single CHO-S remains highly viable on-chip (81.09 ± 13.39%), just as usually cells cultivated in conventional well plates (Figure 4.3C).

Next, the platform was applied for studying the CHO-S productivity in GFP by transient transfection using the different types of lipoplexes. For this purpose, the aqueous phase containing CHO-S cells, liquid agarose and culture medium was supplemented with the CL complexed with pMAX-GFP. CHO-S cells were incubated with lipoplexes for 4 hours in the anchors to interact with pDNA. Then, phase change was performed to wash the excess of lipoplexes from the microchip. The potential toxicity of the lipoplexes was examined by Live/Dead staining and the production of GFP was kinetically monitored by time lapse, immediately after the washing of the excess of lipoplexes. Figure 4.3C demonstrated that CHO-S retained high viability after transfection and long-term culture, whatever the type of lipoplexes (74.69 ± 35.90% for $R_{+/-}$ 5, 70.78 ± 25.52% for $R_{+/-}$ 3 and 88.15 ± 1.32% for $R_{+/-}$ 1.5). In addition, the gradual increase in GFP signal indicated the efficacy of the transfection under the different conditions tested (Figure 4.3D).

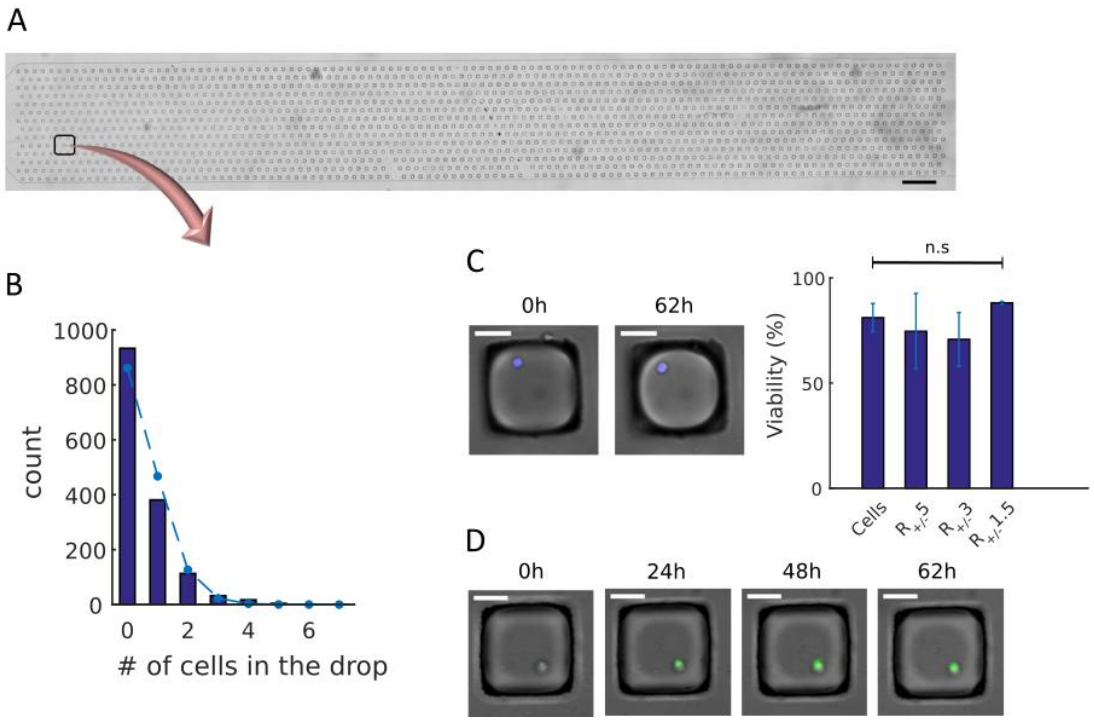

Figure 4.3 – CHO-S cells transfection with lipoplexes at $R_{+/-}$ 5, 3, 1.5 in the microfluidic device. (A) Large scan at 4x magnification of the whole microchip with 1495 anchored droplets. Scale bar: 200 µm. (B) Distribution of the number of cells per droplet (bars), and best fit to a Poisson distribution (dashed line). (C) View of a typical anchor at 10x magnification, showing an overlay of bright-field and DAPI (live) and TRITC (dead) signals. Images at first (0h) and final (62h) time of experiment are shown. Bar graphs show CHO-S viability for different conditions. There is no significant difference (ns) of cell viability between different conditions by Wilcoxon rank sum test at 5% significance level. Scale bars represent 50 µm. Results represent means ± S.D., n = 2. (D) For transfection analysis, FITC filter was used to quantify GFP production and TRITC to track all cells during the time-lapse. Shown here are overlays of bright field and FITC images at time 0, 24, 48 and 62 h.

Others droplet-based microfluidic devices was explored in previous studies with different cell lines, showing their capacity to track cells for long culture period (Annex III), however cell viability and transfection efficiency was compromised.

The platform contrasts with other conventional approaches in well-plates or in bioreactors, where cell productivity is usually assessed at the population level (*e.g.* ELISA or western blot etc.). Alternatively, the standard protocols for assessing single cell protein production make usually use of flow cytometry, which limits the possibility to obtain information of the cell history in culture and protein production kinetics.

Droplet microfluidics provide unique platform for cell encaspulation, biological isolation and tracking in culture. However, to date, the capability of droplet microfluidics to support the transfection and the culture of single genetically engineered animal cells has barely been investigated (22). For instance, while recent studies have demonstrated the electroporation (23) or chemical- based (12) genetic modification of single cells in droplets, the cells were cultivated off-chip after transfection. Consequently, it was not possible to correlate the initial cell properties to the GFP production efficiency.

In contrast to other conventional tools, the integrated platform used in the present study enabled the individualization, the *in situ* transfection as well as to support the long term culture of GFP producing CHO-S population. It was thus possible to follow on line the recombinant protein production in individualized cells, starting from the time of their transfection to the end of the culture period (Figure 4.3D).

3.3. Kinetics of GFP Production at Single CHO-S Level Revealed Distinct Populations

The unique capability of the integrated culture platform for dynamically tracking individual CHO-S enabled to obtain a more complete view of the evolution of GFP production during the culture period. At first, we find the cell distribution according to GFP production for each loop of time lapse (each 2h) (Figure 4.4A, boxplot graphs). Then, since the culture platform let tracking of each cell, we can obtain the evolution of GFP production for each cell during all time lapse (Figure 4.4B, line graphs). The kinetics of GFP production by cells transfected with lipoplexes $R_{+/-}$ 5, 3 and 1.5 (Figure 4.4) showed similar conditions and trends. The broad distribution of the kinetics of GFP production suggests that distinct populations produced different levels of GFP. In addition, since all individual curves followed a first order kinetic (r^2>0.9), the rate of GFP production was not dependant of its relative intensity at the beginning of the culture period (Supplementary Figure S.1).

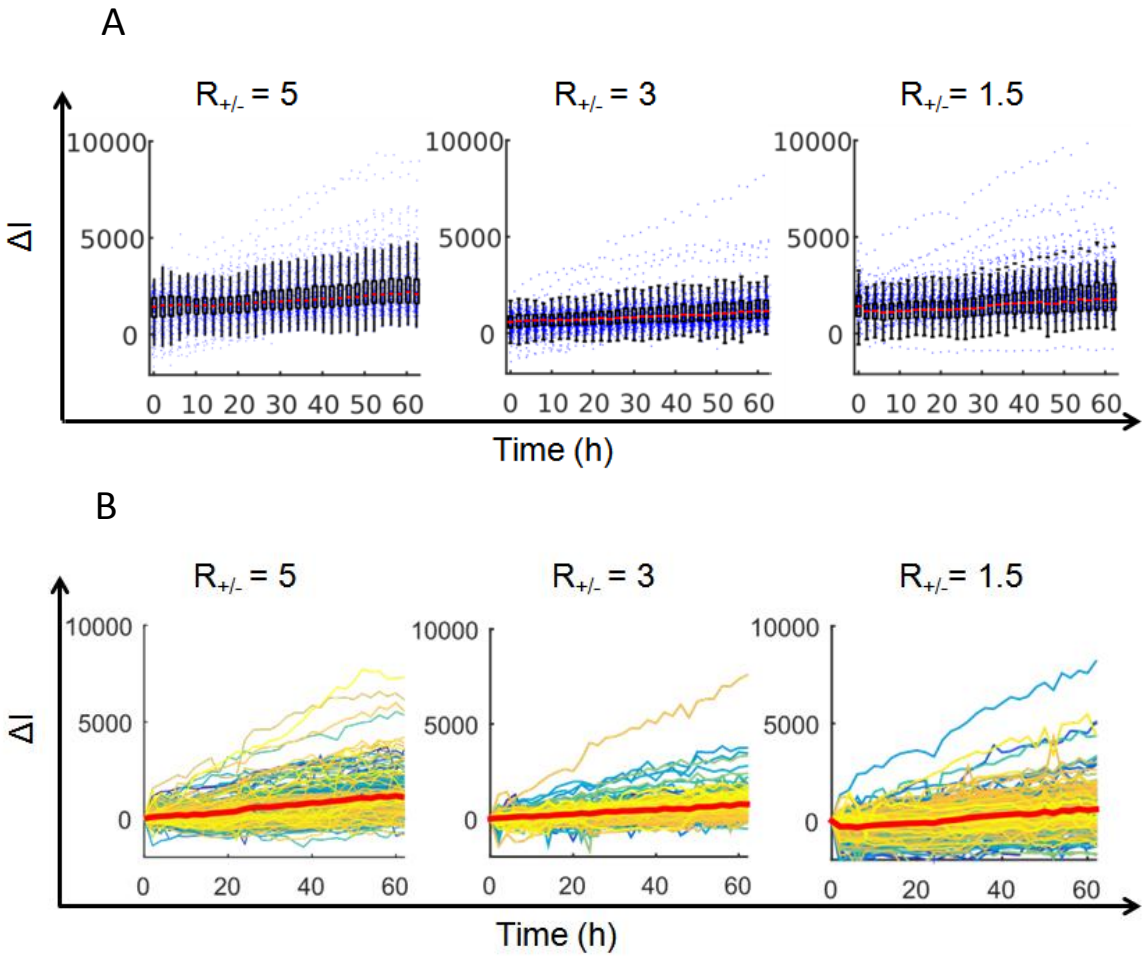

Figure 4.4 - Kinetics of GFP production during the culture period of CHO-S cell in single-cell platform. (A) Boxplots presenting the signal intensity for cells transfected with the lipoplex $R_{+/-}$ 5, 3 and 1.5 at each time step (each 2h). This is how flow cytometry would present the data. (B) The same data where the signal for each cell at the beginning of the experiment is subtracted from the signal as a function of time. The bold red line represents the evolution of the mean GFP production of the population.

To compare the mean of GFP production by CHO-S cell population transfected with lipoplexes $R_{+/-}$ 5, 3 and 1.5, it was plotted in the same graph the three means in Figure 4.5. As a result, it was found the average rate of GFP production by the population transfected with $R_{+/-}$ 5 was significantly higher (1.5 fold) in comparison to the other types of lipoplexes (*i.e.* $R_{+/-}$ 3 and $R_{+/-}$ 1.5) (Figure 4.5).

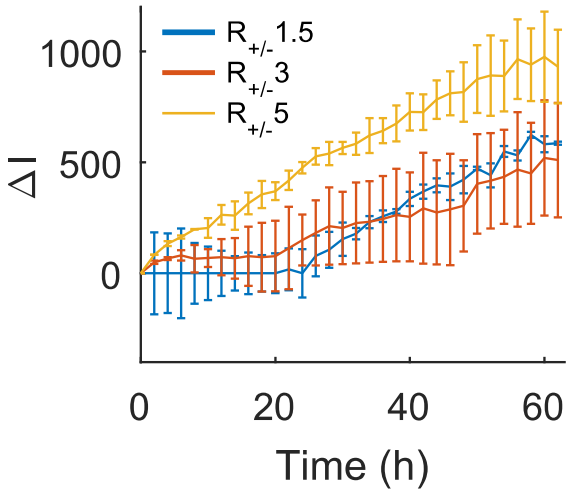

Figure 4.5 – The comparison of GFP mean production by cells transfected with lipoplexes $R_{+/-}$ 1.5, 3 and 5, during the culture period in single-chip platform. The error bars represent the difference between replicas from each lipoplex condition (n=2).

The formation of lipoplexes involves the electrostatic interaction between the positive charge of cationic lipids and the negative charge of the recombinant DNA (24). Consequently, the net charge of the liposome is significantly decreased after DNA complexation, leading to a decrease association with the cell membrane (*i.e.* negatively charged) (25). Consistently, it was found that lipoplexes $R_{+/-}$ 5, which presented positive charge, transfected better the cells than $R_{+/-}$ 3 and 1.5 with negative charge.

Then, in order to better distinguish the different subtypes within the whole CHO-S population, the evolution of the GFP signal distribution was more deeply analyzed. First, it was found that the spreading of the GFP intensity per cell followed a Poisson law, which median slightly shifted to higher values during time in culture (Figure 4.6A). To qualitatively measure this shift to right, we calculated the skweness of GFP intensity distribution over culture time (Figure 4.5B). Skewness is a measure of the asymmetry of the data around the sample mean. Thus, if the skewness is positive, the data are spread out more to the right of the mean than to the left. The skewness of a distribution is defined as (Equation 4.1):

$$s = \frac{E\,(x - \mu)^3}{\sigma^3} \qquad \text{(Equation 4.1)}$$

where μ is the mean of x, σ is the standard deviation of x, and $E(t)$ represents the expected value of the quantity t. Therefore, Figure 4.6B showed a positive skew, which Pearson's moment coefficient of skewness increased linearly with the time in culture. A threshold was determined in the mean of the GFP signal distribution, in which the right side is composed by the high producer cells (HPs) and the left side is composed by the low producers cells (LPs) (Figure 4.6C). Thus, the results demonstrated that a part of the CHO-S population produced GFP at a significantly higher level than other cells (LPS) (Figure 4.6D). Of note, the HPs were evenly distributed within the chip (Supplementary Figure S.2).

The analysis of the GFP production at single cell level revealed that CHO-S contained a distinct sub-population producing higher level of GFP (HPs), whatever the type of lipoplexes used to recombinant DNA delivery (Figure 4.6D). Several cellular parameters can contribute to the heterogeneous level of recombinant GFP production rate, which include 1) the amount of internalized plasmids 2) the rate of RNA transcription, 3) the rate of RNA translation (5). In this study, the contribution of the rate of recombinant protein formation and the cell growth inducing plasmid dilution are considered minimal (5). Moreover, considering identical DNA delivery conditions in droplets containing the same lipoplex, the rate of GFP transcription/translation emerges as a potent parameter promoting the heterogeneity in the level of GFP production (5).

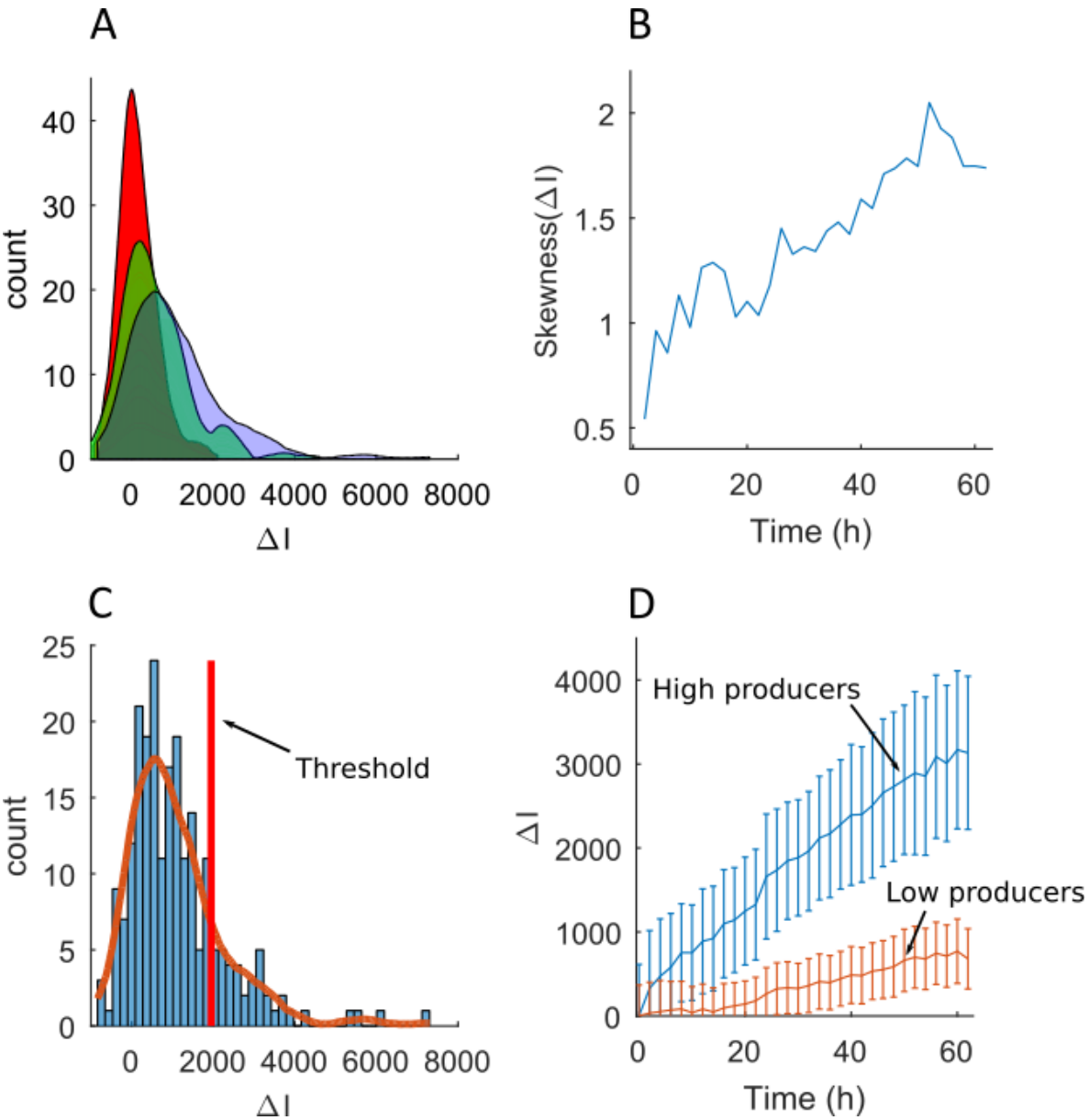

Figure 4.6 - Distribution of GFP production on the single-cell level (A) Histograms of the increase in GFP signal (ΔI) for cells transfected with lipoplexes $R_{+/-}$ 5 at culture-times t = 12h (red curve), t = 32h (green curve) and t = 62 h (blue curve). (B) The asymmetry towards the high values is quantified through the Skewness parameter, which is found to increase linearly in time. (C) The skewness of GFP intensity distribution at the final instant (t=62 h) could be used to define a threshold that divides the population into low-producing and high-producing cells. (D) Time evolution of the signal due to the high producers and other cells. Data for other conditions ($R_{+/-}$ 3 and 1.5) are similar. Results represent means ± S.D., n = 3.

3.4. Characterization and Recovery of the High GFP Producers

To characterize the high GFP producers (HP), the influence of the different types of lipoplexes was investigated on the relative abundance of HPs and their specific productivity. Figure 4.7A showed that a higher percentage of HPs was found using lipoplexes $R_{+/-}$ 5 (15.27% ± 1.77), in comparisons of $R_{+/-}$ 3 and $R_{+/-}$ 1.5 (8.72% ± 1.55 and 4.88% ± 0.12, respectively). Next, we compared the specific GFP productivity of HPs for each lipoplex used $R_{+/-}$ 5, 3 and 1.5 (Figure 4.7B). It was found that the GFP productivity was about 1.5 higher for $R_{+/-}$ 1.5 than $R_{+/-}$ 5 and $R_{+/-}$ 3, after 30h of cell culture (Figure 4.7B). The results suggest that the higher productivity of CHO-S population transfected with $R_{+/-}$ 5 (Figure 4.5) was mainly due to higher percentage of HPs within the whole population. Despite higher productivity, the contribution of the HPs in $R_{+/-}$ 1.5 condition (Figure 4.7B) was not sufficient to reach the same total level of GFP production than for $R_{+/-}$ 5 (Figure 4.5).

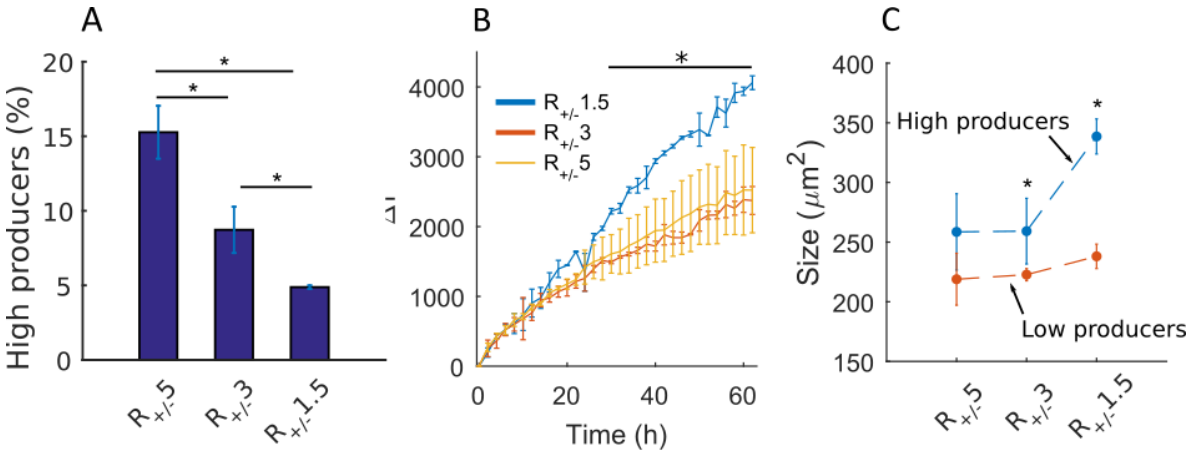

Figure 4.7 - Characterizing high GFP producers. (A) Percentage of total cells characterized as HP for each of the lipoplex conditions indicate a decreasing number of high producing cells with increased DNA charge. (B) The specific productivity for the three conditions shows that the GFP production per transfected cell increases with increased DNA charge. (C) Size difference between high producers and low producers for different conditions. Means statistically significant different by Kruskal-Wallis (B) or by Wilcoxon rank sum test (A and C) at 5% significance level were flagged with an asterisk (*). Error bars represent the values for the two independent experiments.

To better prove the properties distinguishing HPs from the other cells of the population (low producers, LPs), their initial size distribution was first compared (Supplementary Figure S.3). Figure 4.7C showed that the average HPs area was at least 15% higher than LPs whatever the type of lipoplexe tested. In turn, the cells transfected with $R_{+/-}$ 1.5 and 3 lipoplexes had HPs significantly bigger than LPs. In addition, it was found that the initial area of HPs transfected with $R_{+/-}$ 1.5 was significantly larger than those with $R_{+/-}$ 5 and 3 (Figure 4.7C). Thus, the cell size emerged as an important parameter leading to the emergence of HPs in the transfected CHO-S population. Thus, in the present work, it was found that the initial cell size of HPs correlated high GFP production (Figure 4.6C), which suggest that HPs are in a distinct cell cycle phase than the other cells of the population (5,26). Indeed, the specific productivity of CHO is usually found greater in G2/M (*i.e.* early-mid exponential phase) (26). During this cell cycle phase, the cells are found larger and more rRNA are available for recombinant protein translation (27). Moreover, G2/M is associated with a loss of nuclear membrane integrity, facilitating the plasmid internalization through the endosomal pathway (28). Furthermore, as the cytoplasmic membrane is extending prior to mitosis, the decrease of its tension facilitates the endocytosis of nanoparticles (29).

Lipofection provokes a distortion in the cell cycle, which show lower oscillation than non-transfectd cells (30). Moreover, liposome transfection increased the percentage of cells in S and G2/M phase (*i.e.* the phases were the cells displayed the highest diameter), at the expense of cells in G1 (30). In this study, it was found that the different types of lipoplexes differently affected the properties of HPs contained in the bulk of CHO-S. Indeed, a significantly higher percentage of HPs were found in $R_{+/-}$ 5 than $R_{+/-}$ 3 and 1.5 (Figure 4.7A). On the other hand, the GFP production by HPs was higher in cells transfected with lipoplex $R_{+/-}$ 1.5 than $R_{+/-}$ 5 and 3 (Figure 4.7B). Because $R_{+/-}$ 5 displayed higher ζ, it favored increased lipoplexes/cell membrane interactions and, as a consequence, an increase percentage of HPs whitin the population. However, $R_{+/-}$ 1.5 showed higher GFP productivity despite lesser amount of lipoplexes interacting with CHO-S (*i.e.* due to lower ζ), since they enable the delivery of higher amount of plasmid to CHO-S

nucleus. In case of lipoplex $R_{+/-}$ 3, ζ and pDNA content is comprised between $R_{+/-}$ 5 and $R_{+/-}$ 1.5, and so, CHO-S transfected under this conditions showed amount of HPs in cell population and specific productitvity comprised between the two other lipoplexes conditions.

Finally, in view of future functional analysis (transpritomic and proteomic investigations), protocol of a selective recovery from platform was used for the isolation of HPs off-chip. The procedure enabled to non-invasively recover fluorescent cells. Moreover, after one day in culture, the intensity of GFP within the isolated CHO-S was in a similar range as before the extraction, suggesting that cells retain viability and their GFP production capability.

4. Conclusions

A universal droplet microfluidic placed was used to assess the heterogeneities of CHO-S population transiently transfected with different types of lipoplexes. The devise enabled the combined single cell isolation, *in situ* transfection and culture for long time periods. A single cell analysis of GFP production kinetics revealed the presences of a subpopulation producing significantly high levels of recombinant proteins, whatever the properties on lipoplexes. The high producers showed increased cell size in comparison to the average population. The charge and the pDNA content of the different lipoplexes regulated differentially relative abundance of HPs in cell population (higher in lipoplexes with positive charge and less pDNA content) and GFP specific productivity of HPs (higher in lipoplexes with negative charge and more pDNA content).

5. Acknowledgments

The study was financially supported by the São Paulo Research Foundation (FAPESP process number 2014/24797-2, 2014/10557-5 and 2015/26701-0), National Counsel of Technological and Scientific Development (CNPq process number 202086/2015-1) and European Research Council (ERC) under contract number 278248 Multicell. We would like to thank the Condensed Matter Physics Laboratory (PMC) at École Polytechnique for providing the use of Malvern

Zetasizer equipment. We also thank Caroline Frot, Cyprien Guermonprez and Raphaël Tomasi for helpful support of image analysis and discussions about the work.

6. References

1. Hacker DL, Balasubramanian S. Recombinant protein production from stable mammalian cell lines and pools. Vol. 38, Current Opinion in Structural Biology. 2016. p. 129–36.

2. Kim JY, Kim Y-G, Lee GM. CHO cells in biotechnology for production of recombinant proteins: current state and further potential. Appl Microbiol Biotechnol. 2012;93(3):917–30.

3. Wurm FM. Production of recombinant protein therapeutics in cultivated mammalian cells. Nat Biotechnol. 2004;22(11):1393–8.

4. Baldi L, Hacker DL, Adam M, Wurm FM. Recombinant protein production by large-scale transient gene expression in mammalian cells: state of the art and future perspectives. Biotechnol Lett. 2007;29(5):677–84.

5. Subramanian S, Srienc F. Quantitative analysis of transient gene expression in mammalian cells using the green fluorescent protein. J Biotechnol. 1996;49(1):137–51.

6. Kim TK, Eberwine JH. Mammalian cell transfection: The present and the future. Anal Bioanal Chem. 2010;397(8):3173–8.

7. Zuhorn IS, Kalicharan R, Hoekstra D. Lipoplex-mediated transfection of mammalian cells occurs through the cholesterol-dependent clathrin-mediated pathway of endocytosis. J Biol Chem. 2002;277(20):18021–8.

8. Kim J, Hwang I, Britain D, Chung TD, Sun Y, Kim D-H. Microfluidic approaches for gene delivery and gene therapy. Lab Chip. 2011;11(23):3941–8.

9. Kintses B, van Vliet LD, Devenish SRA, Hollfelder F. Microfluidic droplets: new integrated workflows for biological experiments. Curr Opin Chem Biol. 2010;14(5):548–55.

10. Yin H, Marshall D. Microfluidics for single cell analysis. Curr Opin Biotechnol. 2012;23(1):110–9.

11. Schaerli Y, Hollfelder F. The potential of microfluidic water-in-oil droplets in experimental biology. Mol Biosyst. 2009;5(12):1392–404.

12. Chen F, Zhan Y, Geng T, Lian H, Xu P, Lu C. Chemical transfection of cells in picoliter aqueous droplets in fluorocarbon oil. Anal Chem. 2011;83(22):8816–

20.

13. Fradet E, McDougall C, Abbyad P, Dangla R, McGloin D, Baroud CN. Combining rails and anchors with laser forcing for selective manipulation within 2D droplet arrays. Lab Chip. 2011;11(24):4228–34.

14. Balbino TA, Aoki NT, Gasperini AAM, Oliveira CLP, Azzoni AR, Cavalcanti LP, et al. Continuous flow production of cationic liposomes at high lipid concentration in microfluidic devices for gene delivery applications. Chem Eng J. 2013;226(0):423–33.

15. Rigoletto TP, Silva CL, Santana MH, Rosada RS, De La Torre LG. Effects of extrusion, lipid concentration and purity on physico-chemical and biological properties of cationic liposomes for gene vaccine applications. J Microencapsul. 2012;29(8):759–69.

16. Amselem G, Guermonprez C, Drogue B, Michelin S, Baroud CN. Universal microfluidic platform for bioassays in anchored droplets. Lab Chip. 2016;16(21):4200–11.

17. Cifone MA, Fidler IJ. Correlation of patterns of anchorage-independent growth with in vivo behavior of cells from a murine fibrosarcoma. Proc Natl Acad Sci. 1980;77(2):1039–43.

18. Amselem G, Brun PT, Gallaire F, Baroud CN. Breaking anchored droplets in a microfluidic Hele-Shaw cell. Phys Rev Appl. 2015;3(5):1–5.

19. Balbino TA, Gasperini AAM, Oliveira CLP, Azzoni AR, Cavalcanti LP, De La Torre LG. Correlation of the Physicochemical and Structural Properties of pDNA/Cationic Liposome Complexes with Their in Vitro Transfection. Langmuir. 2012;28(31):11535–45.

20. Balbino TA, Serafin JM, Malfatti-Gasperini AA, de Oliveira CLP, Cavalcanti LP, de Jesus MB, et al. Microfluidic assembly of pDNA/Cationic liposome lipoplexes with high pDNA loading for gene delivery. Langmuir. 2016;32(7):1799–807.

21. Dangla R, Kayi SC, Baroud CN. Droplet microfluidics driven by gradients of confinement. Proc Natl Acad Sci. 2013;110(3):853–8.

22. Rakszewska A, Tel J, Chokkalingam V, Huck WT. One drop at a time: toward droplet microfluidics as a versatile tool for single-cell analysis. NPG Asia Mater. 2014;6(10):e133.

23. Zhan Y, Wang J, Bao N, Lu C. Electroporation of Cells in Microfluidic Droplets. Anal Chem. 2009;81(5):2027–31.

24. Felgner PL, Gadek TR, Holm M, Roman R, Chan HW, Wenz M, et al. Lipofection: a highly efficient, lipid-mediated DNA-transfection procedure. Proc Natl Acad Sci USA. 1987;84(21):7413–7.

25. da Cruz MTG, Simões S, Pires PPC, Nir S, de Lima MCP. Kinetic analysis of the initial steps involved in lipoplex–cell interactions: effect of various factors that influence transfection activity. Biochim Biophys Acta (BBA)-Biomembranes. 2001;1510(1):136–51.

26. Lloyd DR, Holmes P, Jackson LP, Emery AN, Al-Rubeai M. Relationship between cell size, cell cycle and specific recombinant protein productivity. Cytotechnology. 2000;34(1–2):59–70.

27. Tait AS, Brown CJ, Galbraith DJ, Hines MJ, Hoare M, Birch JR, et al. Transient production of recombinant proteins by Chinese hamster ovary cells using polyethyleneimine/DNA complexes in combination with microtubule disrupting anti-mitotic agents. Biotechnol Bioeng. 2004;88(6):707–21.

28. Remaut K, Symens N, Lucas B, Demeester J, De Smedt SC. Cell division responsive peptides for optimized plasmid DNA delivery: The mitotic window of opportunity? J Control Release. 2014;179:1–9.

29. Raucher D, Sheetz MP. Membrane Expansion Increases Endocytosis Rate during Mitosis. J Cell Biol. 1999;144(3):497–506.

30. Fuge G, Zeng A-P, Jandt U. Weak cell cycle dependency but strong distortive effects of transfection with Lipofectamine 2000 in near-physiologically synchronized cell culture. Eng Life Sci. 2016;17(4):348-356.

31. Israelachvili JN, Mitchell DJ. A model for the packing of lipids in bilayer membranes. Biochim Biophys Acta (BBA)-Biomembranes. 1975;389(1):13–9.

32. Lasic DD. Liposomes in Gene Delivery. Boca Raton-Florida: CRC Press; 1997. 295 p.

7. Supplementary data

7.1. Lipoplexes per cell estimation

To estimate the number of lipoplexes per cell, at first we estimated the number of liposomes synthesized for each condition: 1.85 µL ($R_{+/-}$ = 5), 1.11 µL ($R_{+/-}$ = 3) and 0.55 µL ($R_{+/-}$ = 1.5). Considering lipossomes with a spherical geometry and unimodal size distribution, the aggregation number is (31):

$$N \approx {4\pi[R_C^2 + (R_C - t)^2]}/{a_0}$$

where R_C is the critical radius assumed here as the average hydrodynamic radii of 50 nm, t is the bilayer hydrocarbon thickness of 4 nm (32) and a_0 is the optimal value of surface headgroup area. In this case of mixed bilayer, a_0 corresponded

the lipid cross-sectional area for DOTAP, DOPE and EPC are 0.7, 0.55 and 0.71 nm^2, respectively (31,32). The final lipid concentration of liposome was 2.27 mM. Thus, we used approximate 9.7 x 10^9 liposomes for $R_{+/-}$ = 5, 5.8 x 10^9 liposomes for $R_{+/-}$ = 3 and 2.9 x 10^9 liposomes for $R_{+/-}$ = 1.5.

In terms of lipoplexes, the system can generate a ternary phase system with single, double, and multiple bilayers, depending on the molar charge ratio (19). Analyzing the extreme conditions, $R_{+/-}$ = 5 formed around 20% of double bilayers and 80% "empty" liposomes, $R_{+/-}$ = 1.5 formed around 20% of multiple bilayers, 66% of double and 14% "empty" liposomes. Thus, effectively $R_{+/-}$ = 5 and $R_{+/-}$ = 1.5 contained about 6 x 10^5 lipoplexes / cell and 2 x 10^5 lipoplexes / cell, respectively.

7.2. Graphics of GFP production by CHO-S cells

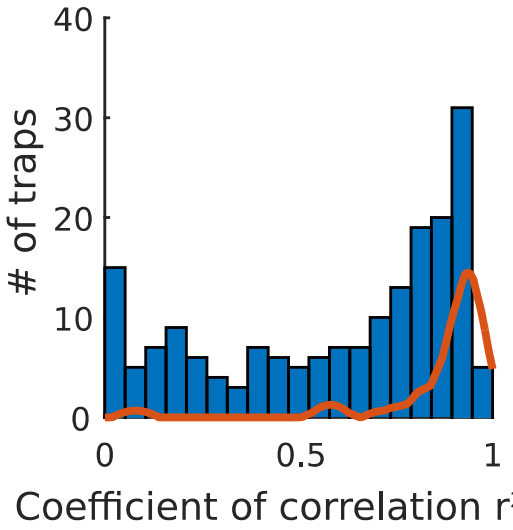

Figure S.1 – GFP production kinetics characterization. An example of linear coefficient correlation distribution (r^2) of GFP produced by CHO-S cells transfected with lipoplexes $R_{+/-}$ 5 for all single cells (blue columns) and for high GFP producers (red line) is exhibited.

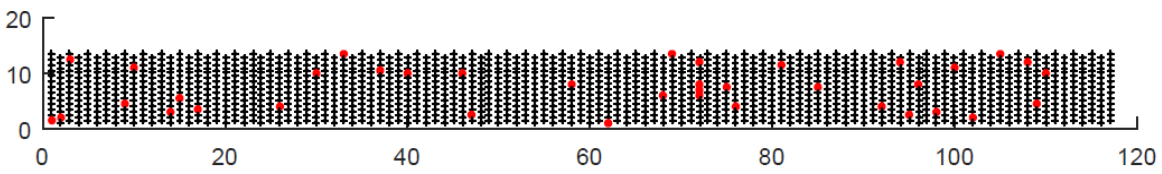

Figure S.2 - High GFP producers evenly distributed within the microchip. HPs are represented as red points on the microchip's map.

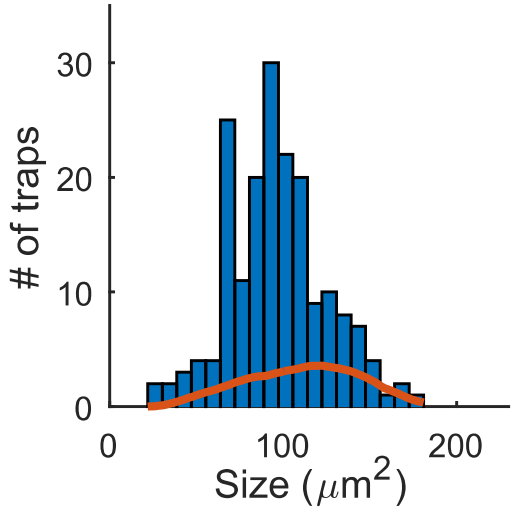

Figure S.3 - High GFP producers characterization in terms of cell-size. An example of graphs comparing size of HPs (red line) and all cell population (blue columns) for CHO-S cells transfected with lipoplexes $R_{+/-}$ 5 is shown.

Chapter V – Conclusions

In the first part of this work, droplet-based microfluidic system was applied to synthesize lipoplexes. In the second part, a single-cell platform was used to investigate transient transfection of CHO-S cells. We conclude that liposomes maintain their properties after processing in droplet system, allowing more advanced applications. Microchip design with thin serpentine channel or wide serpentine channel with a split region increase lipoplex homogeneity. This system allows the loading of larger amounts of pDNA in liposomes ($R_{+/-}$ 1.5) without changing lipoplexes properties (size, PdI and zeta potential), specially desired for gene therapy applications. Lipoplexes synthesized in droplet system with wide serpentine channel and split region, operating at ratio aqueous/oil flow rate 0.25 and $R_{+/-}$ 1.5, 3, 5, 7, and 10, transfect DCs showing the transfection efficiency equivalent to that presented by lipoplexes produced by bulk method. In addition to transfecting, lipoplexes synthesized in droplet system also activate DCs. Therefore, the droplet-based microfluidic system shows as a potential tool to synthesize lipoplexes for cell lines transfection. The single-cell platform was shown to be efficient to transfect CHO-S cells by lipoplexes, while maintaining cells viability. With the single-cell analysis, it is possible to study the heterogeneities of CHO-S population, during transient transfection. The GFP production kinetics is tracked for each cell during culture time, allowing to determinate two different subtypes of cell population, high and low GFP producers. High producers increase cell size in comparison to the average population. The charge of lipoplexes shows an important role to transfect CHO-S, since the unique positive charged lipoplex $R_{+/-}$ 5 produces more HPs. The amount of pDNA delivered affects the protein production, since $R_{+/-}$ 1.5 with more pDNA, increase GFP specific productivity of HPs. The universal platform shows as a powerful tool to investigate mammalian cell transfection and to identify / characterize high protein producer cells.

Chapter VI - Perspectives

Lipoplexes synthesized in the droplet-based microfluidic system were suitable to transfect dendritic cells. Moreover, the universal platform can be used to investigate mammalian cell transfection and heterogeneities in cell population. In this context, one future perspective envisaged for this work is to use the universal platform to transfect dendritic cells. The aim would be to investigate DCs transfection, characterize the transfected DCs and high-producer screening, in order to find the way to increase the DC transfection efficiency while providing cells activation. In general, this universal platform opens good perspectives to investigate the transfection of immune system cells, which frequently present a heterogeneous behavior and are hard-to-transfect cells, since they are usually provided by primary cell cultures. Another possible future work is to use the droplet-based microfluidic system to complex other nanoparticles with nucleic acids, which require more controllable environment. For example, chitosan nanoparticles are very sensible to changes in the solvent and in amount of nucleic acids, leading to precipitations in different complexation conditions. Thus, the controlled microenvironment generate in the droplet system could favor the synthesis of these complexes, even if in adverse conditions.

ANNEX I – Plasmid vectors

Positive control vector pEGFP-N1 from Clontech (Figure 1) is a plasmid with florescent tag for mammalian cell expression presenting bacterial resistance for kanamycin. This vector was used in Chapter III to quantify DC transfection efficiency.

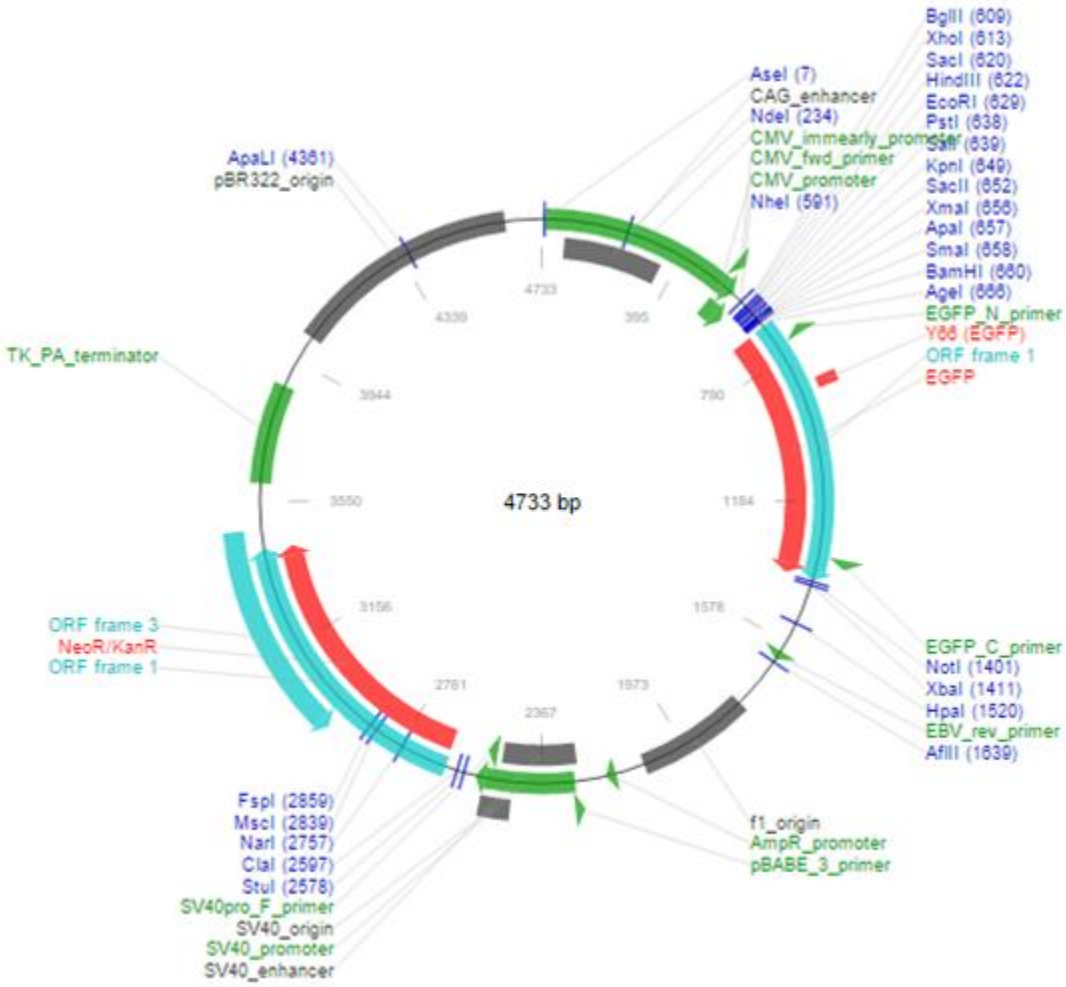

Figure 1 - Plasmid map of pEGFP-N1 Vector from Clontech.

Positive control vector pmaxGFP from Lonza (Figure 2) is ideal positive control protein especially for fluorescence microscopy. The plasmid encodes the

green fluorescent protein from *Pontellina* sp. This vector was used in Chapter IV to obtain the kinetics of recombinant protein production by CHO-S cells.

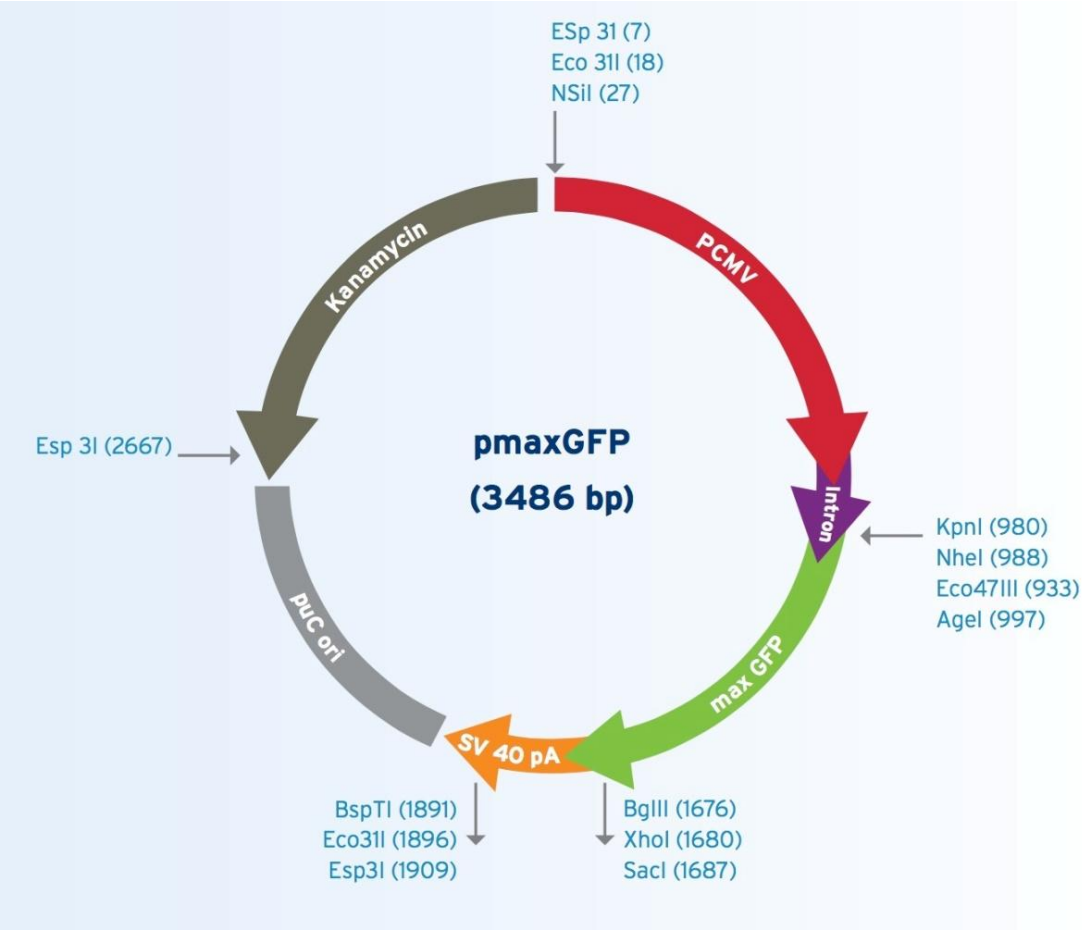

Figure 2 - Plasmid map of pmaxGFP Vector from Lonza.

ANNEX II –Preliminary studies in droplet microfluidic system to synthesize lipoplexes

Before investigating the lipoplexes synthesis in droplet-based microfluidic system, previous studies were carried out, such as investigation of flow rates to droplets formation in a water/oil emulsion using less expensive reagents and study of CL formation in different diluents in order to obtain nanoparticles with required physico-chemical characteristics to DC transfection.

1. Study of flow rates for droplets formation

For investigation of droplet formation in microfluidic system (Figure 3.1B, TC), two aqueous solutions were prepared with water added with green and red dyes in order to facilitate visualization of droplets and the mixing inside them. The oil phase of emulsion was composed of mineral oil from Vetec Química Fina (RJ, Brazil) with 2% v/v of surfactant sorbitan monooleate (Span 80) from Sigma Aldrich (MO, USA). We should highlight that this oil phase was not chosen for complexation process due to the low biocompatibility of mineral oil. However, we decided to use it to estimate flow rates for droplets formation in microfluidic device because of the lower cost of these reagents than FC-40 oil and Pico-Surf 1.

Thus, we studied several inlet flow rates for aqueous phase ($Q_{aqueous}$) and for oil phase (Q_{oil}) in the droplet-based microfluidic system thin serpentine channel (200 μm) and split region and (Figure 1 and Table 1). The solutions were introduced in each respective inlet by syringe pump, in which as aqueous phase was introduced the green and the red dye solution and as oil phase the mineral oil with Span 80. The following strategy was used to investigate the flow rates: at first the oil phase flow was fixed at 2 μL min^{-1} while aqueous flow rate varied from 0.1 to 4 μL min^{-1}. Then, the inverse was made, the aqueous flow rate remained constant at 0.67 μL min^{-1} and the oil phase flow varied from 0.1 to 19.2 μL min^{-1}, as described in Table 1. The fixed flow rates of aqueous and oil phases and the microfluidic device were chosen based on the previous study realized by (1), which

used Q_{oil} = 2 µL min^{-1} and $Q_{aqueous}$ = 0.67 µL min^{-1} to produce droplets in a similar droplet-based microfluidic system.

Table 1 - Variation in flow rates $Q_{aqueous}$ (aqueous phase composed of green and red dye in water) and Q_{oil} (oil phase composed of mineral oil with 2% v/v of surfactant Span 80) for droplet formation in the droplet-based microfluidic system with serpentine-TC and split region (Figure 3.1B).

Flow rates study		
Fixed	Q_{oil} = 2 µL min^{-1}	$Q_{aqueous}$ = 0.67 µL min^{-1}
Variant	$Q_{aqueous}$ (µL min^{-1})	Q_{oil} (µL min^{-1})
	0.1	0.1
	0.29	0.67
	0.48	1.4
	0.67	2
	1.11	4
	1.55	8
	2	19.2
	3	
	4	

Flow rate combinations were observed and images were taken by using the trinocular stereo microscope from Bel Photonics (STMPRO-T model, Monza, Italy). For each moment in which system operating conditions changed, it was waited five minutes for system stabilization. General behaviors observed in the droplet-based microfluidic system were illustrated in Figure 1 and described as follow:

(i) If the flow rate is considered good, droplet formation will be well defined and similar to that seen in Figure 1A;

(ii) If the ratio between $Q_{aqueous}$ and Q_{oil} increases, droplet size tends to increase (Figure 1B) until reach a parallel flow streams (Figure 1C).

(iii) However, if this ratio decreases ($Q_{aqueous}/Q_{oil}$), droplet size tends to decrease (Figure 1D) until the oil phase invades aqueous phase inlet channels (Figure 1E). We also observed an intermediate stage between Figures 1D and E not shown, in which system was unstable altering in droplet formation and in oil phase entering into aqueous phase inlets.

As a result, the range of $Q_{aqueous}$ between 0.48 to 2 µL min^{-1} and Q_{oil} fixed at 2 µL min^{-1} was chosen for further assays of water fraction estimation with FC-40 oil with 5% v/v of surfactant Pico-Surf 1 as oil phase in droplet-based microfluidic system.

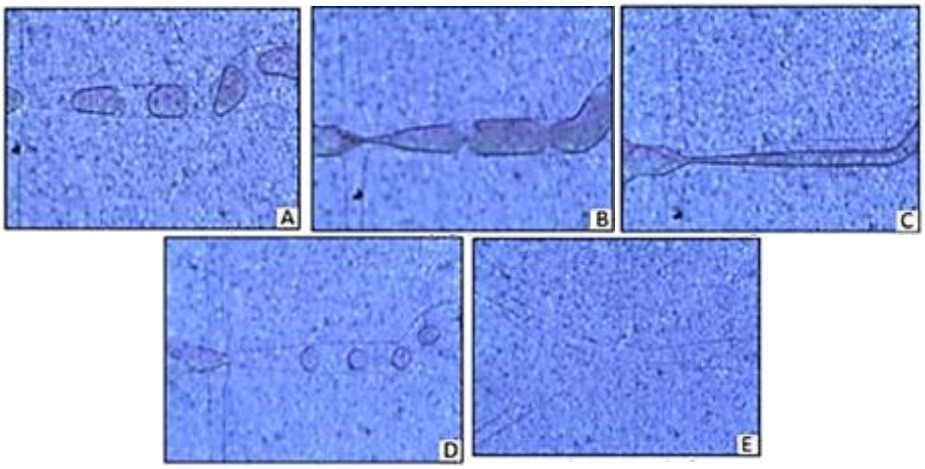

Figure 1 – Images of droplet formation with aqueous phase composed of green and red dye in water and oil phase composed of mineral oil with 2% v/v of surfactant Span 80 in the droplet-based microfluidic system with serpentine-TC and split region (Figure 3.1B). Following droplet behaviors were observed in the microfluidic system: (A) ideal droplets when flow rates were Q_{oil} = 2 µL min^{-1} and $Q_{aqueous}$ = 0.67 µL min^{-1}, large droplets when Q_{oil} = 2 µL min^{-1} and $Q_{aqueous}$ = 2 µL min^{-1} (B), until reached a parallel flow when Q_{oil} = 2 µL min^{-1} and $Q_{aqueous}$ = 3 µL min^{-1} (C), and small droplets were formed decreasing $Q_{aqueous}$ to 0.29 µL min^{-1} with Q_{oil} = 2 µL min^{-1} (D), until the oil phase invaded aqueous phase inlet in Q_{oil} = 2 µL min^{-1} and $Q_{aqueous}$ = 0.10 µL min^{-1}(E).

2. Cationic liposome diluent

Cationic liposomes composed of EPC/DOTAP/DOPE (50/25/25 % molar, respectively) were produced in a cross-junction microfluidic device by a single hydrodynamic focusing, like BALBINO *et al.* (2) (Figure 3.1A). Lipid dispersion was inserted in the central entrance and in the two lateral inlets were introduced the aqueous phase, which could be water, PBS buffer solution or OptiMEM culture medium (Figure 3.1A). The three lipids were dispersed in anhydrous ethanol to achieve 25 mM of total lipid concentration, following the protocol established by Rigoletto *et al.* (3). The lipid dispersion was injected into the system at 10.92 µL min^{-1} in a glass syringe (Hamilton, NV, USA, 1 mL) via syringe pump (KDScientific, model KDS-200, USA). Simultaneously, two glass syringes (Hamilton, NV, USA, 2.5 mL) with aqueous phase (water, PBS buffer or OptiMEM) were injected at 54.6 µL min^{-1} into two sides of T-chip. Liposome samples were collected from the exit and leaved for at least 2 hours at 4 °C. Then, samples were collected to physico-

chemical characterization of size, polydispersity and zeta potential in Zetasizer equipment, as shown in Table 2 and Figure 2.

The cationic liposomes obtained using water as aqueous solution had small polydispersity (0.202), positive zeta potential (59.9 mV) and small size (76.6 nm), like showed in Table 2. On the other hand, liposomes obtained using PBS buffer as aqueous solution had higher polydispersity (0.322), larger size (approximately 85% of the population at 135.8 nm and the other 15% at 376.4 nm) and zeta potential slightly smaller (41.8 mV) than those obtained in water (Table 2). Similarly to PBS buffer solution, cationic liposomes formed in OptiMEM had higher polydispersity (0.257), larger size (approximately 99% of the population at 88.1 nm and the other 1% at 532.2 nm) and smaller zeta potential (38.6 mV) than those obtained in water (Table 2). In addition, Figure 2 showed the size distribution graphs of cationic liposomes in intensity and number for all conditions. Graphs demonstrated more clearly the polydispersity of liposomes formed in PBS and in OptiMEM that had two populations, and liposomes synthesized in water had only one homogeneous population. Because of these characteristics, water indicated to be more suitable as aqueous solution than PBS and culture medium for cationic liposomes formation in the cross-junction microfluidic device. Moreover, complexing process, incorporation of DNA into liposomes, tends to increase more nanoparticles size and polydispersity, leading to decrease internalization by DCs, and consequently, in transfection efficiency (4).

Table 2 - Physico-chemical properties of cationic liposomes obtained by single hydrodynamic focusing in cross-junction microfluidic device using as aqueous phase water, OptiMEM culture medium or PBS buffer solution.

Cationic liposomes	Mean diameter (± S.D.) nm and distribution (± S.D.) %		Pdl[iii]	Zeta potential
	Intensity[i]	Number[ii]		(± S.D.) mV
PBS	444.7 ± 46.5 (67.4 ± 8.4) 146.1 ± 33.1 (32.7 ± 8.4)	376.4 ± 26.5 (15.3 ± 0.1) 135.8 ± 31.0 (84.7 ±0.1)	0.322 ± 0.059	41.8 ± 0.0
OptiMEM	129.8 ± 34.4 (76.4 ± 12.6) 479.8 ± 186.0 (23.6 ± 12.6)	88.1 ± 0.4 (98.9 ± 1.3) 532.2 ± 270.2 (1.1 ± 1.3)	0.257 ± 0.066	38.6 ± 1.7
Water	119.7 ± 16.7 (100 ± 0)	76.6 ± 17.8 (100 ± 0)	0.202 ± 0.038	59.9 ± 2.1

Results represent means ± S.D., n = 2.
[i] Intensity-weighted average diameter and distribution (I-distribution).
[ii] Number-weighted average diameter and distribution (N-distribution).
[iii] PdI: Polydispersity index of samples vary in ascending order from 0 to 1.

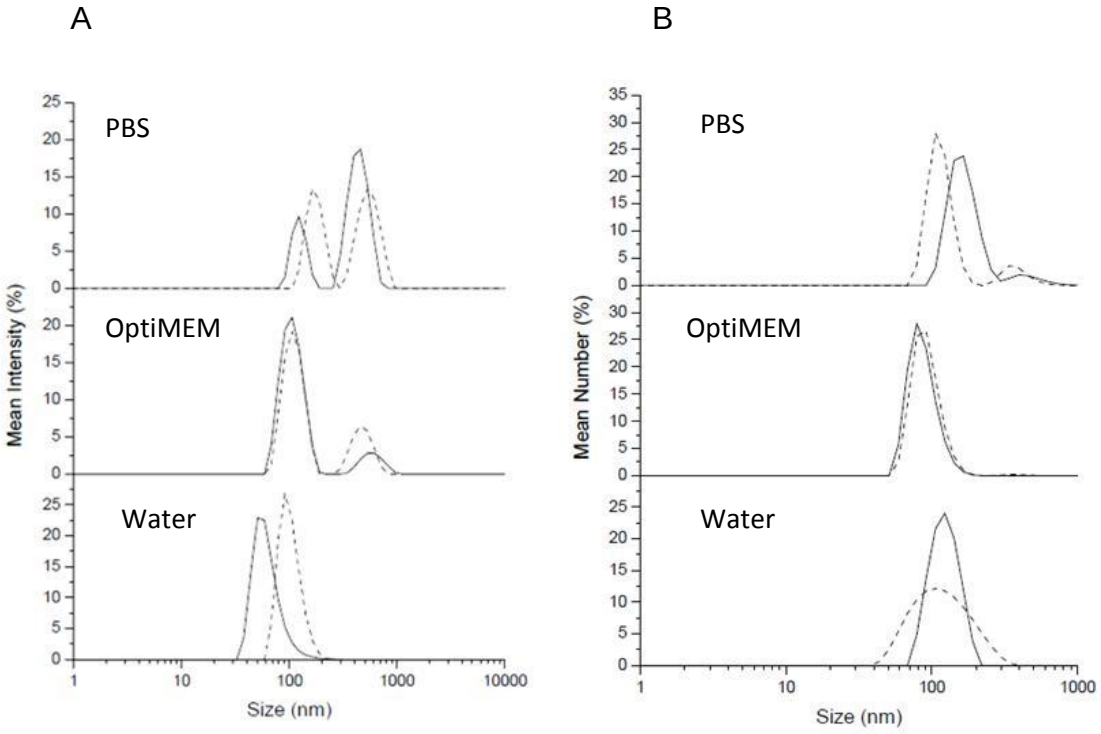

Figure 2 - Intensity-weighted distribution (A) and number-weighted distribution (B) of cationic liposomes obtained in water, OptiMEM culture medium or PBS buffer solution as aqueous phase. The dashed and solid lines in each graph represent one independent size distribution (n=2).

3. References

1. Hsieh AT-H, Hori N, Massoudi R, Pan PJ-H, Sasaki H, Lin YA, et al. Nonviral gene vector formation in monodispersed picolitre incubator for consistent

gene delivery. Lab Chip. The Royal Society of Chemistry; 2009;9(18):2638–43.

2. Balbino TA, Aoki NT, Gasperini AAM, Oliveira CLP, Azzoni AR, Cavalcanti LP, et al. Continuous flow production of cationic liposomes at high lipid concentration in microfluidic devices for gene delivery applications. Chem Eng J. 2013;226(0):423–33.

3. Rigoletto TP, Silva CL, Santana MH, Rosada RS, De La Torre LG. Effects of extrusion, lipid concentration and purity on physico-chemical and biological properties of cationic liposomes for gene vaccine applications. J Microencapsul.. 2012;29(8):759–69.

4. Vitor MT, Bergami-Santos PC, Zômpero RHF, Cruz KSP, Pinho MP, Barbuto JAM, et al. Cationic liposomes produced via ethanol injection method for dendritic cell therapy. J Liposome Res. 2016;7:1-15.

ANNEX III – Preliminary studies in droplet microfluidic system to transfect CHO-S cells

Before reach the system presented in Chapter III to transfect CHO-S cells, others cells and microdevices were explored, as showed in this annex. However, the low viability or transfection of cells lead us to leave them. Even though, the device showed a potential to understand key parameters that influence *in vitro* mammalian cells transfection process. Thus, a droplet-based microfluidic system was used to transfect *in vitro* mammalian cells (smooth muscle cells (SMCs), mesenchymal stem cells (MSCs) and lymphoma cells (S49.1)) under a 3D microenvironment provided by hydrogels (collagen and agarose) as extracellular matrices. Additionally, this system also provided a study of cells morphology by changing cells concentration (from 0.1 to 0.5 x 10^6 cells/mL), using Rho–ROCK–myosin inhibitors (like blebbistatin and Y27632) and modifying hydrogel stiffness (1.2 and 6 mg/mL collagen concentration); being a potential tool to signalize transfection pathways.

1. Objectives

The general purpose of this part of work was to develop a microchip to transfect mammalian cells *in vitro* within soft 3D droplets hydrogel, using cationic liposomes incorporated with nucleic acids as nanovectors. Thus, with this system, we are able to investigate and compare transfection parameters in different types of mammalian cells, like transfection kinetics and pathways, optimum molar ratio between nanoparticles/nucleic acids and nanoparticles/cell.

2. Materials and methods

2.1. Materials

Collagen rat tail type I to make hydrogel droplets for adherent mammalian cells and agarose (1% w/v) as an extracellular matrix for non-adherent mammalian cells. Oil phase was composed by Fluorinert Eletronic Liquid FC-40 from 3M with surfactant poly(ethylene glycol-*ran*-propylene glycol) (PEG-*ran*-PPG) at 1 % (w/v).

Cationic liposomes consisted of egg phosphatidylcholine (EPC), 1,2-dioleoyl-3-trimethylammonium propane (DOTAP) and 1,2-dioleoylphosphatidylethanolamine (DOPE) from Lipoid (Germany), were complexed with DNA (Clontech pGFP Vector) encoding green fluorescent protein (GFP). Cells were marked with CellTracker^{TM} red CMTPX or Live/Dead® Viability/Cytotoxicity Assay Kit both from Life Technologies.

2.2. Microfluidic device fabrication

The microfluidic device (Figure 1) was fabricated following protocols established at Professor Charles' laboratory. We used dry film photo-lithography, which allows the simple fabrication of complex geometries (1). Briefly, a solid film of photo-resist is laminated on a glass slide, using an office laminator. It is then exposed to UV light through a specially designed mask that corresponds to the desired channel shape. This then serves as a mold for patterning the channels themselves, which corresponds to the top part of the chip made with poly(dimethylsiloxane) (PDMS) (see e.g. SQUIRES e QUAKE (2)). The bottom part was a thin film of PDMS with five hundred droplet traps, obtained from a metal model designed in a Micro Engraving Machine, in which the polymer dried bonded over a glass slide. The top and bottom part of PDMS are then bonded and the inner surfaces are functionalized with silane groups that provide a hydrophobic environment that is suitable for the generation and manipulation of aqueous droplets in oil (1).

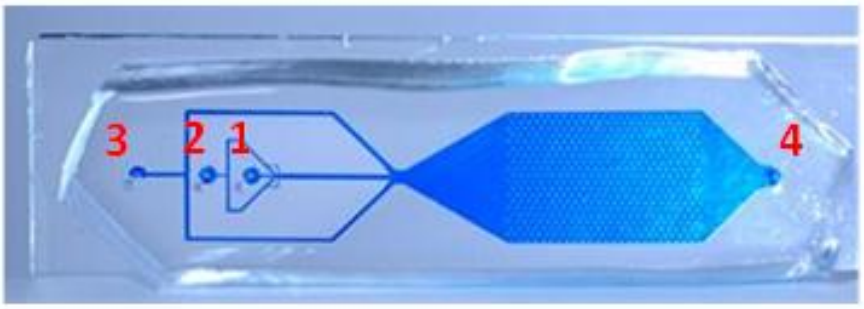

Figure 1 - Droplet-based microfluidic system.

2.3. Adherent mammalian cells transfection in the droplet-based microfluidic system

Smooth muscle cells (SMCs) and mesenchymal stem cells (MSCs) were cultivated until be in confluence and then inserted in microchip with collagen. SMCs and MSCs were mixed with collagen in 1:3 ratio and then inserted in the microdevice shown in Figure 1. Cell concentration varied from 0.1 to 0.5 x 10^6 cells/mL and collagen concentration 1.2 and 6 mg/mL. In this step, the system was kept at -4 ºC to avoid collagen gelation before droplets formation. The cells suspension was pumped in the system by the first entrance (Figure 1) at 5 µl/min, while two oil flows were incorporated by second entrance at 5.8 µl/min to form droplets in a flow-focusing design, and by third entrance at 35 µl/min to pull droplets to be trapped in the chamber and to increase their covering with surfactant, avoiding coalescence. After fill all traps with hydrogel droplets, the system was incubated at 37 ºC to collagen gelation, and then we changed the continuous phase from oil to aqueous phase. For this, about 2 ml of FC40 oil pure (without surfactant) was passed through the system at 40 µl/min to wash droplets covered with surfactant, and then, at least 100 µl culture medium was inserted at 1 µl/min. Depending on what we wanted to investigate, lipoplexes or culture inhibitors might be diluted in this medium. Then, images from the cells inside hydrogel droplets were taken by a motorized microscope (Nikon, Eclipse Ti-E) to study cell behavior over time.

2.4. Non-adherent mammalian cells transfection in the droplet-based microfluidic system

Likewise, 0.25 x 10^6 lymphoma cells (S49.1)/ml were inserted in the system, but in this case, because of involving non-adherent cells, agarose was used as hydrogel. Thus, the system was kept on 37 ºC during droplets formation, and then put at 4 ºC for agarose gelation. After that, phases were changed from oil to aqueous composed by medium with or without lipoplexes. Cells were also marked with live/dead staining to study cells viability, besides transfection kinetics. Images

were taken by the motorized microscope to investigate these behaviors of S49.1 over time.

3. Results and discussion

3.1. Smooth muscle cells and mesenchymal stem cells in collagen microdroplets

At a first moment, we started to work with adherent mammalian cells looking for more complex cells transfection applications, like induced pluripotent stem (iPS) cells reprogramming (3). However, adherent mammalian cells need a growth matrix like collagen to regulate integrin-mediated adhesion to the extracellular matrix, to bind growth factors to their receptors (4) and to mediate cells spreading (5), among other things. Additionally, cellular morphology is closely linked to transfection efficiency. Cellular microenvironment can modulate non-viral gene delivery, since proteins that promoted well spread cells resulted in complexes being trafficked to the nucleus and enhanced gene transfer (6). And also the act of integrin engagement and spreading itself may have an effect on cells uptake of non-viral vectors (7). Thus, as preliminary results (data not shown), we cultivated DC3F cells (Chinese hamster lung fibroblasts) inside and on the top of collagen, in and off chip, aiming to investigate cell morphology. Then, we started to work with Smooth Muscle cells (SMCs) in chip to investigate the behavior of a high contraction cell model according to matrix stiffness. For this, we filled the microchamber like showed in Figure 2 with five hundred collagen droplets containing cells inside, providing a huge number of experimental repetitions to be analyzed. In this first moment, we analyzed the results only in few droplets (n=10 to 20), but in the future the purpose is to use computational tools for image analysis, like MATLAB, to analyze more samples and increase the experimental accuracy of results.

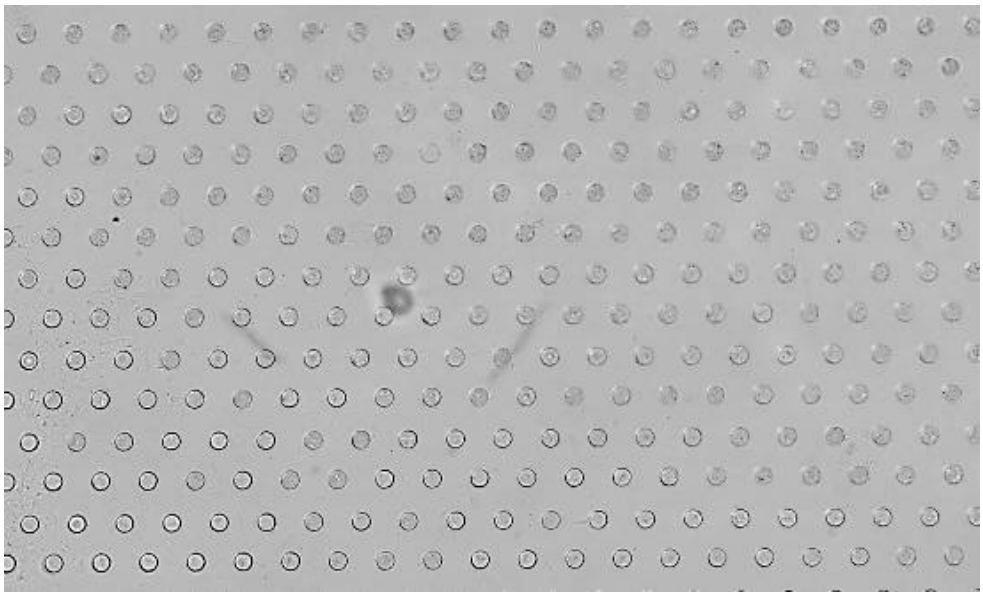

Figure 2 – Microchamber with 500 cylindrical traps with 250 µm of diameter by 250 µm of height.

The first aspect tested was to change the matrix stiffness by changing hydrogel concentration. Thus, we fixed SMCs concentration at $4x10^6$ cells/ml and compared their mechanism in the early hours of incubation in 1.2 mg/ml and 6 mg/ml of collagen in the matrix (Figure 3). As we can see in the images, when SMCs were cultured in a softer matrix (1.2 mg/ml) in 5 hours they spread (Figure 3 B), in 16 hours of incubation they shrink the hydrogel with their strong force traction (Figure 3 C) and, in 1 day, almost 90% of droplets are like an agglomeration ball of cells and collagen (Figure 3 D). On the other hand, when SMCs were cultured in a more rigid matrix (6 mg/ml), they spend more time to start to spread (around 16 hours incubation, Figure 3 G) and, consequently, to make these typical cell agglomerations showed in Figure 3 H. About 60% of cells are in these cluster structures after 1 day in culture.

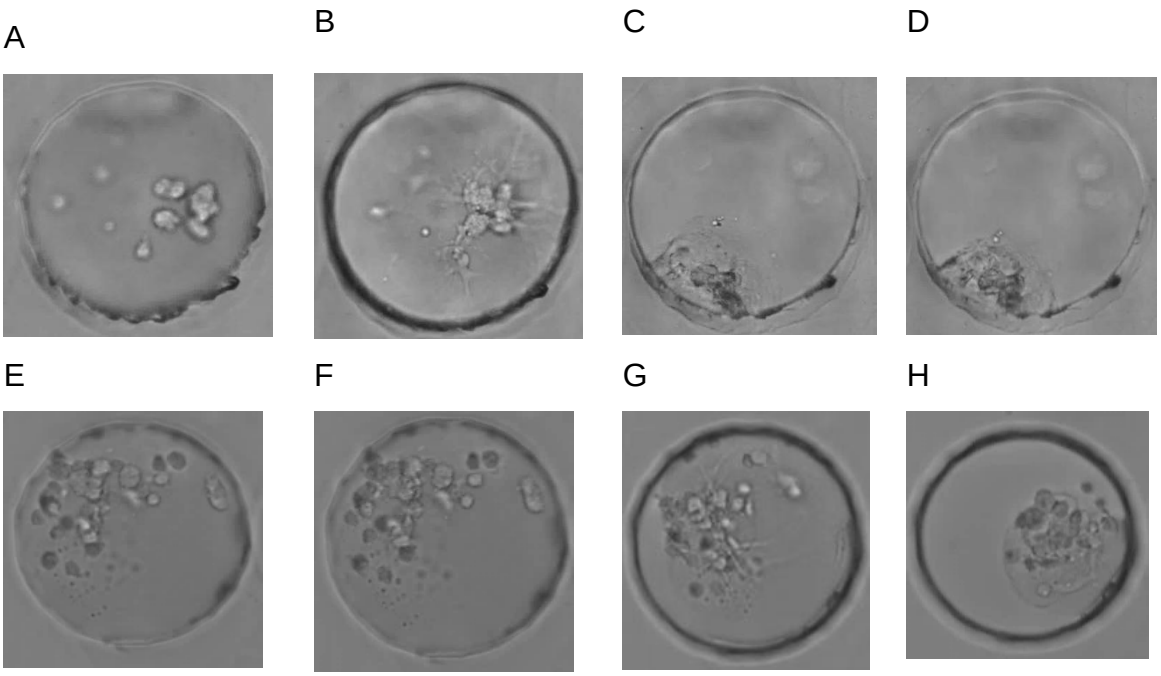

Figure 3 – Time-lapse images from 0, 5, 16 and 24 hours of smooth muscle cells (C_{cell} = 4x10^6 cells/ml) cultivated in collagen hydrogel droplets at 1.2 mg/ml (A, B, C and D) and 6 mg/ml (E, F, G, H).

Then, since spreaded cells could provide nanoparticles traffic to the nucleus (6), we transfected SMCs in the same cell concentration (4x10^6 cells/ml) and collagen droplets at 6 mg/ml (Figure 4), in order to stay a larger period of time in a favorable morphology to transfection. We complexed cationic liposomes EPC/DOTAP/DOPE (50/25/25% molar) with pDNA encoding green fluorescent protein (GFP), in a molar charge ratio between nucleic acids and cationic lipids ($R_{+/-}$) at 5 and around 1.3x10^{-4} µg of DNA/droplet. However, as shown in Figure 4C and D, cells in agglomerated structures make difficult to quantify cells transfected for over than 1 day incubation, seeing that the green fluorescence comes from a cluster, not from an individual cell.

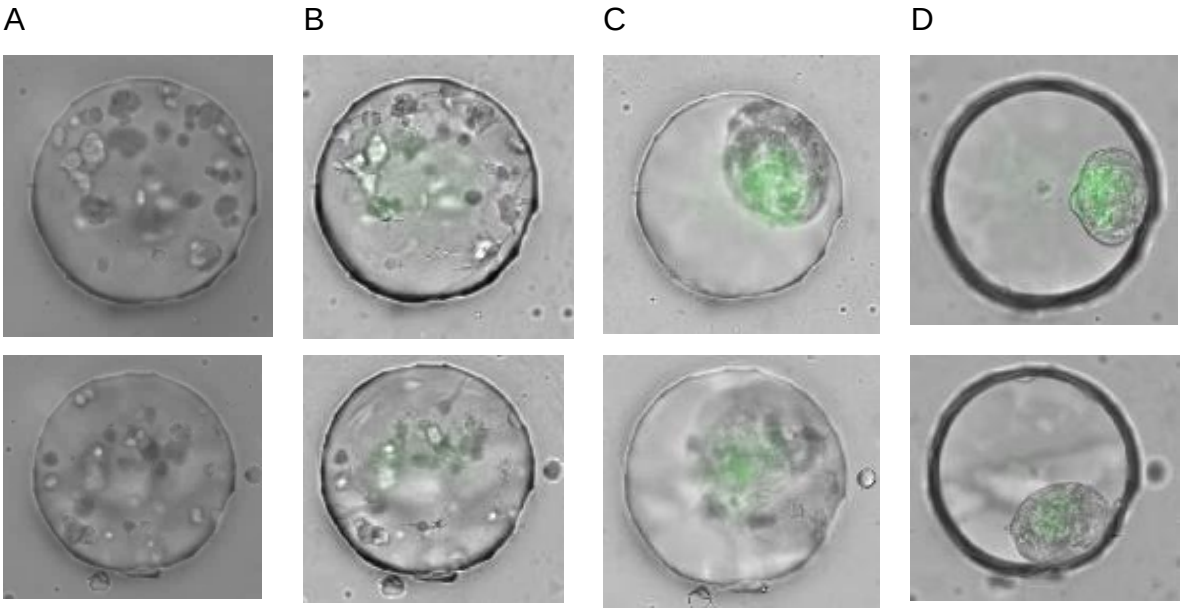

Figure 4 – Images of smooth muscle cells (C_{cell} = 4x10^6 cells/ml) cultivated in collagen at 6 mg/ml and transfected with lipoplexes (DNA/cationic liposomes at a molar charge ratio of $R_{+/-}$=5 for 0 day (A), 1 day (B), 2 days (C) and 3 days (D).

After, in such a way to avoid these cluster structures, we decreased SMCs concentration from 4 to 1x10^6 cells/ml, but study cell behavior also in the two collagen concentration, 1.2 mg/ml (Figure 5 A and B) and 6 mg/ml (Figure 5 C and D) for 1 day. As a result, almost 70% of droplets did not form an agglomeration after 1 day incubation (Figure 5 B and D), *i.e.* fewer cells in droplets, in both collagen concentrations, slowed down hydrogel shrink. Nevertheless, cell distribution on microdroplets follows Poisson distribution (8), which makes that many droplets in the chamber do not have cells inside hydrogel, decreasing results accuracy.

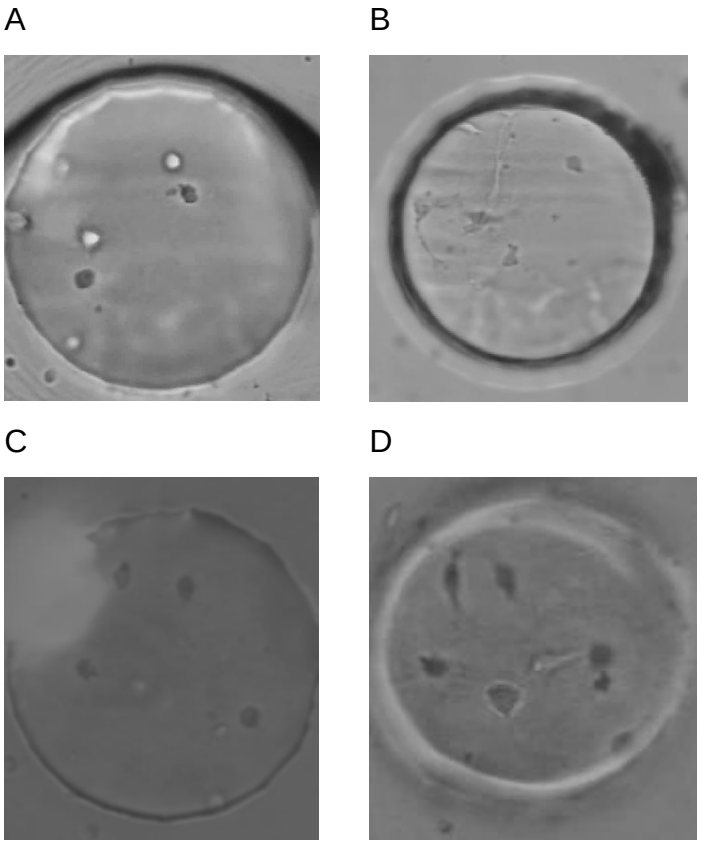

Figure 5 – Images from 0 and 1 day incubation of smooth muscle cells $1x10^6$ cells/ml cultivated in collagen hydrogel droplets at 1.2 mg/ml (A and B) and 6 mg/ml (C and D).

Thus, to maintain hydrogel droplets without shrinking but assuring the majority of 500 droplets in the chamber with SMCs, we inserted $2.5x10^6$ cells/ml mixed with 6 mg/ml of collagen in microdevice, reaching around 10 cells/droplet (Figure 6). About 95% of hydrogel droplets stayed attached to the trap surface for 1 day incubation even with cells spreaded, like showed in Figure 6 A. Even though, when cells are stained with cell tracker to facilitate cell localization and added with lipoplexes to transfect, they did not spread as we can verify in Figure 6 B. Continuous exposure of cells to fluorescent probes, such as rhodamine, can lead to be cytotoxic for some type of cells (9); and also cationic liposomes, more specifically cationic lipids (10,11). Therefore, cells maybe react against cytotoxic from these reagents, not spreading.

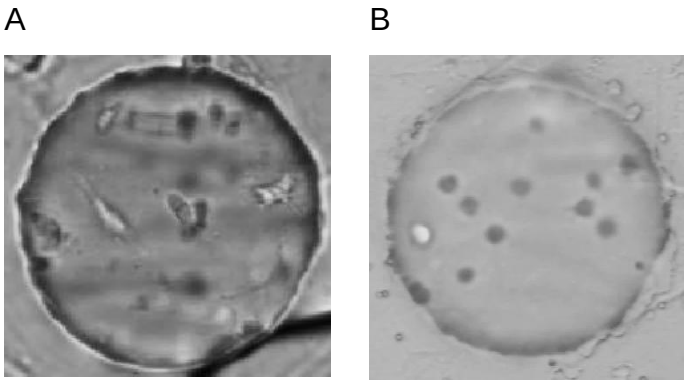

Figure 6 – Images incubation of smooth muscle cells $2.5x10^6$ cells/ml cultivated in collagen hydrogel droplets at 6 mg/ml for 1 day without staining (A) or with cell tracker and lipoplexes (B).

Hence, we transfected SMCs in this cell concentration ($2.5x10^6$ cells/ml), collagen droplets at 6 mg/ml and cells marked with a tracker (Figure 7). The lipoplexes cationic liposomes/pDNA were also in a molar charge ratio at ($R_{+/-}$) at 5 and around $1.3x10^{-4}$ µg of DNA/droplet. Almost 30% of cells were transfected after 1 day incubation and in 7 days it increased to 35% of transfection, but in 10 days of transfection does not increase more, maybe because they do not proliferate more.

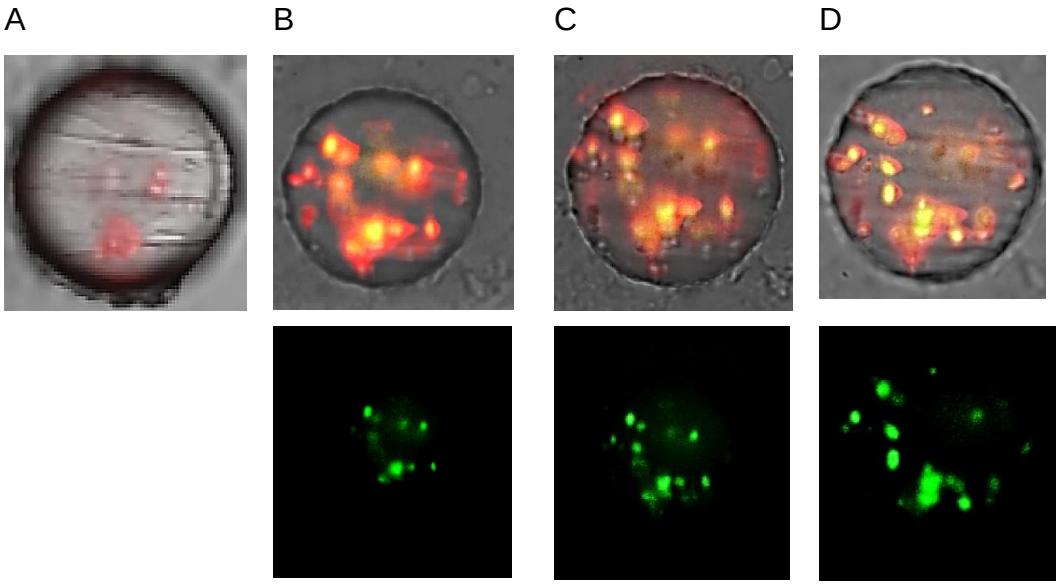

Figure 7 – Images of smooth muscle cells (C_{cell} = $2.5x10^6$ cells/ml) stained with cell tracker, cultivated in collagen at 6 mg/ml and transfected with lipoplexes (DNA/cationic liposomes at a molar charge ratio of $R_{+/-}$=5) for 0 day (A), 1 day (B), 7 days (C) and 10 days (D). Detached green fluorescent images of transfected cells in their respectively day of incubation.

Cells inside 3D microenvironment interact with cell-surface receptors, extracellular matrix and cell-cell adhesions, stimulating to generate changes in the actin cytoskeleton at primarily through engagement of clathrin endocytosis pathways, more specifically, RhoGTPases proteins (12). So, as a first step, we investigate few parameters, like hydrogel and cell concentration, to modify matrix stiffness and, consequently, activate molecular pathways related to actin cytoskeleton, which can regulate internalization and effective intracellular processing of nanoparticles resulting in an efficient gene transfer (6). But after, as a second step, we started to use few cell inhibitors to study cell behavior with regard to specific pathways related to matrix stiffness (13).

Cell spreading increase with cell traction force, RhoA activity and is also controlled by extracellular matrix stiffness. So, when grown in soft matrices, many cell types exhibit less spreading, as well as, reductions in proliferation, traction forces, stress fibers, and focal adhesions (14). However, Mih *et al.* (13) showed that putting some Rho ROCK inhibitors (like blebbistatin and Y27632) in fibroblasts cultivated in soft matrices generate an “excessive” contractile force that switches actomyosin from suppression to promote cell proliferation in soft matrices. We remarked by time-lapse images (Figure 3) with high SMCs concentration ($4x10^6$ cells/ml) in a very soft matrices ($C_{collagen}$ = 1.2 mg/ml) that collagen hydrogel is so soft that cells cannot stay a long time spreaded. Thus, we put 100 µM of Y27632 inhibitor in this cell culture conditions to promote cell proliferation and spreading even in soft matrix (Figure 8) and, maybe in future steps, we can use the same strategy to determinate the transfection pathways.

A

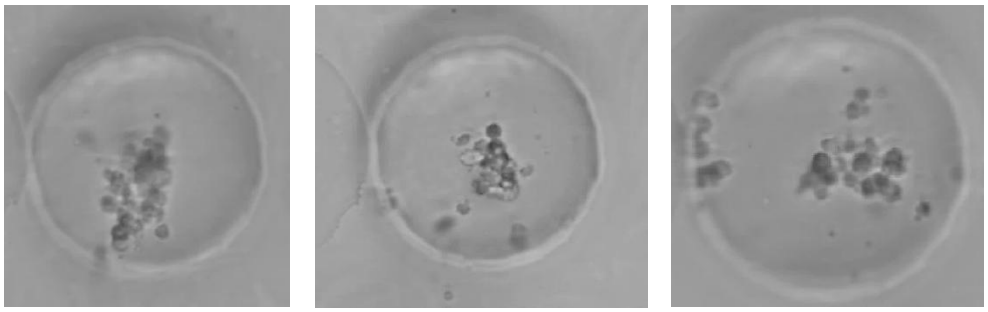

B

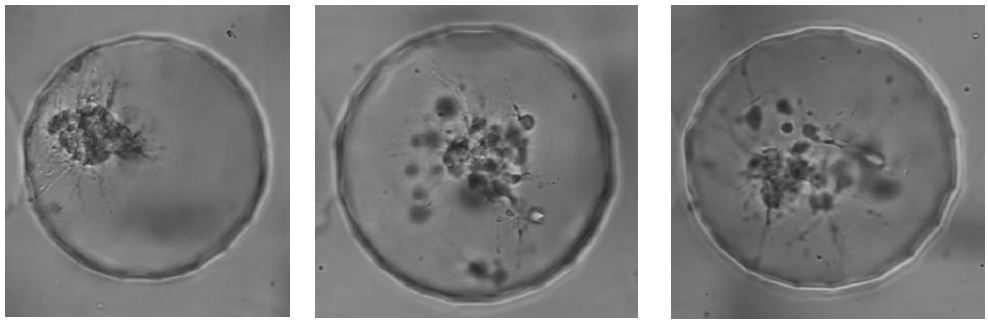

Figure 8 – Images of smooth muscle cells (C_{cell} = $4x10^6$ cells/ml) added with Y27632, cultivated in collagen hydrogel droplets at 1.2 mg/ml for 0 (A) and 16 hours (B).

As we can see in Figure 8 B, after 16 hours of incubation SMCs continue spreaded (approximately 90% of microdroplets) and without making an aggregated structure like showed in Figure 3 C. On the other hand, the spreading morphology of smooth muscle cells is different from Figure 3 B to Figure 8 B, because of different pathways used to activate actin cytoskeleton. In fact, members of RhoGTPase family are key regulatory molecules that link surface receptors to the organization of the actin cytoskeleton; more specifically RhoA forms stress fibers and focal adhesion, Rac1 provides structures like lamellipodia and Cdc42 like filopodia (12). According to images shown in HALL (15) work, in the case of SMCs without inhibitors (Figure 3B) it seems that RhoA pathway is activated, since spreading is only regulated by matrix stiffness (14); on the other hand, SMCs with Y27632 inhibitor (Figure 8 B) seems to activated Cdc42 pathway, forming protrusions like filopodia. And also LI; ZHOU e GAO (16) showed that small molecule inhibitors Y27632 markedly enhanced Cdc42 activity and the association of p-ERM with activated Cdc42, increasing cell motility.

In addition, for mesenchymal stem cells microenvironments appears to be an important for reprogramming them, for example, soft matrices that mimic brain provide neurogenic phenotypes, stiffer matrices that mimic muscles providing myogenic and comparatively rigid matrices that mimic collagenous bone prove osteogenic (17). Thus, we cultivated MSCs at $4x10^6$ cells/ml inside collagen microdroplets at 1.2 mg/ml for 1 day, without inhibitors (Figure 9 A and B), with 10 µM of Y27632 (Figure 9 C and D) and with 33 µM of blebbistatin (Figure 9 E and F). As a result, the positive control, *i.e.* without adding inhibitors, 40% of cell microdroplets maintained spreaded and without shrink for 1 day like showed in Figure 9 B. When added Y27632, 65% of MSCs microdroplets were spreaded like in Figure 9 D, and when added blebbistatin, 90% of hydrogel droplets with MSCs are like showed in Figure 9 F. Thus, blebbistain seems to be the most efficacy inhibitor for MSCs to not shrink, but differently from the other Rho ROCK inhibitor (Y27632), cells with blebbistain do not spread well in soft matrix (Figure 9 D and F). ENGLER *et al.* (17) also added blebbistain in naïve MSCs cultured in matrices with different elasticity, concluding that blebbistain blocks cell spreading in every matrix tested.

In addition, for mesenchymal stem cells microenvironments appears to be an important for reprogramming them, for example, soft matrices that mimic brain provide neurogenic phenotypes, stiffer matrices that mimic muscles providing myogenic and comparatively rigid matrices that mimic collagenous bone prove osteogenic (17). Thus, we cultivated MSCs at $4x10^6$ cells/ml inside collagen microdroplets at 1.2 mg/ml for 1 day, without inhibitors (Figure 9 A and B), with 10 µM of Y27632 (Figure 9 C and D) and with 33 µM of blebbistatin (Figure 9 E and F). As a result, the positive control, *i.e.* without adding inhibitors, 40% of cell microdroplets maintained spreaded and without shrink for 1 day like showed in Figure 9 B. When added Y27632, 65% of MSCs microdroplets were spreaded like in Figure 9 D, and when added blebbistatin, 90% of hydrogel droplets with MSCs are like showed in Figure 9 F. Thus, blebbistain seems to be the most efficacy inhibitor for MSCs to not shrink, but differently from the other Rho ROCK inhibitor (Y27632), cells with blebbistain do not spread well in soft matrix (Figure 9 D and

F). ENGLER *et al.* (17) also added blebbistain in naïve MSCs cultured in matrices with different elasticity, concluding that blebbistain blocks cell spreading in every matrix tested.

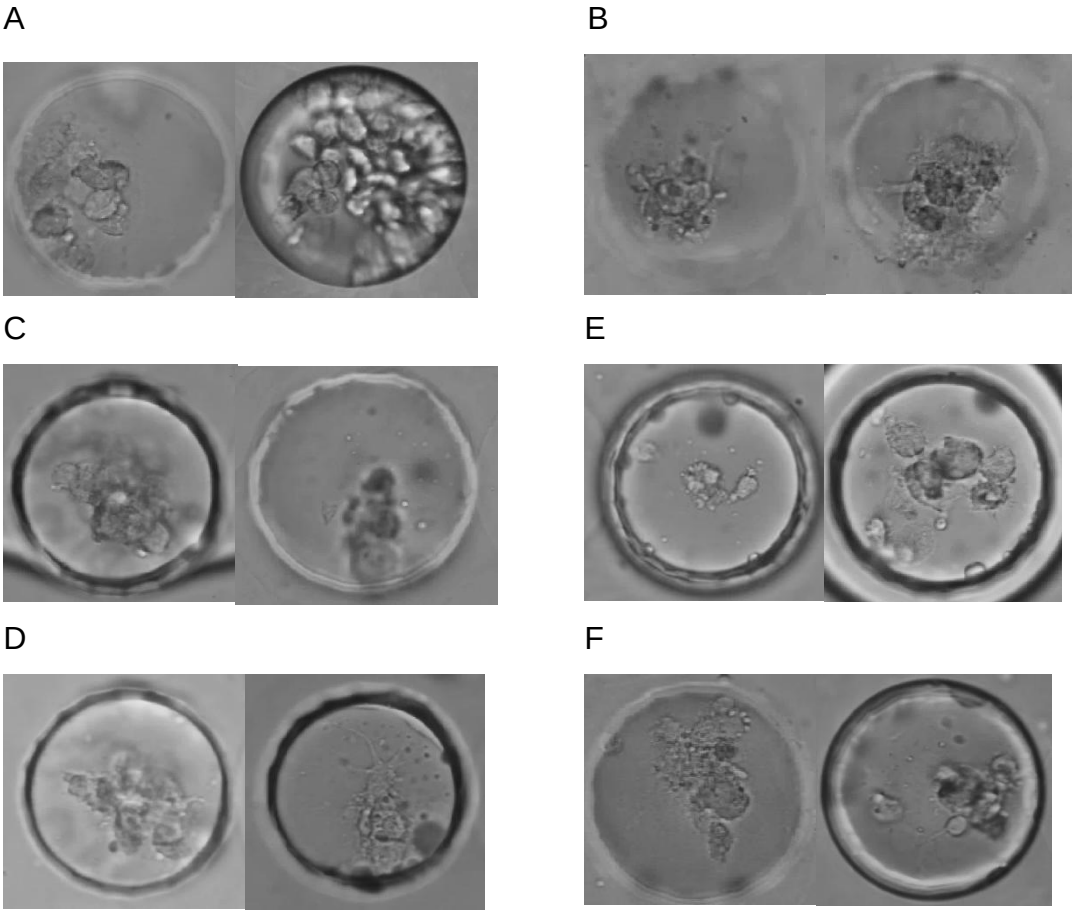

Figure 9 – Images of mesenchymal stem cells (C_{cell} = 4x10^6 cells/ml) cultivated in collagen hydrogel droplets at 1.2 mg/ml for 0 and 1 day without inhibitors (A and B), added with Y27632 (C and D) or with Blebbistatin (E and F).

Furthermore, this study with adherent mammalian cells will help in the next step of the PhD project, since collagen seems to be an adequate support for dendritic cells transfection (18).

3.2. Lymphoma cells in agarose microdroplets

After study adherent mammalian cells, we studied non-adherent mammalian cells, such as lymphoma cells (S49.1), to consider the application of the same microchip to transfect both mammalian cells types. In this case, the hydrogel used

was agarose, because non-adherent cells do not need a complex extracellular matrix to attach, interact with other cells or soluble factors, as provided by collagen. As lymphoma cells are smaller than SMCs and MSCs, at first, we studied the cell concentration with which we can count cells after proliferate for some days, but also not so few cells that many droplets in chamber stay without cells. For this, we compared two S49.1 concentrations, $2.5x10^6$ cell/ml (Figure 10 A and B) and $5x10^6$ cell/ml (Figure 10 C and D), cultivated for 1 day in agarose droplets and marked with cell tracker. When cell concentration was $2.5x10^6$ cell/ml, there were almost 10 cells/droplet after 1 day (Figure 10 A), and when $5x10^6$ cell/ml, there were about 20 cells/droplet (Figure 10 D). So, we decided to use $2.5x10^6$ cell/ml in the next studies to have a reasonable quantity of cells after at least 7 days incubation during transfection processes, and to produce less quantity of metabolites that could be toxic for cells.

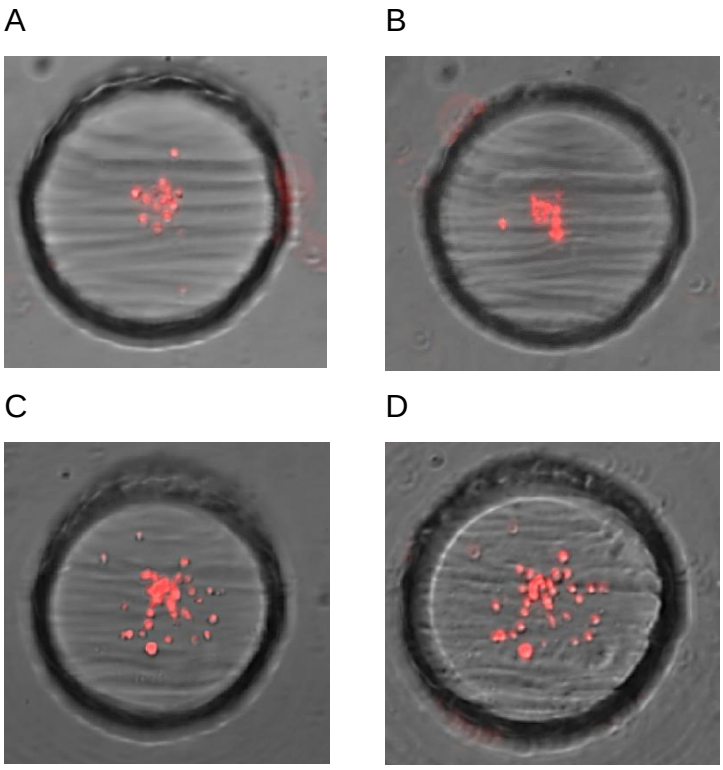

Figure 10 – Images of lymphoma cells market with cell tracker cultivated in agarose hydrogel droplets for 0 and 1 day incubation at $2.5x10^6$ cells/ml (A and B) and $5x10^6$ cells/ml (C and D).

Then, we transfected $2.5x10^6$ lymphoma cells/ml marked with cell tracker inside agarose droplets for 7 (Figure 11 B) and 11 days (Figure 11C). The lipoplexes cationic liposomes/pDNA were in a molar charge ratio at ($R_{+/-}$) at 5 and around $1.3x10^{-4}$ µg of DNA/droplet. About 10% of cells were transfected after 7 day incubation and in 11 days it increased to 20% of transfection. However, after 7 days of incubation we realized that cells were not typically round as in the beginning (Figure 11 A), showing that they maybe were in apoptosis or dead. But, seeing movies of changing phases process (from oil to medium) we saw that there was still oil around droplets, and these would be the cause to cells death. Because of that, we changed trap design from cylindrical to hexagonal form in order to drain the oil easier by trap angles. Other transfection experience drawback was the high green background showed in fluorescence images, which hinders the detection of transfected cells. We verified, by taking fluorescence images from the medium, that probably the background showed came from the medium. As a strategy, we decided to change the medium for PBS buffer only when taking pictures.

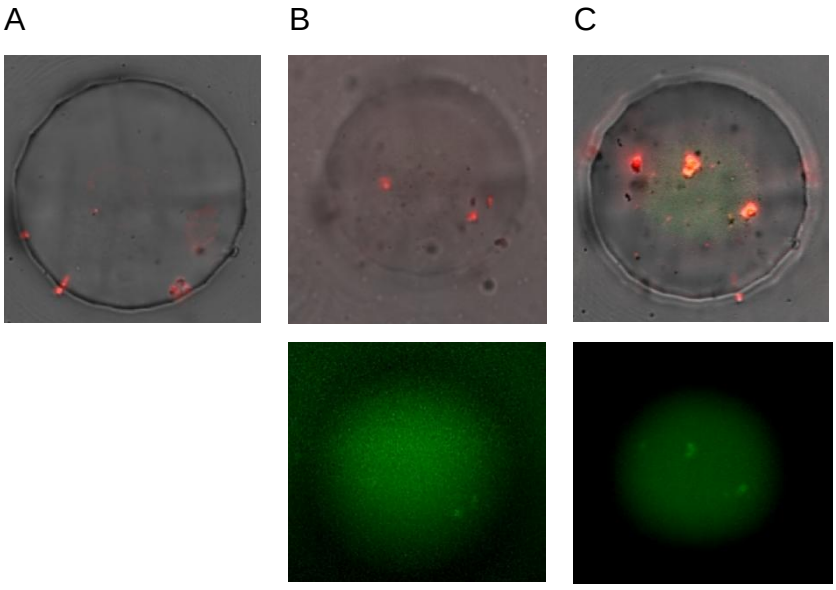

Figure 11 – Images of lymphoma cells (C_{cell} = $2.5x10^6$ cells/ml) stained with cell tracker, cultivated in agarose and transfected with lipoplexes (DNA/cationic liposomes at a molar charge ratio of $R_{+/-}$=5) for 0 day (A), 7 days (B) and 11 days (C). Detached green fluorescent images of transfected cells in their respectively day of incubation.

Then, we transfected lymphoma cells again (C_{cell}=2.5x10^{6}cell/ml) with lipoplexes at $R_{+/-}$ 5 inside agarose droplets kept in hexagonal traps for 1 (Figure 11 A) and 7 days (Figure 11 B) incubation. In one day incubation, there was almost no transfection, but in 7 days, 20% of cells were transfected. So, comparing to the last transfection result, we can see that the number of cells transfected in the same period of cells incubation, 7 days, increased 10% and also the green background in the fluorescence images disappeared, changing medium for PBS buffer when taking images.

Aiming to quantify cell viability in this transfection condition, we marked cells with live/dead staining and took images in 1 day (Figure 11 C) and 7 days (Figure 11 D) of culture. Since cells marked with green are alive and with red are died, around 50% of them were dead in the first day and 70% in 7 days. We do not know why many of them were died in chip, maybe they were high exposure to live/dead probes being toxic for them, or the oil were still not well drained around droplets.

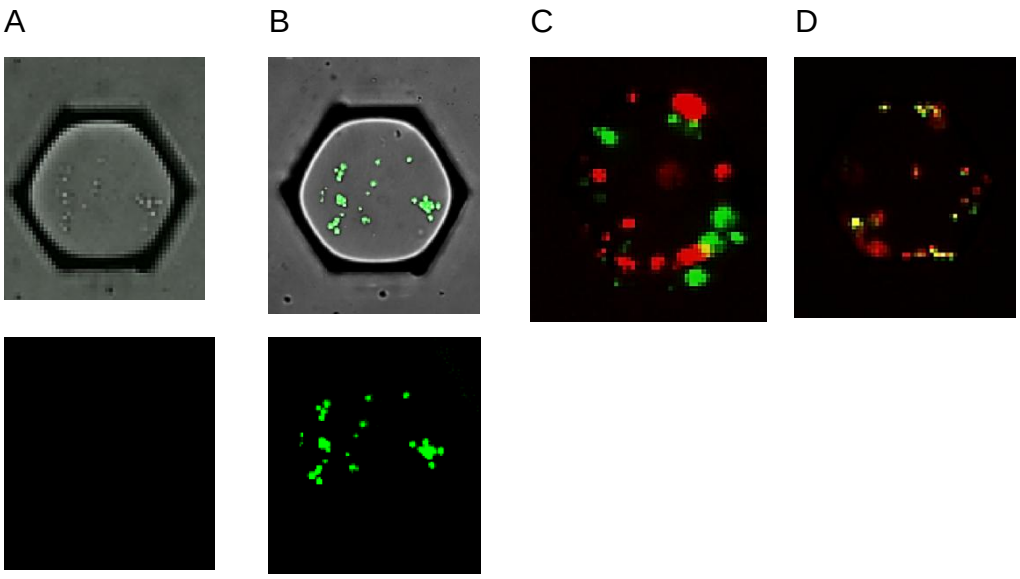

Figure 12 – Images of lymphoma cells (C_{cell} = 2.5x10^6 cells/ml) cultivated in agarose, transfected with lipoplexes (DNA/cationic liposomes at a molar charge ratio of $R_{+/-}$=5) for 1 day (A) and 7 days (B), or marked with live/dead staining for 1 day (C) and 7 days (D). Detached green fluorescent images of transfected cells in their respectively day of incubation.

4. Conclusions

We develop a microchip which with we were able to transfect adherent (SMCs and MSCs) and non-adherent (S49.1) mammalian cells spending little quantities of reagents and obtaining many replicates and data in only one experiment. High SMCs concentration ($4x10^6$ cells/ml) in collagen at 1.2 mg/ml and 6 mg/ml make cluster structures after 1 day in culture, being difficult to identify number of cells transfected. But, decreasing cell concentration to $2.5x10^6$ cells/ml in collagen at 6 mg/ml, SMCs stayed spreaded after 1 day, however if we marked cells with cell tracker, they did not do the cluster structure, but they do not spread as well. SMCs transfected in this condition achieve almost 35% of transfection in 7 days incubation. Using Rho ROCK inhibitors, like Y27632 and blebbistatin, in soft matrices (C_{cell} = $4x10^6$ cells/ml and $C_{collagen}$=1.2 mg/ml) seems to be a good strategy to maintain SMCs and MSCs spreaded and without shrinking, and also a potential tool to investigate the pathway used by cells for transfection. In the case of lymphoma cells, we showed that transfection was better in microchip with hexagonal traps to drain better the oil around droplets, reaching about 20% of transfection in 7 days incubation, however with cells viability very low.

5. References

1. Fradet E, McDougall C, Abbyad P, Dangla R, McGloin D, Baroud CN. Combining rails and anchors with laser forcing for selective manipulation within 2D droplet arrays. Lab Chip. The Royal Society of Chemistry; 2011;11(24):4228–34.

2. Squires T, Quake S. Microfluidics: Fluid physics at the nanoliter scale. Reviews of Modern Physics. 2005. p. 977–1026.

3. Takahashi K, Yamanaka S. Induction of pluripotent stem cells from mouse embryonic and adult fibroblast cultures by defined factors. Cell. Elsevier; 2006;126(4):663–76.

4. Schwartz M a, Assoian RK. Integrins and cell proliferation: regulation of cyclin-dependent kinases via cytoplasmic signaling pathways. J Cell Sci. 2001;114(Pt 14):2553–60.

5. Price LS, Leng J, Schwartz M a, Bokoch GM. Activation of Rac and Cdc42 by integrins mediates cell spreading. Mol Biol Cell. 1998;9(7):1863–71.

6. Dhaliwal A, Maldonado M, Lin C, Segura T. Cellular cytoskeleton dynamics modulates non-viral gene delivery through RhoGTPases. PLoS One. 2012;7(4):e35046.

7. Adler AF, Speidel AT, Christoforou N, Kolind K, Foss M, Leong KW. High-throughput screening of microscale pitted substrate topographies for enhanced nonviral transfection efficiency in primary human fibroblasts. Biomaterials. 2011;32(14):3611–9.

8. Joensson HN, Samuels ML, Brouzes ER, Medkova M, Uhlén M, Link DR, et al. Detection and Analysis of Low-Abundance Cell-Surface Biomarkers Using Enzymatic Amplification in Microfluidic Droplets. Angew Chemie Int Ed. Wiley Online Library; 2009;48(14):2518–21.

9. Lampidis TJ, Bernal SD, Summerhayes IC, Chen LB. Selective toxicity of rhodamine 123 in carcinoma cells in vitro. Cancer Res. AACR; 1983;43(2):716–20.

10. Bringmann A, Held SAE, Heine A, Brossart P. RNA vaccines in cancer treatment. J Biomed Biotechnol. 2010;2010:1–12.

11. Gilboa E, Vieweg J. Cancer immunotherapy with mRNA-transfected dendritic cells. Immunol Rev. 2004;199:251–63.

12. Sit S-T, Manser E. Rho GTPases and their role in organizing the actin cytoskeleton. J Cell Sci. The Company of Biologists Ltd; 2011;124(5):679–83.

13. Mih JD, Marinkovic A, Liu F, Sharif AS, Tschumperlin DJ. Matrix stiffness reverses the effect of actomyosin tension on cell proliferation. J Cell Sci. 2012;125(Pt 24):5974–83.

14. Wozniak MA, Chen CS. Mechanotransduction in development: a growing role for contractility. Nat Rev Mol cell Biol. Nature Publishing Group; 2009;10(1):34–43.

15. Hall A. Rho GTPases and the actin cytoskeleton. Science (80-). American Association for the Advancement of Science; 1998;279(5350):509–14.

16. Li Y, Zhou C-X, Gao Y. Snail regulates the motility of oral cancer cells via RhoA/Cdc42/p-ERM pathway. Biochem Biophys Res Commun. Elsevier; 2014;452(3):490–6.

17. Engler AJ, Sen S, Sweeney HL, Discher DE. Matrix elasticity directs stem cell lineage specification. Cell. Elsevier; 2006;126(4):677–89.

18. Singh R, Kostarelos K. Designer adenoviruses for nanomedicine and

nanodiagnostics. Trends Biotechnol. 2009;27(4):220–9.